(2)

Defense Nuclear Agency
Alexandria, VA 22310-3398

DNA-TR-92-130

One-Dimensional Modeling of Ground Shock Propagation in Spatially Random Geologic Media

Audrey A. Martinez
The Board of Regents of
New Mexico State University
Civil Engineering Department
P.O. Box 30002
Las Cruces, NM 88003-0002

March 1993

Technical Report

CONTRACT No. DNA MIPR-91-645

Destroy this report when it is no longer needed. Do not return to sender.

PLEASE NOTIFY THE DEFENSE NUCLEAR AGENCY, ATTN: CSTI, 6801 TELEGRAPH ROAD, ALEXANDRIA, VA 22310-3398, IF YOUR ADDRESS IS INCORRECT, IF YOU WISH IT DELETED FROM THE DISTRIBUTION LIST, OR IF THE ADDRESSEE IS NO LONGER EMPLOYED BY YOUR ORGANIZATION.

DISTRIBUTION LIST UPDATE

This mailer is provided to enable DNA to maintain current distribution lists for reports. (We would appreciate your providing the requested information.)

NOTE:
Please return the mailing label from the document so that any additions, changes, corrections or deletions can be made easily.

☐ Add the individual listed to your distribution list.

☐ Delete the cited organization/individual.

☐ Change of address.

NAME: _____

ORGANIZATION: _____

OLD ADDRESS	CURRENT ADDRESS
_____	_____
_____	_____
_____	_____

TELEPHONE NUMBER: (___) _____

DNA PUBLICATION NUMBER/TITLE	CHANGES/DELETIONS/ADDITIONS, etc.) *(Attach Sheet if more Space is Required)*
_____	_____
_____	_____
_____	_____

DNA OR OTHER GOVERNMENT CONTRACT NUMBER: _____

CERTIFICATION OF NEED-TO-KNOW BY GOVERNMENT SPONSOR (If other than DNA):

SPONSORING ORGANIZATION: _____

CONTRACTING OFFICER OR REPRESENTATIVE: _____

SIGNATURE: _____

CUT HERE AND RETURN

DEFENSE NUCLEAR AGENCY
ATTN: TITL
6801 TELEGRAPH ROAD
ALEXANDRIA, VA 22310-3398

DEFENSE NUCLEAR AGENCY
ATTN: TITL
6801 TELEGRAPH ROAD
ALEXANDRIA, VA 22310-3398

REPORT DOCUMENTATION PAGE

Form Approved
OMB No. 0704-0188

1. AGENCY USE ONLY *(Leave blank)*	2. REPORT DATE	3. REPORT TYPE AND DATES COVERED
	930301	Technical

4. TITLE AND SUBTITLE
One-Dimensional Modeling of Ground Shock Propagation in Spatially Random Geologic Media

5. FUNDING NUMBERS
C - DNA-MIPR-91-645
PE - 62715H, 62601F
PR - RS
TA - RB
WU - DH00277

6. AUTHOR(S)
Audrey A. Martinez

7. PERFORMING ORGANIZATION NAME(S) AND ADDRESS(ES)
The Board of Regents of
New Mexico State University
Civil Engineering Department
P. O. Box 30002
Las Cruces, NM 88003-0002

8. PERFORMING ORGANIZATION REPORT NUMBER

9. SPONSORING/MONITORING AGENCY NAME(S) AND ADDRESS(ES)
Defense Nuclear Agency
6801 Telegraph Road
Alexandria, VA 22310-3398

SPWE/Tremba

10. SPONSORING/MONITORING AGENCY REPORT NUMBER
DNA-TR-92-130

11. SUPPLEMENTARY NOTES
This work was sponsored by the Defense Nuclear Agency under RDT&E RMC Code B 4662 D RS RB SPWE 4400 A 25904D.

12a. DISTRIBUTION/AVAILABILITY STATEMENT
Approved for public release, distribution is unlimited.

12b. DISTRIBUTION CODE

13. ABSTRACT *(Maximum 200 words)*

Field experiments have shown that scattering by random geologic heterogeneity has a significant influence on explosively induced stress wave propagation. Physical models of stress wave propagation created by explosive tests are based on the traditional assumption that the subsurface geologic material can be divided into homogeneous layers. This simplistic approach may be responsible for much of the discrepancy which remains between observations from field experiments and computational results. Stochastic modeling techniques were applied to the problem of ground shock propagation through spatially random geologic media. Using these techniques, the spatial variability in the material model is defined by 1) the type of statistical distribution which defines the subsurface heterogeneity; 2) the scale or correlation distance of the variability; and 3) the mean and standard deviation of the material property under consideration. For the particular site under study, these statistical parameters have been estimated from cone penetrometer testing, laboratory material property testing, and seismic surveys. The statistical estimates of the properties are used in the stochastic modeling technique to modify

14. SUBJECT TERMS		15. NUMBER OF PAGES
Spatially random geologic media subsurface heterogeneity stress wave propagation	stochastic modeling scattering	116
		16. PRICE CODE

17. SECURITY CLASSIFICATION OF REPORT	18. SECURITY CLASSIFICATION OF THIS PAGE	19. SECURITY CLASSIFICATION OF ABSTRACT	20. LIMITATION OF ABSTRACT
UNCLASSIFIED	UNCLASSIFIED	UNCLASSIFIED	SAR

CLASSIFIED BY: N/A since Unclassified

DECLASSIFY ON: N/A since Unclassified

13. ABSTRACT (Continued)

the output of a random number generator. The output, termed spatially random geologic variability factors in this study, was then incorporated into a finite difference ground shock code to simulate the subsurface in homogeneities. The results from the stochastic calculations were compared with the results of calculations utilizing a homogeneous material model in order to determine the relative influence of spatial geologic variability on ground motions. The results of the calculations were also compared to closed form solutions and with experimental data. The comparisons indicate that the introduction of spatial subsurface heterogenity into ground shock calculations causes changes in ground shock attenuation rates and broadening of peaks relative to the homogeneous calculations. The late time perturbations seen in the random calculations are similar to those often seen in experimental data.

14. SUBJECT TERMS (Continued)

Statistical Characterization
Random Geology Generator

PREFACE

This report describes research performed by the author in partial fulfillment of the requirements for the Degree of Master of Science in Civil Engineering at New Mexico State University, Las Cruces, New Mexico. The research consisted of developing one-dimensional techniques for modeling ground shock propagation through spatially random geologic media.

The research was performed under the guidance of Dr. A. K. Aiyer, the author's graduate committee chairman. Other members of the committee were Dr. William McCarthy, Dr. Morris Southward, and Dr. Timothy Ward who provided comments, technical support and helpful discussions regarding this thesis.

The author's Master program was sponsored by the Air Force Phillips Laboratory under project 88091357, and the Defense Nuclear Agency under MIPR 91-645 monitored by Dr. Edward L. Tremba.

CONVERSION TABLE

(This Conversion Table is Unclassified)

MULTIPLY → TO GET	BY	TO GET ← DIVIDE
angstrom	1.000 000 X E -10	meters (m)
atmosphere (normal)	1.013 25 X E +2	kilo pascal (kPa)
bar	1.000 000 X E +2	kilo pascal (kPa)
barn	1.000 000 X E -28	meter^2 (m^2)
British thermal unit (thermochemical)	1.054 350 X E +3	joule (J)
calorie (thermochemical)	4.184 000	joule (J)
cal (thermochemical/cm^2)	4.184 000 X E -2	mega joule/m^2 (MJ/m^2)
curie	3.700 000 X E +1	*giga becquerel (GBq)
degree (angle)	1.745 329 X E -2	radian (rad)
degree Fahrenheit	$t_k = (t^{\circ}f + 459.67)/1.8$	degree kelvin (K)
electron volt	1.602 19 X E -19	joule (J)
erg	1.000 000 X E -7	joule (J)
erg/second	1.000 000 X E -7	watt (W)
foot	3.048 000 X E -1	meter (m)
foot-pound-force	1.355 818	joule (J)
gallon (U.S. liquid)	3.785 412 X E -3	meter^3 (m^3)
inch	2.540 000 X E -2	meter (m)
jerk	1.000 000 X E +9	joule (J)
joule/kilogram (J/kg) radiation dose absorbed	1.000 000	Gray (Gy)
kiloton	4.183	terajoules
kip (1000 lbf)	4.448 222 X E +3	newton (N)
kip/inch^2 (ksi)	6.894 757 X E +3	kilo pascal (kPa)
ktap	1.000 000 X E +2	newton-second/m^2 (N-s/m^2)
micron	1.000 000 X E -6	meter (m)
mil	2.540 000 X E -5	meter (m)
mile (international)	1.609 344 X E +3	meter (m)
ounce	2.834 952 X E -2	kilogram (kg)
pound-force (lbs avoirdupois)	4.448 222	newton (N)
pound-force inch	1.129 848 X E -1	newton-meter (N'm)
pound-force/inch	1.751 268 X E +2	newton/meter (N/m)
pound-force/foot^2	4.788 026 X E -2	kilo pascal (kPa)
pound-force/inch^2 (psi)	6.894 757	kilo pascal (kPa)
pound-mass (lbm avoirdupois)	4.535 924 X E -1	kilogram (kg)
pound-mass-foot^2 (moment of inertia)	4.214 011 X E -2	kilogram-meter^2 (kg'm^2)
pound-mass/foot^3	1.601 846 X E +1	kilogram/meter^3 (kg/m^3)
rad (radiation dose absorbed)	1.000 000 X E -2	**Gray (Gy)
roentgen	2.579 760 X E -4	coulomb/kilogram (C/kg)
shake	1.000 000 X E -8	second (s)
slug	1.459 390 X E +1	kilogram (kg)
torr (mm Hg, 0° C)	1.333 22 X E -1	kilo pascal (kPa)

*The becquerel (Bq) is the SI unit of radioactivity; 1 Bq = 1 event/s.
**The Gray (GY) is the SI unit of absorbed radiation.

TABLE OF CONTENTS

LIST OF FIGURES

LIST OF TABLES

Chapter 1

INTRODUCTION

1.1 General Problem

Knowledge of the stress wave field created within the earth by an explosive detonation is required for the design of hardened protective structures for weapon systems and for the verification of compliance with nuclear testing treaties. Models for this stress wave propagation are developed in the "explosive effects community" by using large scale finite difference codes and geologic material models based on field and laboratory testing. These models are validated and improved by comparing calculated stress and motion fields with observations from field explosive experiments. "Explosive effects community" is used in this study to represent the scientists and engineers involved in planning, designing, and analyzing nuclear and conventional explosive experiments.

A series of small scale field experiments conducted over the past several years has established that scattering by random geologic heterogeneity has a significant influence on explosively induced stress wave propagation (Reinke and Stump, 1988; Reinke and Stump, 1991). Existing physical

models of stress wave propagation in the explosive effects community are based on the assumption that the subsurface geologic material properties can be divided into homogeneous layers. This type of representation is often inadequate as demonstrated by small scale explosive experiments, and may be responsible for much of the discrepancy which remains between observations from field experiments and computational results.

Site investigation efforts performed at sites where field experiments were conducted have shown subsurface heterogeneities (Reinke and Stump, 1988). These heterogeneites are not considered in the geologic material models used in ground shock codes. The mean soil conditions at test sites are defined by constant soil parameters in the geologic material model. While the constant soil parameters may be a reasonable description of the mean conditions at a test site, this simplistic representation of the subsurface geology cannot allow ground shock calculations to correctly model the phenomenology which occurs as the shock propagates through the soil medium.

1.2 Goal

This study develops one-dimensional techniques for modeling ground shock propagation through spatially random geologic media. A geologic material property at a given point is unknown until accurately measured, but it is not practical to perform a site characterization effort in enough detail to delineate each and every heterogeneity in the subsurface soil (Vanmarcke, 1983). Therefore, stochastic modeling techniques borrowed from the geophysical community were applied to the problem of ground shock propagation through spatially random geologic media (Frankel and Clayton, 1986; Sudicky, 1986). Using these techniques, the spatial variability (as distinguished from point variability due to imprecision in measurement of the properties at a given location) in the material model is defined by (1) the type of statistical distribution which defines the subsurface heterogeneity; (2) the scale or correlation distance of the variability; and (3) the mean and standard deviation of the material property under consideration. For the site used in this study, these statistical parameters have been estimated from cone penetrometer testing, laboratory material property testing, and seismic surveys.

The site of interest for this study is McCormick Ranch,

composed of dry alluvium. McCormick Ranch is a test site located on Kirtland Air Force Base (AFB), south of Albuquerque, New Mexico. The subsurface spatial variability at McCormick Ranch can be seen in Figure 1. Figure 1 contains a set of data plots from 3 cone penetrometer tests performed on the same azimuth (270 degrees) and at varying distances from the reference point (center of test bed). Test cv27012 was 3.66 m (12 ft) from the test bed center, and tests cv27024 and cv27040 were 7.32 m (24 ft) and 12.2 m (40 ft) from the center, respectively. As shown in Figure 1, a large degree of variability is present in the data as a function of depth. The tip resistance in cv27012 varies from 55 to 320 kg/cm^2 (782-4551 psi), and from 70 to 425 kg/cm^2 (996-6045 psi) in cv27040. There is also a significant amount of lateral spatial variability present as evidenced by differences from one hole to the next. To illustrate this, the tip resistances from two arbitrary depths were selected to describe the lateral variability:

DEPTH (m)	cv27012	cv27024 (kg/cm^2)	cv27040
1.22	209	373	235
4.88	176	180	414

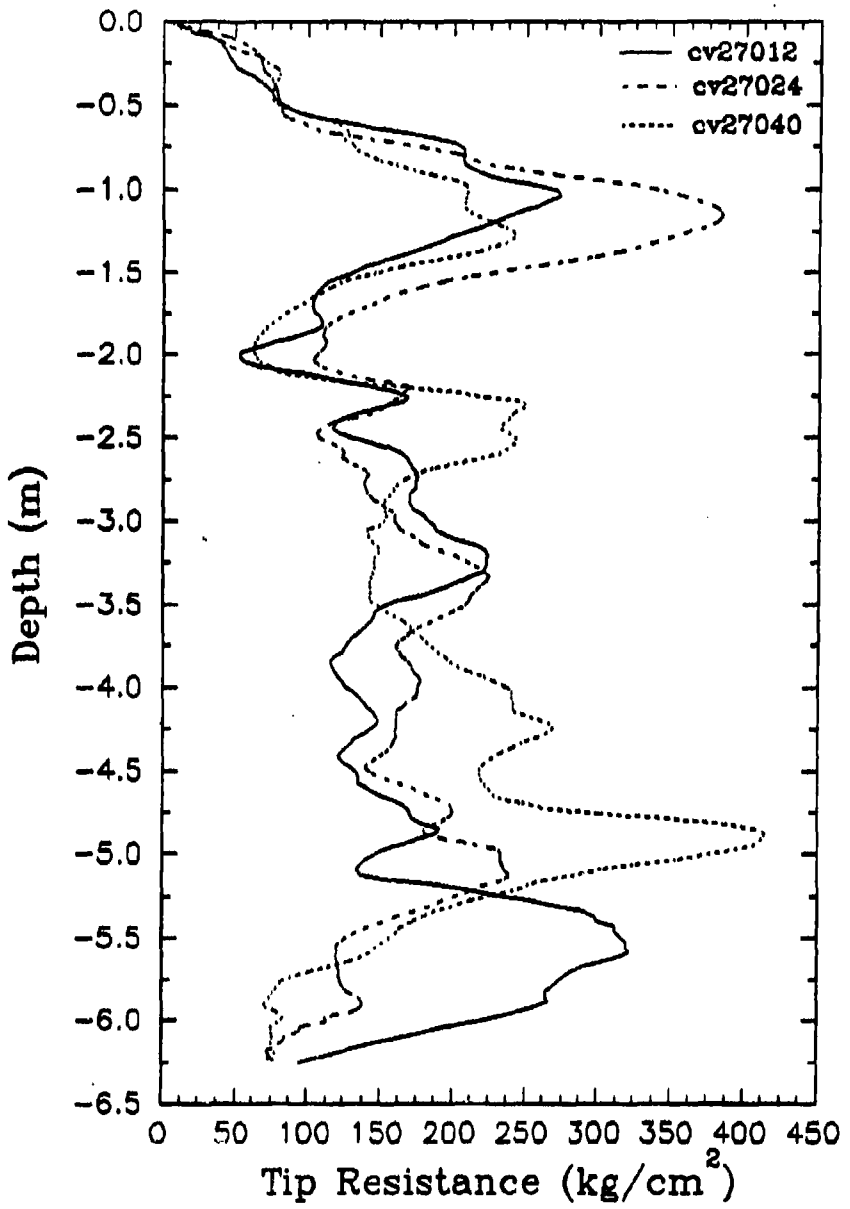

Figure 1. Set of three cone penetrometer soundings performed at McCormick Ranch, New Mexico.

Figure 1 demonstrates the geologic variability present in the subsurface material which is not considered in ground shock calculations. The subsurface geologic material properties in ground shock calculations are defined as homogeneous layers. Figure 2 shows a simplified site profile of the McCormick Ranch, New Mexico test site developed for use in ground shock calculations of high explosive test events at this site (Grant, 1988). This profile was developed from a series of laboratory and field test data which were cone penetrometer tests, seismic refraction surveys, and borehole logs. Figure 2 shows the subsurface material divided into 3 homogeneous layers. The properties associated with each layer are p-wave velocity (C_p), shear wave velocity (C_s), and soil density (ρ). These values are constants, which do not account for the geologic variability present in Figure 1. The profile in Figure 2 simply describes the mean conditions at the site.

The main application of results from this study will be used to reduce or quantify the uncertainty in performing ground shock/motion calculations/predictions based upon conventional and nuclear detonations.

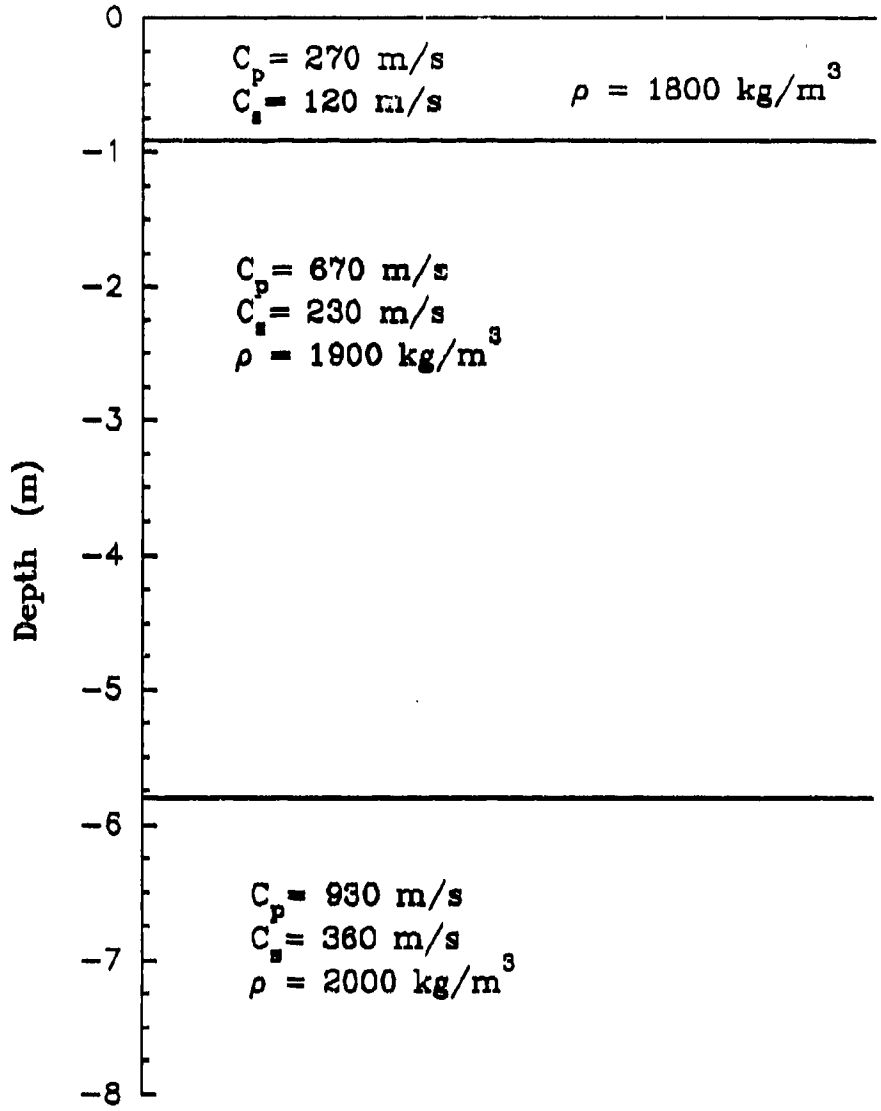

Figure 2. Simplified site profile developed for the McCormick Ranch test site.

1.3 Previous Work

Several studies have found that medium inhomogeneities are characterized by correlation analysis. The application of correlation analysis to the study of wave propagation in a medium with random inhomogeneities goes back to Chernov (1960). Chernov developed techniques to categorize medium inhomogeneities. He studied the problem of amplitude and phase fluctuations of wave fields when sound waves propagated in the atmosphere and the sea, the twinkling of stars, and the fading of radio signals.

Correlation analysis has also been used to characterize spatial variation in earthquake induced ground motions. The El Centro differential array data from the 1979 Imperial Valley earthquake (Smith et al., 1982) were analyzed using correlation analysis and spectral ratios of array averages. The differential array consisted of 6 DCA-300 digital recording accelerographs in a north-south line at distances of 0, 18.3, 54.9, 128.1, 213.4, and 304.9 m (0, 60, 180, 420, 700, and 1000 ft). The exact location of the array was not referenced by Smith et al. (1982). However, a map in the paper indicated that the Imperial fault was located 5 km (3.1 miles) from the first recording station (at 0 meters). For the Imperial Valley earthquake

the recording station at 304.9 m (1000 ft) did not trigger (reasons were not given). In the correlation analysis, a set of normalized covariance functions were calculated for all possible pairs of recording stations to examine the nature of the motion recorded on the differential array. The covariance function measures the "fraction of the power in the seismic signal that can be attributed to a single nondispersive propagating wave". (Smith et al., 1982, p. 248). The degree of correlation between pairs of stations and velocity at which the propagating wave moves across the array were obtained from the covariance functions of the accelerations. The normalized covariance functions for the P-wave group demonstrated that about 95 percent of the power is in the form of a single propagating wave across the array to about 50 m (164 ft), but the power drops rapidly to about 75 percent at 85 m (279 ft). Across the entire triggered array, a distance of 213 m (700 ft), the normalized covariance is about 60 percent. The amount of power or energy uncorrelated between stations appeared to be related to scattering. Scattering is caused by the interaction of seismic waves with the inhomogeneities present in the material properties of the geologic medium.

The same type of measurable variability was observed at a small-aperture seismic array at Pinyon Flat, California

where eight local earthquakes were recorded (Vernon et al., 1991). The array consisted of nine recording stations set up in three nested equilateral triangles. Three stations were located 300 m (984 ft) from the center point at angles of 0, 120, and 240 degrees. The middle triangle of stations were located at a distance of 100 m (328 ft) from the center point at 60, 180, and 300 degrees. The inner triangle stations were located 30 m (98.4 ft) from the center point at 30, 150, and 270 degree angles. Pinyon Flat was selected because of its homogeneous geology (granite) and its planar topography. If the geology were truly homogeneous, the waves would propagate effectively as a plane across the array. However, this did not occur. There was measurable variability in the power spectra and the waveform coherence was low when the station spacing was greater than 300 m (984 ft) for wavelengths shorter than 300-400 m (984-1312 ft). Coherence is a measure of the correlation between two processes as a function of wavelength.

Characterizing spatial variability is also of great importance to groundwater pollution problems. The complexity of groundwater systems, physical and chemical properties of the subsurface materials that affect solute transport, is being analyzed as spatially random fields.

Sudicky (1986) examined the spatial variability of hydraulic conductivity at a site where a long term tracer test was performed in the Borden aquifer. Permeability measurements were obtained from a series of core samples taken along two cross sections at the Borden tracer test site. The samples revealed that the aquifer was comprised of numerous thin, discontinuous lenses of contrasting hydraulic conductivity. An exponential autocorrelation function was used to obtain a statistical model which would represent the aquifer. The exponential model with a vertical correlation distance of 0.12 m (0.4 ft), and horizontal correlation distance of 2.8 m (9.2 ft) closely approximated the estimated autocorrelation functions. The statistical description of the Borden aquifer was used to determine the dispersion of the injected tracer, and then compared to the dispersion rates observed during the long-term tracer test. Because the results were consistent, Sudicky believes that a statistical understanding of random hydraulic parameters will provide meaningful estimates of transport parameters in other aquifers.

Correlation functions were used by Frankel and Clayton (1986) to study the scattering of elastic and acoustic waves in two-dimensional media with random spatial variations in seismic velocity. The paper was concerned

with variations in seismic velocity in the earth's crust with scale lengths (correlation distances) ranging from tens of kilometers down to tens of meters. The scattering model consisted of a random velocity perturbation applied to a homogeneous velocity field. The perturbation fields (also called random media in the paper) were characterized by a correlation function, correlation distance, and standard deviation. The Gaussian, exponential, and Von Karman correlation functions were used to construct the random media.

The method used by Frankel and Clayton to construct the random media is of great importance to this study because a similar procedure was utilized. The procedure used to construct the random media on a two-dimensional grid was outlined in the paper as follows: "First, a random number generator assigned a velocity $v(x,z)$ sequentially to each point of the grid. The random velocity field was then Fourier transformed to wave number space, filtered to achieve the desired spectrum, and transformed back to the spatial domain to yield the velocity field for the simulations" (Frankel and Clayton, 1986, p. 6469). The results from the simulations were then compared to actual observations to constrain models of the crustal heterogeneity. The results demonstrated that the Gaussian,

exponential, and Von Karman random media with correlation distances greater than 10 km (6.2 miles) produce correlation functions similar to the actual observations.

This literature review concentrated on the usage of correlation analyses in various disciplines. The correlation analysis was used to characterize the spatial variation in strong ground motions, examine the spatial variability of hydraulic conductivity, and study the scattering of elastic and acoustic waves in media with random spatial variations in seismic velocity.

1.4 Objectives of Study

To achieve the goal, the specific objectives of this study were to do the following:

1. Develop a one-dimensional random geology generator to generate the random geologic variability profiles to be used in finite difference calculations.
2. Modify a ground shock finite difference code to incorporate the random geologic variability factors. The factors will be used to perturb the average soil material properties to generate random geologic material property profiles that represent the

inhomogeneities present in the subsurface material.

3. Perform linear elastic calculations using the modified code.

4. Compare the results of the calculations with closed form solutions and with experimental data.

1.5 Specifics of This Study

This research is unique within the explosive effects community in the following ways. First, stochastic techniques are used to produce spatial perturbations in the material model. These perturbations simulate the subsurface heterogeneities. Existing solutions for plane wave propagation in a heterogeneous material have been obtained by using probabilistic techniques (Rohani, 1982), which do not incorporate the concept of spatial variability. Second, the spatial random geologic variability factors are directly incorporated into the AFTON-1D finite difference ground shock code which has not been done previously (Trulio, 1966).

1.6 Organization of Thesis

The organization of this thesis is as follows: chapter 1 is the Introduction which states the problem, goal, review of literature, and objectives. Chapter 2 is Theory and Methodology. The topics covered in chapter 2 are autocorrelation functions, random geology generator, theoretical and computed autocorrelations, AFTON-1D finite difference code, and code modifications and calculations. The results and analysis are presented in chapter 3. In chapter 4, conclusions are drawn based on the results from the various calculations and recommendations are given for future work in this area.

Chapter 2

THEORY AND METHODOLOGY

2.1 Autocorrelation Function

Random or stochastic processes are commonly characterized through autocorrelation functions or spectral density functions. The spectral density function is simply the Fourier transform of the autocorrelation function of a random process.

The autocorrelation function is defined as a measure of the degree of linear relationships between neighboring values in a random process (Bendat and Piersol, 1971). The general autocorrelation function is defined as

$$R_{xx}(t, t+\tau) = \frac{1}{N} \sum_{k=1}^{N} x_k(t) x_k(t+\tau) \qquad (2.1)$$

N = number of samples

where, R_{xx} = autocorrelation function of $x_k(t)$

t = reference point

τ = spatial separation

The quantity R_{xx} is always a real-valued even function with

a maximum at $\tau=0$, and may be either positive or negative. In terms of the autocorrelation function, the mean value of x(t) is given by

$$\mu_x = \sqrt{R_{xx}(\infty)} \tag{2.2}$$

Another form of the autocorrelation function is the normalized autocorrelation function (correlation coefficient)

$$R_{xx}(t, t+\tau) = \frac{\frac{1}{N}\sum_{k=1}^{N} x_k(t)\, x_k(t+\tau)}{\sqrt{Var\ x_k(t)\ Var\ x_k(t+\tau)}} \tag{2.3}$$

$$-1 \leq R_{xx}(\tau) \leq 1 \tag{2.4}$$

When the autocorrelation function is at a peak, the random process has a high degree of linear correlation with itself at t and $t+\tau$. When the autocorrelation function is near zero, the random process is uncorrelated with itself at t and $t+\tau$.

The autocorrelation function is used in many disciplines, which include geotechnical engineering, statistics, geophysics, and hydrology. The autocorrelation function is commonly referred to as simply the correlation function in

the literature. Throughout this paper, the terms autocorrelation and correlation will be used interchangeably.

The most common autocorrelation functions used to characterize random geologic variability in the seismological and hydrological communities are the Gaussian, exponential, and von Karman functions (Frankel and Clayton, 1986; Sudicky, 1986). The correlation function and corresponding 1-D power spectra equations are shown in Table 1. The correlation functions in Table 1 are theoretical equations for a Gaussian, exponential, and von Karman distribution, respectively, and are always positive.

The data set from McCormick Ranch used to statistically characterize the subsurface heterogeneity suggests that the exponential and Gaussian correlation functions are most appropriate for describing the spatial variability. Therefore, this study has focussed on the Gaussian and exponential correlation functions to define the subsurface heterogeneities. The correlation functions and 1-D power spectra are plotted in Figure 3. The 1-D power spectra plots were generated with a correlation distance (a) of 50 cm.

For Gaussian and exponential correlation functions shown in Table 1, the correlation distance (a) marks the lag (r) where the correlation function has the value of e^{-1}. Therefore, when r=a the normalized lag (r/a) is equal to R_{xx}=0.37 as shown in Figure 3.

Table 1. Correlation functions and 1-D power spectra equations.

	Correlation Function	1-D Power Spectra
GAUSSIAN	e^{-r^2/a^2}	$a\sqrt{\pi}e^{-k^2a^2/4}$
EXPONENTIAL	$e^{-r/a}$	$\frac{2a}{1+k^2a^2}$
von KARMAN	$K_0(r/a)$	$\frac{a}{(1+k^2a^2)^{1/2}}$

where,

r = offset (or spatial lag)

a = correlation distance

k = wave number, $k=2\pi/\lambda$, where λ is wavelength

K_0 = Bessel function

e = exponential function

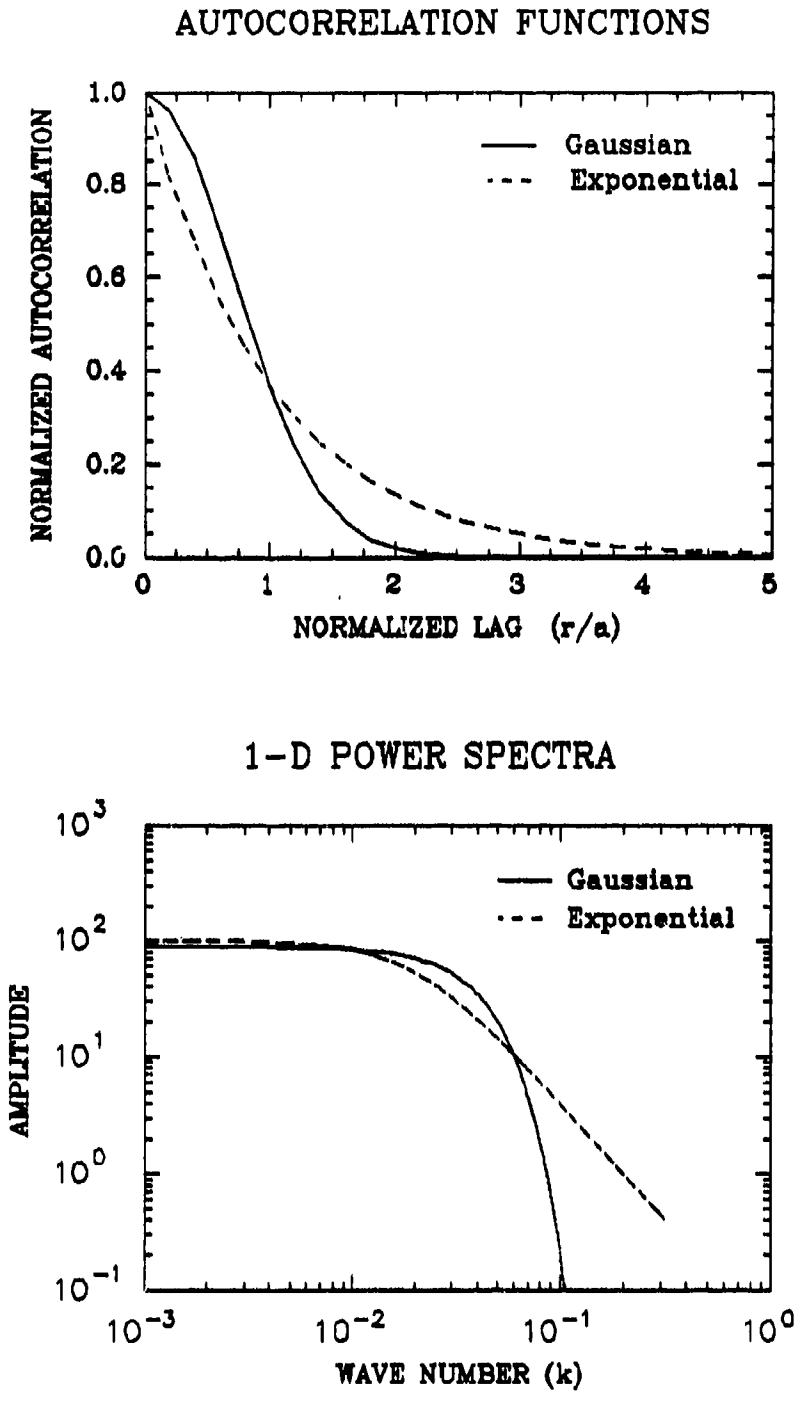

Figure 3. Gaussian and Exponential theoretical autocorrelation functions and 1-D power spectra.

2.2 Random Geology Generator

A technique was developed to construct spatially random geologic variability factors which would be incorporated into the AFTON-1D finite difference code (Trulio, 1966) to simulate the subsurface inhomogeneities. The technique has been named the random geology generator. The procedure used to develop the random geology generator is as follows.

1. First, the desired correlation function, f, is constructed in the wave number domain using the equations (1-D power spectrum) in Table 1.

2. Next, a random sequence, y_i, is generated using a random number generator (discussed later in this chapter). This random sequence is then transformed to the wave number domain by means of a fast Fourier transform.

3. A random phase term, θ, is obtained by $\theta = \tan^{-1}[imag(Y(k))/real(Y(k))]$, where Y(k) is the Fourier transform of the sequence y_i. θ is known as the phase angle of the Fourier transform, and *imag* and *real* stand for the imaginary and real part of the

Fourier transform, respectively.

4. Since a complex number (x+iy) can be written as

$$x + iy = \sqrt{x^2 + y^2}\, e^{i(\tan^{-1}(\frac{y}{x}))} \qquad (2.5)$$

the random sequence is written as

$$X(k) = \sqrt{f}\, e^{i\theta} \qquad (2.6)$$

where X(k) is a random sequence in the wave number domain having the desired correlation function (f). Transforming X(k) back to the space domain yields x_i, which is a random sequence in space.

5. The random sequence is then standardized to a specific mean and standard deviation. The transforming equation is

$$\left(\frac{x_i - \mu_x}{\sigma_x}\right)\sigma_d + \mu_d = x_n \qquad (2.7)$$

where μ_x and σ_x are the mean and standard deviation of the random sequence x_i, μ_d and σ_d are the desired mean and standard deviation, and x_n is the sequence of random geologic variability factors.

The program to generate the random geologic variability

factors is listed in Appendix A. The input parameters needed to run the program are 1) the desired correlation function (Gaussian or exponential), 2) number of random variables to be generated, 3) the desired mean and standard deviation, 4) correlation distance, and 5) a seed for the random number generator. The correlation distance in the program is defined in terms of the number of sample intervals.

2.2.1 Correlation Distance

The correlation distance is a stochastic parameter used to measure the size of variations in a data set. The correlation distance is defined as a measure of the separation distance where two measurements are essentially independent of each other.

The correlation distance used in this study is based on work done by Jewell (1988). A cone penetrometer data set from the McCormick Ranch test site on Kirtland AFB composed of alluvium was analyzed for stochastic and statistical properties. Various autocorrelation functions were used to determine the spatial variability in the subsurface properties. Correlation distances of 30-50 cm provided a

good fit between the model and data. For this study, two correlation distances of 30 and 50 cm were investigated.

2.2.2 Random Variability Factors

The Gaussian and exponential functions were used to generate the random variability factors. The variability factors are used to perturb the average soil material model to generate random geologic material property profiles that represent the inhomogeneities in the subsurface material in the ground shock code. Since the grid in the ground shock code has a limit of 500 cells or zones and the number of variability factors generated must equal 2^n for the random geology generator, n was chosen to be 9. Therefore, 512 variability factors were generated.

Figure 4 shows the variability factors constructed with the Gaussian function. The variability factors constructed with the exponential function are shown in Figure 5. The profiles shown in Figures 4 and 5 represent the subsurface heterogeneities with depth. The variability factor profiles were computed with different zone sizes. Therefore, in order to compare the profiles directly, the

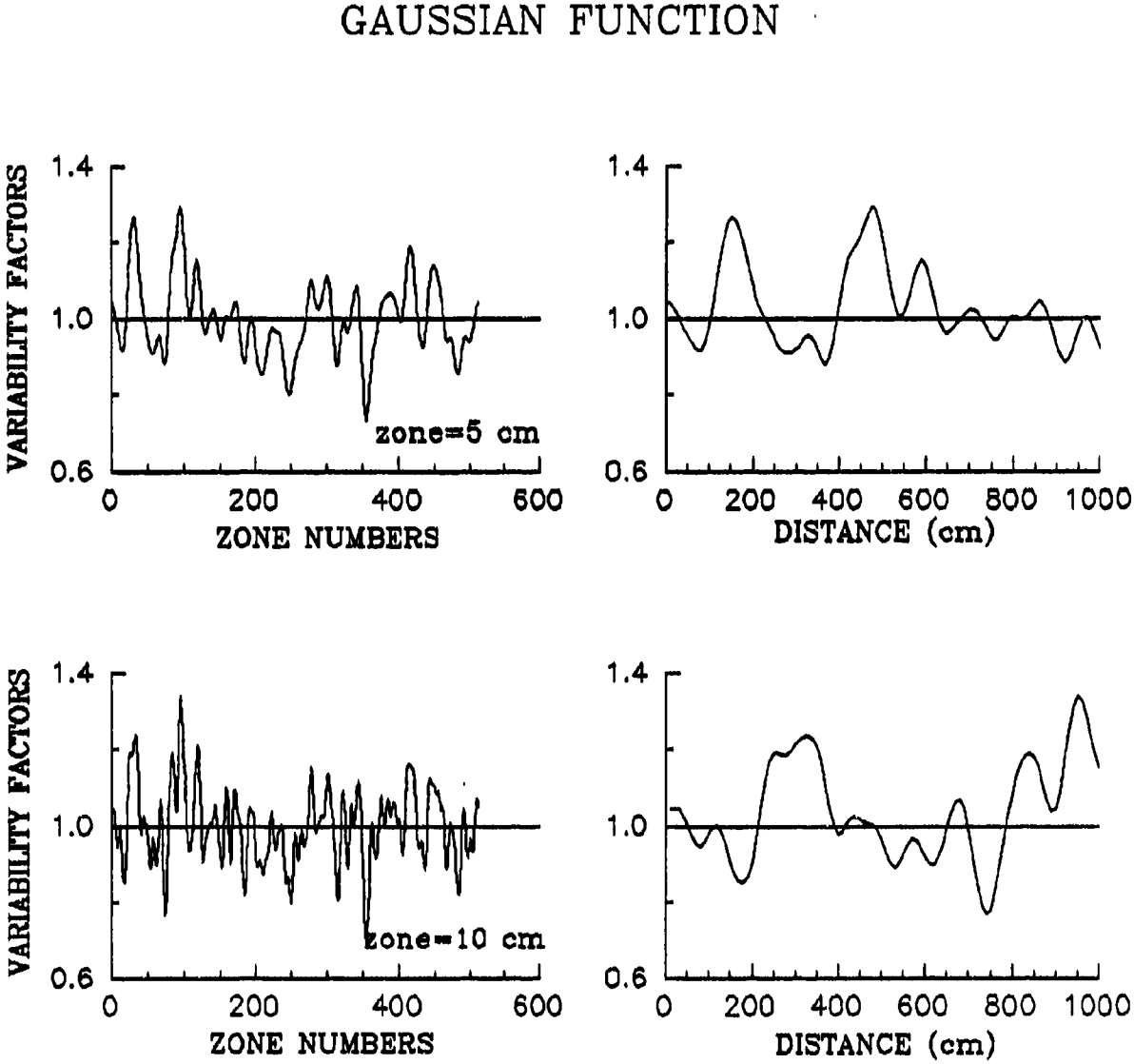

Figure 4. Variability factor profiles for the Gaussian function at different zone sizes, and with respect to normalized distance.

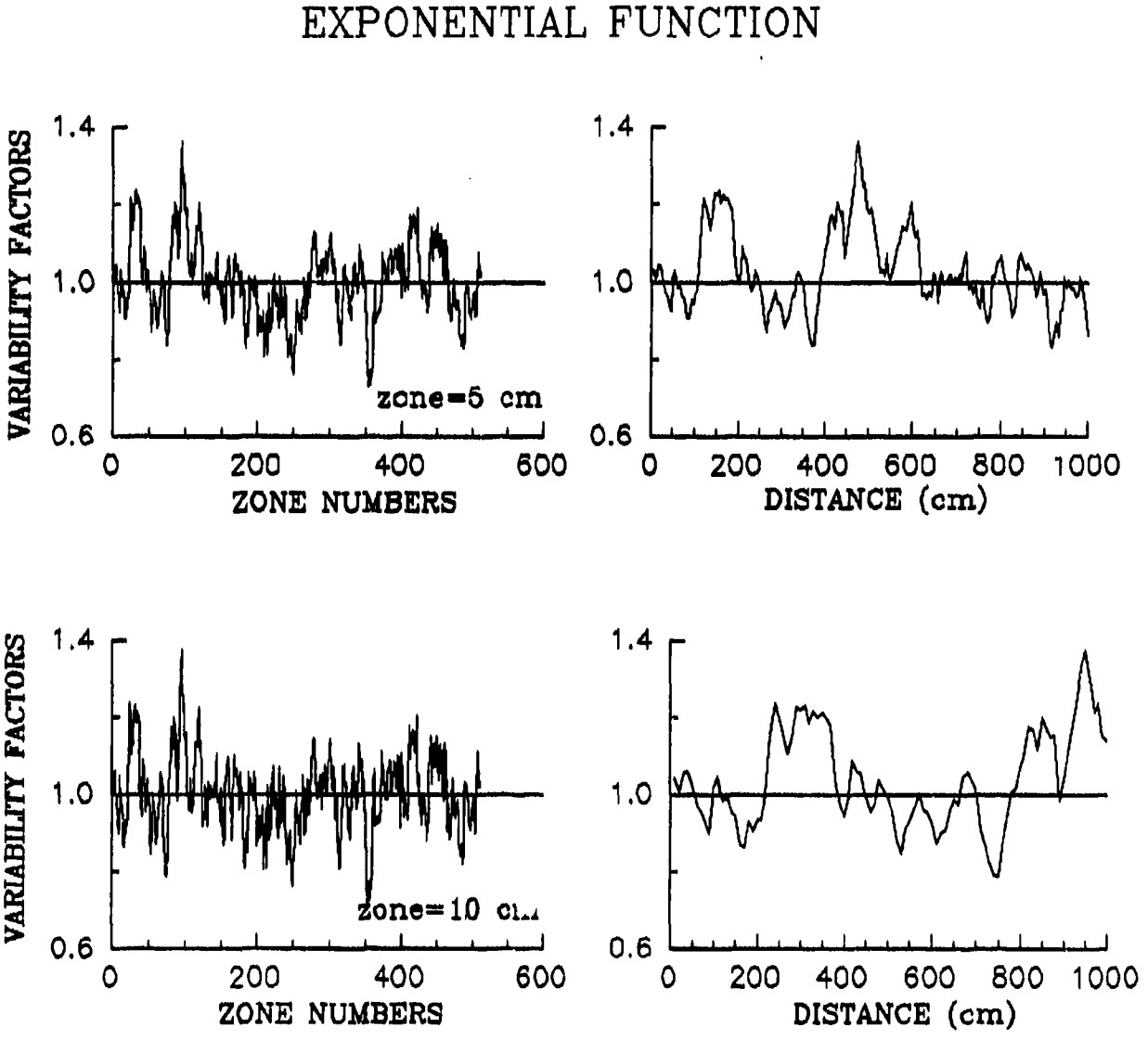

Figure 5. Variability factor profiles for the Exponential function at different zone sizes, and with respect to normalized distance.

variability factors are shown with respect to the normalized distance in the figures. The same input parameters were used to generate the different profiles. When these generated profiles are compared with the cone data profiles in Figure 1, they appear quite realistic (see Figure 6).

The variability factors from the exponential function show more high frequency roughness or noise than those from the Gaussian function. The roughness is due to the fall off rate in the spectral amplitude between the two correlations (see Figure 3). Both spectra are flat out to a specific wave number (k), but at higher wave numbers the exponential falls off at $k^{-(N+1)}$, where N is the number of space dimensions (Fisk et al., 1991). The amount of roughness in the profile is controlled by the fall off rate of the spectra. The spectrum with more energy at higher wave numbers shows more roughness in the generated variability profiles.

2.2.3 Random Number Generator

The random number generator from the MATLAB software

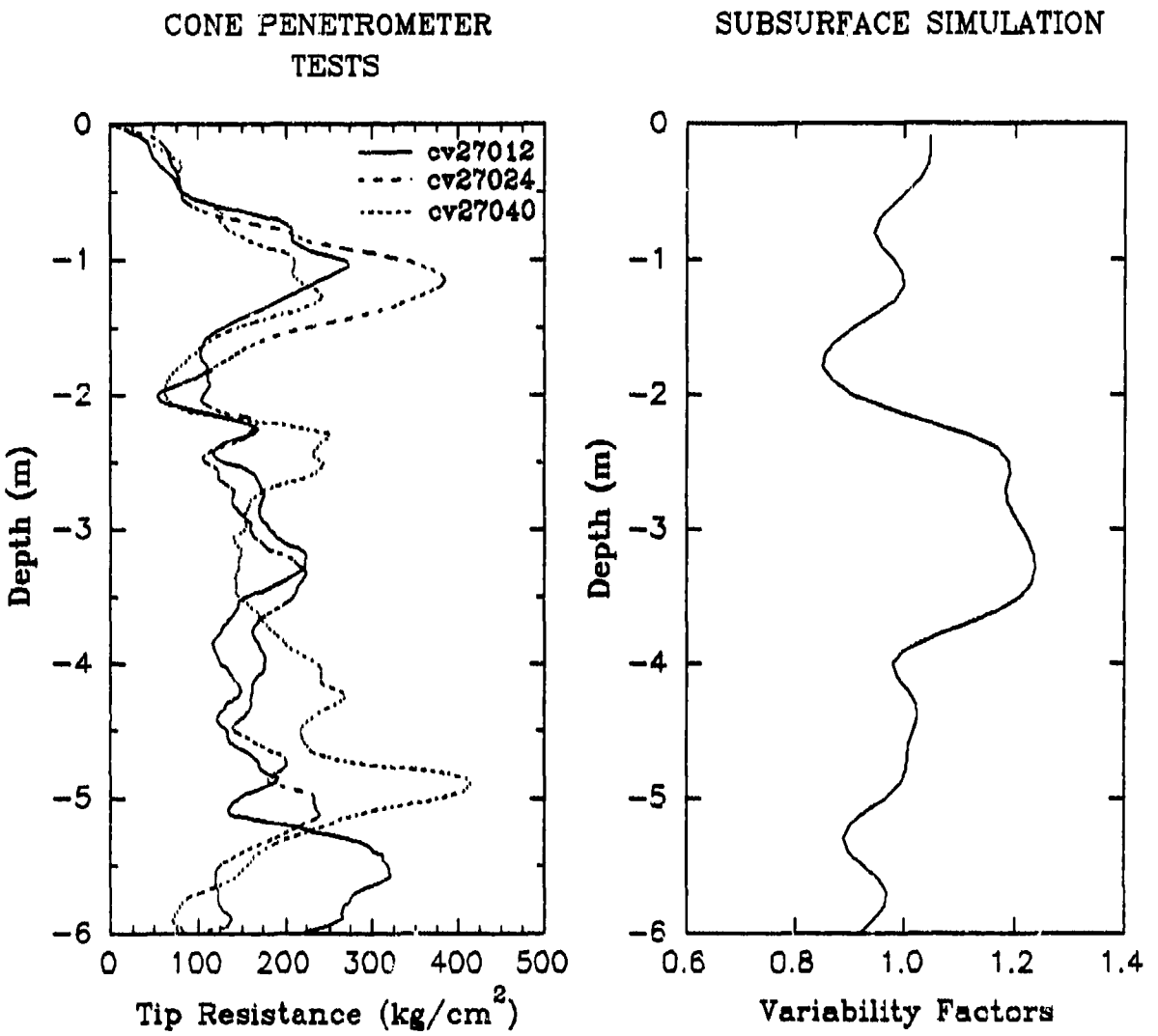

Figure 6. Comparison between cone penetrometer tests and generated subsurface variability simulations.

package (PC-MATLAB, 1989) was utilized in this research (in Section 2.2). MATLAB is a high-performance interactive software package used for scientific and engineering numerical computations. MATLAB provides an easy-to-use environment where problems and solutions are expressed almost exactly as they are written mathematically. A specific programming language is not required. Typical uses for MATLAB are general purpose numerical computations, algorithm prototyping, and solving problems with matrix formulations that arise in disciplines such as automatic control theory, statistics, and digital signal processing.

The MATLAB function RAND is a uniform random number generator based on linear congruential methods. The algorithm for this random number generator was proposed by D. H. Lehmer (1951). The algorithm involves the choice of two fixed integer parameters

(i) modulus: m - a large prime integer

(ii) multiplier: a - an integer in the range 2, 3,....,m - 1

and the generation of the integer sequence $Z_1, Z_2, Z_3, \ldots, Z_{m-1}$ is defined by the recursive formula

(iii) $Z_i = (aZ_{i-1}) \pmod{m}$ for $i = 1, 2, \ldots$

where Z_0 is the seed or starting value. To obtain the desired random numbers, U_i on (0,1), the sequence of Z's is normalized by

$$\text{(iv)} \quad U_i = Z_i/m \qquad \text{for } i = 1, 2, \ldots$$

The values of a and m must be selected in the manner that the function, f(Z), is a full period generating function, and the full period sequence, $Z_1, Z_2, \ldots, Z_{m-1}$, is random. The modulus $m = 2^{31} - 1$ was suggested by Lehmer (1951). The multiplier $a = 7^5 = 16807$ was suggested by Lewis, Goodman and Miller (1969), based on the fact that

$$f(Z) = 16807Z \bmod 2147483647 \qquad (2.5)$$

is a full period generating function. This function has also demonstrated evidence of randomness through various tests (Lehmer, 1951).

Random number generators can be subjected to empirical and theoretical tests to determine how well the generated U_i's resemble values of a true independent and identically distributed (IID) random variable. In addition to the statistical tests conducted in by Lehmer (1951), the chi-square (empirical) test of uniformity was applied to equation (2.5) in this study. The results from the chi-square test indicate the U_i's generated do not behave in a

way which is significantly different from what would be expected from truly independent identically distributed random variables. The computations and results from the chi-square test are included in Appendix B.

2.3 Theoretical and Computed Autocorrelations

The Gaussian and exponential correlation functions were used to generate the random geologic variability factors. The random factors are applied to the homogeneous soil material model to develop synthetic heterogeneous soil profiles. In order to determine the validity of the random geology generator, the autocorrelations of the variability factors were compared to the theoretical autocorrelations. The theoretical autocorrelation functions shown in Table 1 were developed based on integral Fourier transform theory from $-\infty$ to $+\infty$ over space. In order to construct a numerical realization (random geologic variability factors), a discrete process was used. The integral is no longer from $-\infty$ to $+\infty$, but rather from 0 to 512. Therefore, the adequacy of the computed autocorrelations obtained from the discrete, limited realizations was compared to the theoretical autocorrelations.

Figure 7 shows the theoretical and computed auto-correlations for the Gaussian and exponential functions, respectively, for a correlation distance of 50 cm. Figure 8 shows the autocorrelations for a correlation distance of 30 cm. The characteristics associated with the random factors in Figures 7 and 8 are a mean of 1, a standard deviation of 10 percent, and zone size of 10 cm. The random number generator seed was set at 100.

The comparison between the theoretical and computed autocorrelations in both cases was extremely good. Therefore, one would conclude that the random geology generator constructing the discrete, limited realizations is working correctly.

2.4 1-D Finite Difference Code

The AFTON 1-D (one dimensional) finite difference code was used in this study. The AFTON 1-D code is a finite difference ground shock code designed to solve problems in the field of dynamic continuum mechanics (Schuster el at., 1984). AFTON 1-D may be used in any of the three 1-D symmetric modes; plane, cylindrical or spherical. Figure 9 shows the three symmetric modes. The only direction of

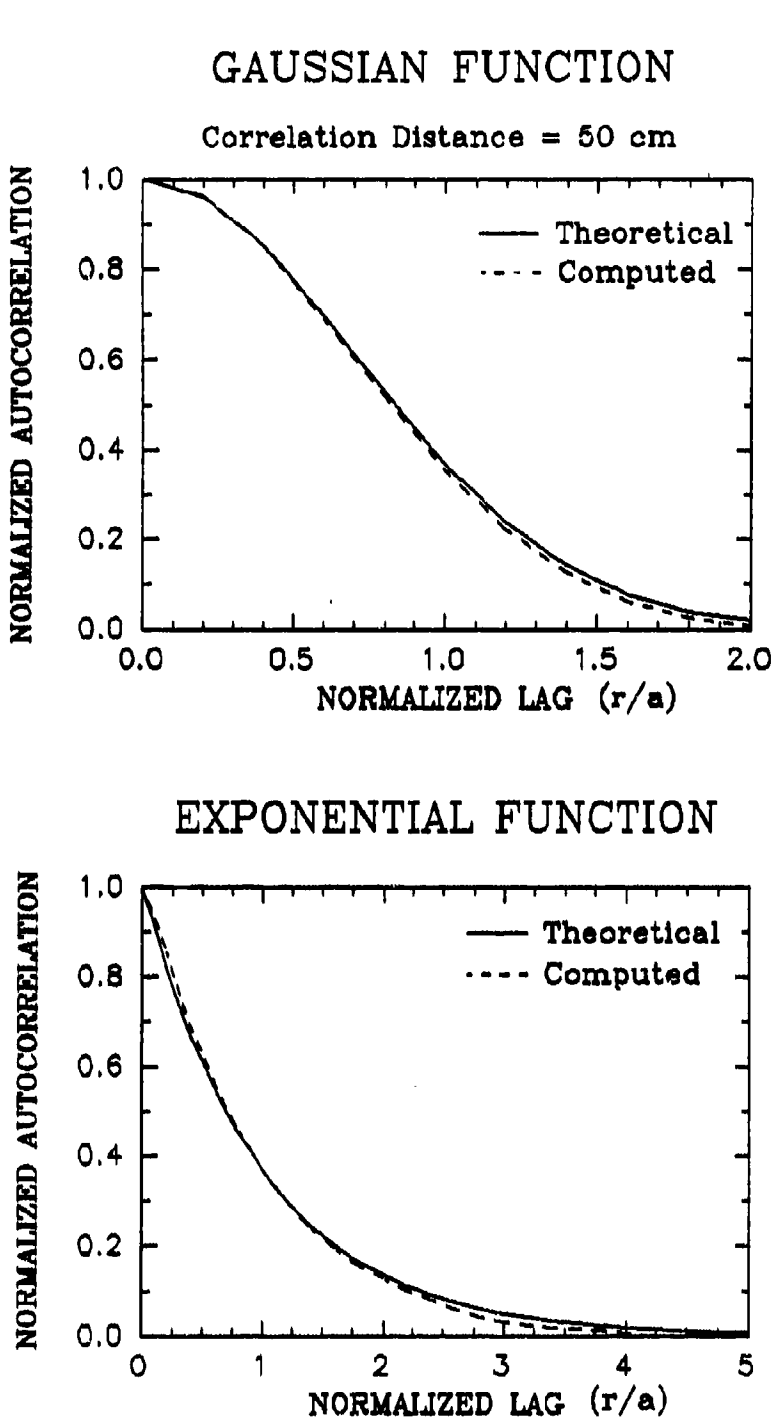

Figure 7. Theoretical and computed autocorrelations for the Gaussian and Exponential functions for a correlation distance of 50 cm.

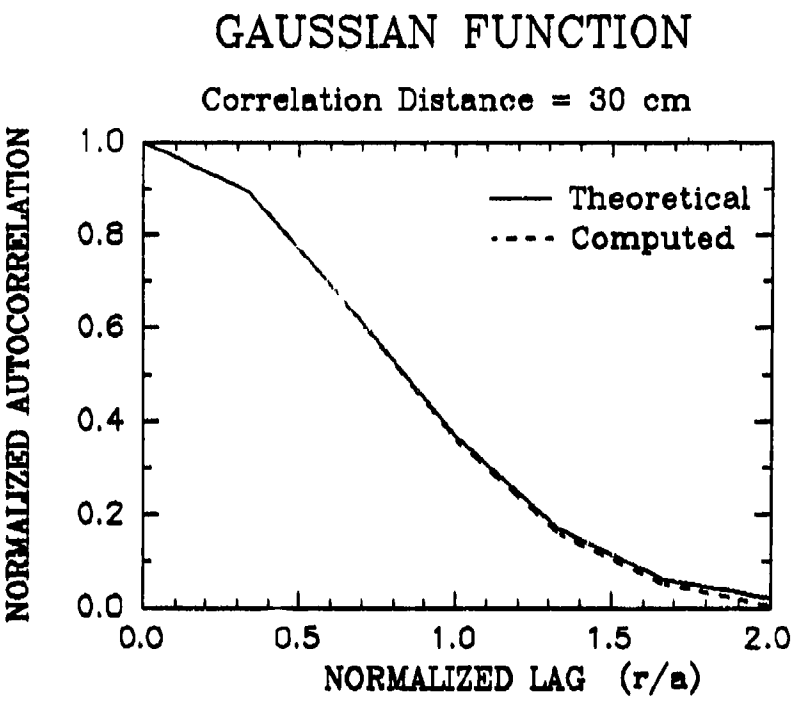

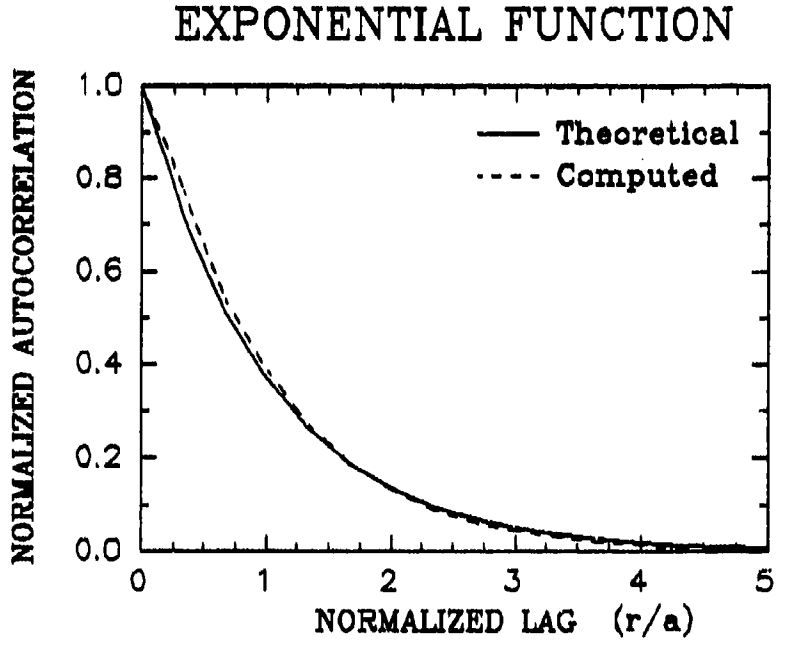

Figure 8. Theoretical and computed autocorrelations for the Gaussian and Exponential functions for a correlation distance of 30 cm.

Plane: $d\varepsilon_x = \frac{d\Delta x}{\Delta x}$; $d\varepsilon_y = d\varepsilon_z = 0.$

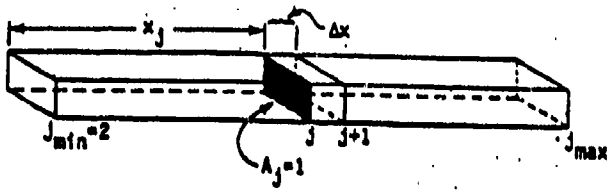

Cylinder: $d\varepsilon_x = \frac{d\Delta x}{\Delta x}$; $d\varepsilon_y = \frac{dx}{x}$; $d\varepsilon_z = 0$

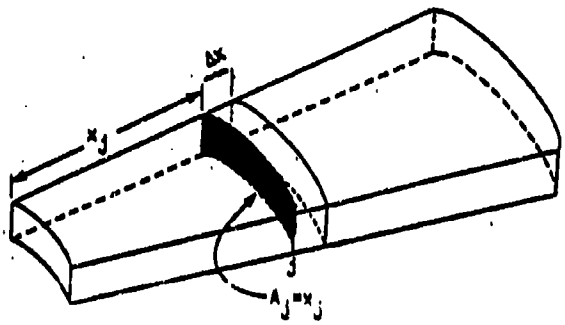

Sphere: $d\varepsilon_x = \frac{d\Delta x}{\Delta x}$; $d\varepsilon_y = d\varepsilon_z = \frac{dx}{x}$

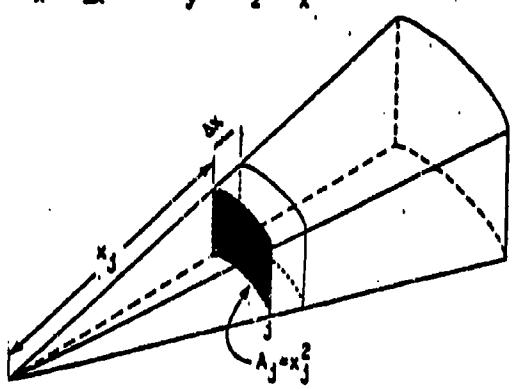

where, ε = *strain*
j = *number of zones*
x_j = *distance to zone*
Δx = *zone size*

Figure 9. Three 1-D symmetric modes for the AFTON-1D code. (From Schuster et al., 1984)

motion allowed in the three modes is that perpendicular to the shaded area (A_j) in the figure. The media are divided into discrete cells, identified by J, and the code cycles through the equation of motion for all active J's using the output of the previous cycle to advance each timestep. The state of stress in each cell or zone was calculated by a linear elastic model. The parameters that define the linear elastic model are material density (ρ = 1643 kg/m^3), compressional wave velocity (c = 508 m/s), and Poisson's ratio (ν = 0.25).

This code was used to perform homogeneous and random calculations in the spherical mode with a pressure step function (p = 1 MPa) applied at the grid boundary (spherical cavity wall) to simulate ground shock propagating through the grid from an explosive source. A zone size of 10 cm was used throughout the grid.

2.4.1 Validation of Calculational Technique

As a check on the validity of the calculational technique, the homogeneous finite difference calculations were compared to a closed form solution of wave motion

developed by Sharpe (1942). Sharpe states the problem as follows: "Given a spherical cavity of radius *a* within a homogeneous, ideally elastic, infinite medium of density ρ and compressional wave velocity *c*; to find the elastic wave motion which results from application of an arbitrary pressure *P(t)* to the interior surface of the cavity" (Sharpe, 1942, p. 146). The problem is illustrated in Figure 10.

The primary reason for the waveform comparisons between the homogeneous finite difference and closed form calculations was to validate both the parameter setup of the code, as well as the geometric setup of the finite difference grid.

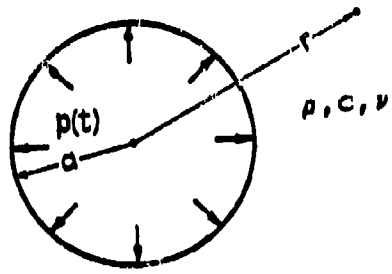

Figure 10. Illustration of the idealized model. (From Sharpe, 1942, p. 146)

A computer program was written for Sharpe's closed form solution and is included in Appendix C along with the equation derivations. The program was written to generate velocity and displacement time histories at several distances from the center of the cavity.

Comparisons between the closed form solution and the AFTON calculations are shown in Figures 11 through 13 at arbitrary ranges of 200, 500, and 900 cm from the cavity center, respectively. The vertical scales in the figures vary to show the maximum velocities and displacements at the different ranges. Also shown in Figures 11 through 13 are the time histories generated with different zone sizes. In order to check the influence of frequency and boundary effects on the calculations due to the zone size, several zone sizes were compared. The homogeneous calculations were performed with 2, 5, 10, and 20 cm zone sizes.

The velocity and displacement waveforms from the closed form solution and AFTON calculations are similar. The waveform agreement increased as the distance from the cavity wall also increased. The reason for the agreement is explained by the simplified displacement equation used by Sharpe (1942). The simplified equation is adequate for displacements at distances more than a few times the radius

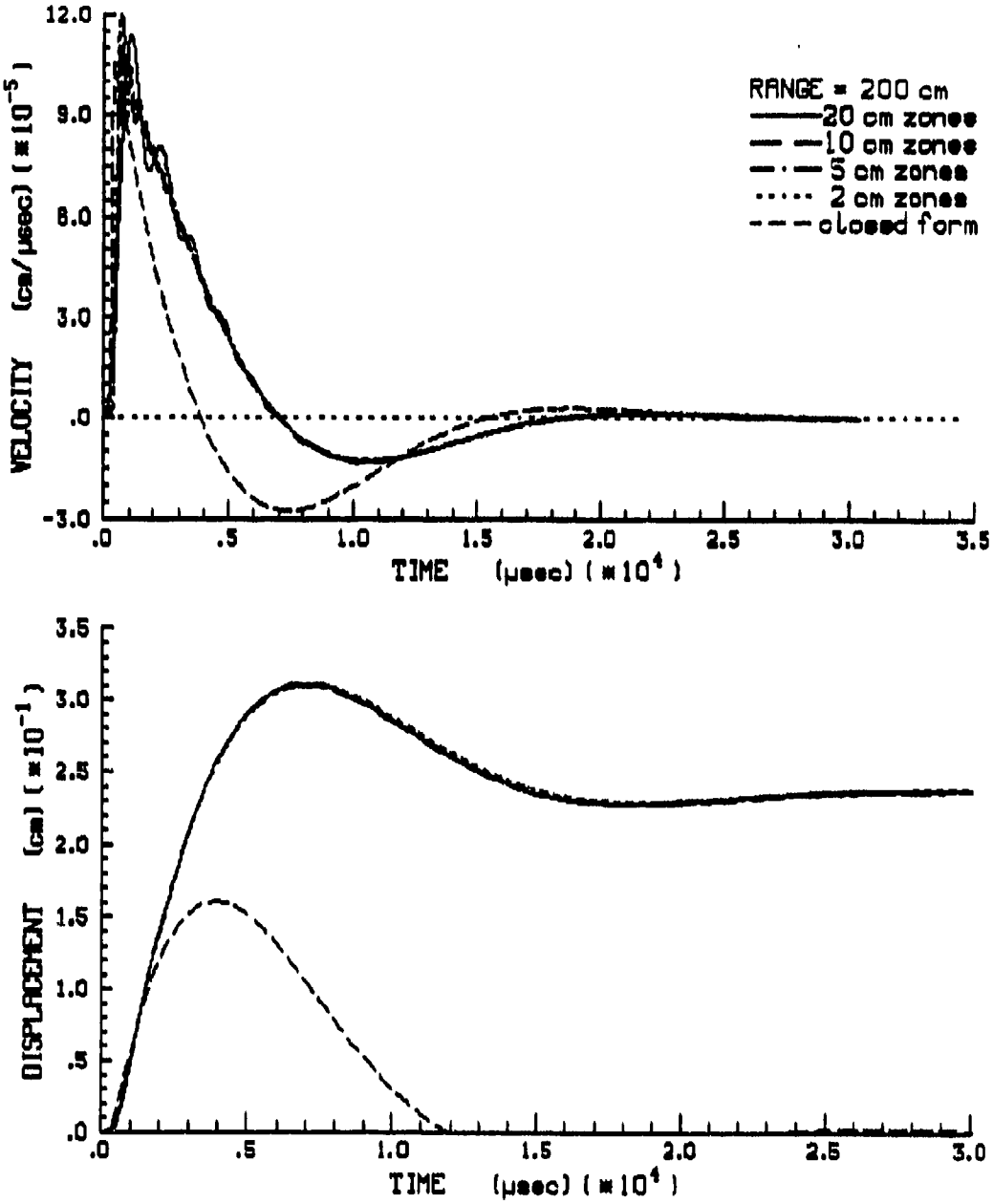

Figure 11. Comparisons between the closed form solution and AFTON-1D calculations for 2, 5, 10, and 20 cm zones at 200 cm from the cavity center.

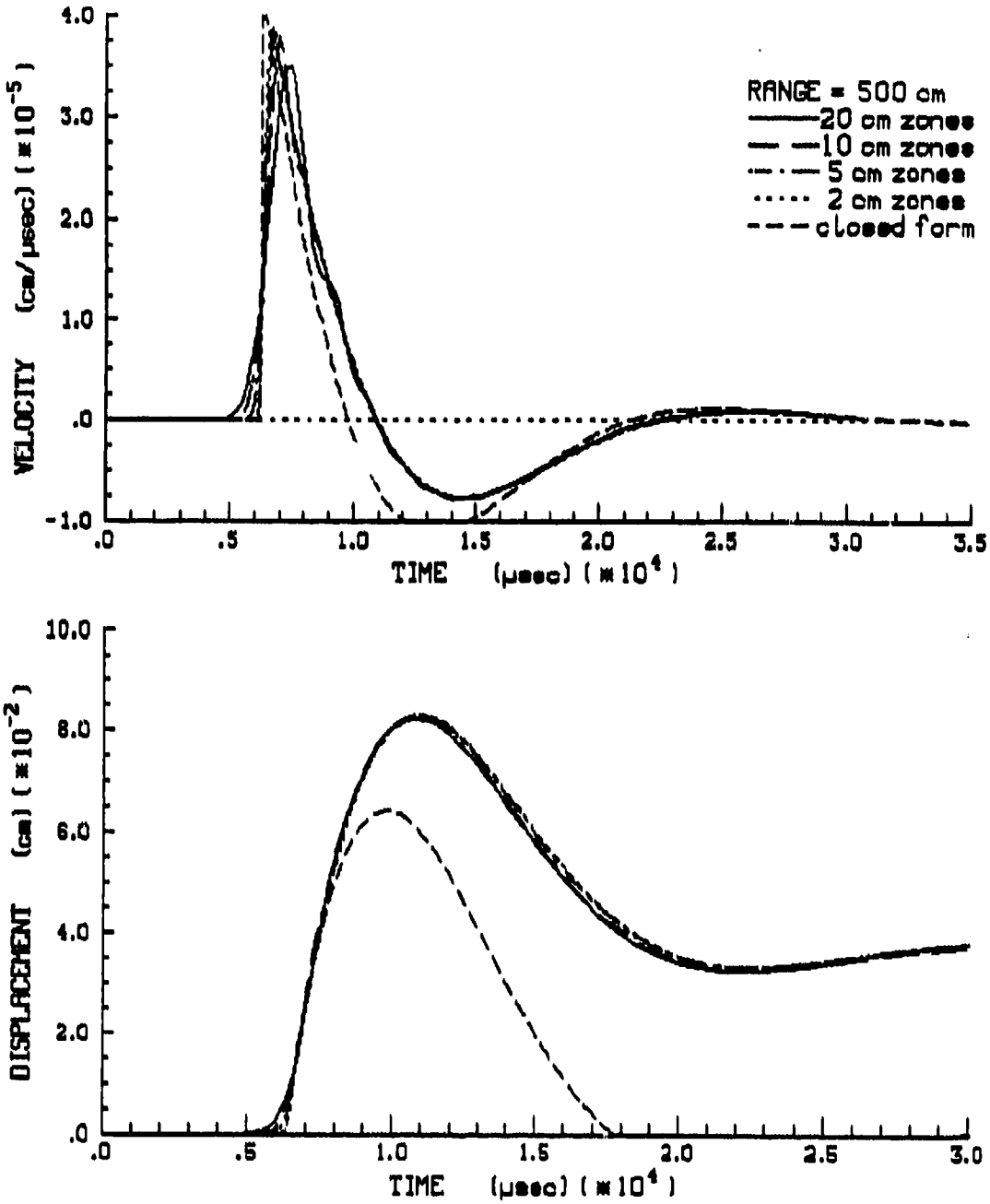

Figure 12. Comparisons between the closed form solution and AFTON-1D calculations for 2, 5, 10, and 20 cm zones at 500 cm from the cavity center.

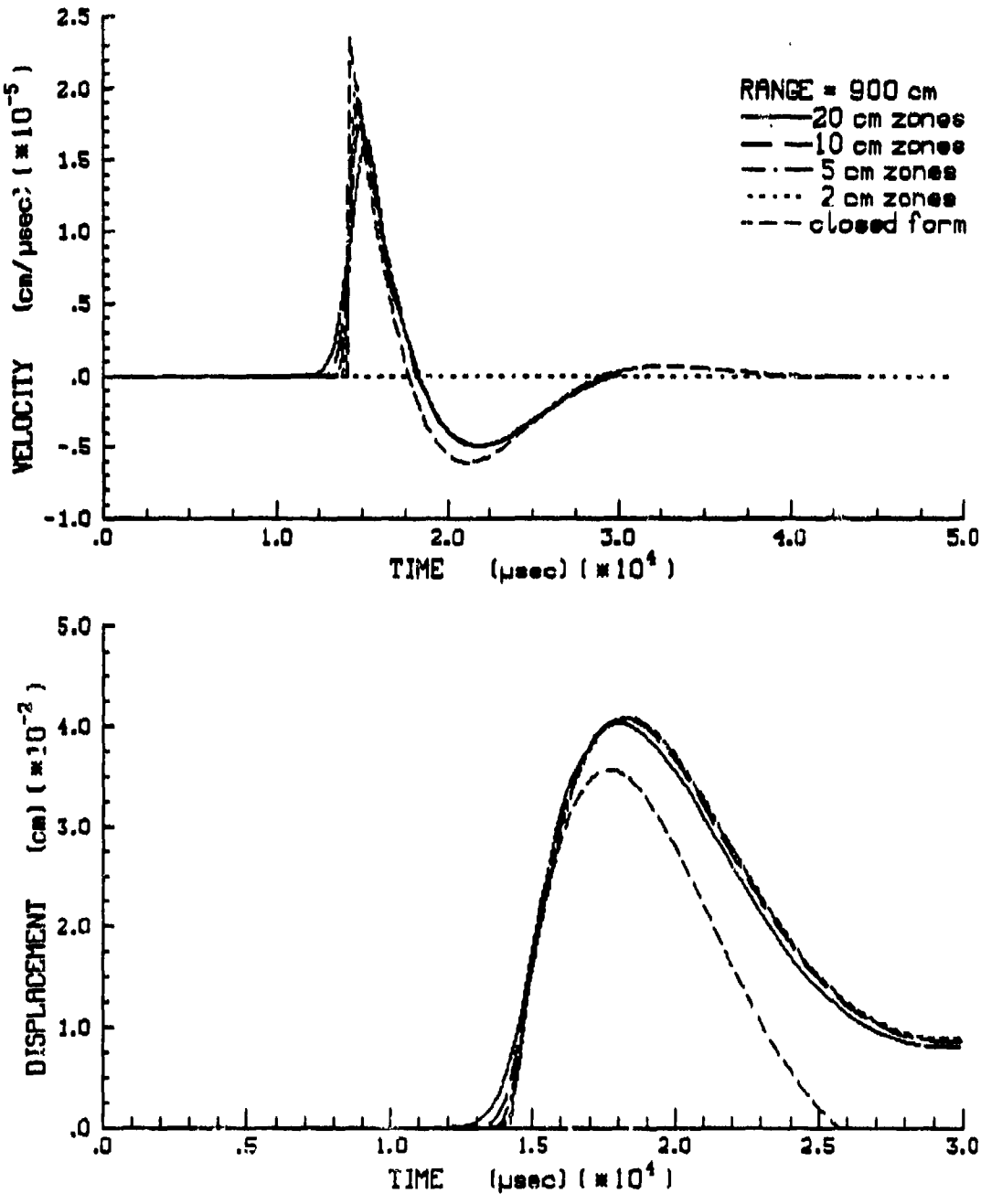

Figure 13. Comparisons between the closed form solution and AFTON-1D calculations for 2, 5, 10, and 20 cm zones at 900 cm from the cavity center.

of the cavity. The cavity radius for the calculations was set at 175 cm. Based on the agreement between the closed form solution and AFTON calculations, one would conclude the parameter setup used in the code is adequate.

As shown in Figures 11 through 13, the difference in zone size, between the 2, 5, and 10 cm zones, in the finite difference grid was not significant. However, numerical noise was present in the 20 cm zone calculation, and the velocity peak values were lower. Therefore, a zone size greater than 10 cm would not be recommended. Based on these comparisons, the geometric setup of 10 cm zones for the homogeneous and random calculations was used throughout this study.

2.5 AFTON 1-D Code Modifications

In order to determine the influence of spatial geologic variability on ground motion, the AFTON 1-D finite difference code was modified to incorporate the random geologic variability factors. The variability factors were assigned to each zone or cell on the grid. They were then used to perturb the average soil material properties to represent the inhomogeneities in the subsurface material.

The AFTON 1-D code consists of 53 subroutines which include functions for initializing constants, setting up the problem, adding new cells as the problem progresses, setting the new timestep, and storing output data. The subroutine of interest for this study was SUBROUTINE ESINIT. The parameters from the linear elastic model are read in at this subroutine and assigned to the zones. This subroutine was modified so that the set of variability factors could be read in to the material model and applied to the parameters in each zone. Since only a linear elastic material model is being explored in this study, the material parameters perturbed by the variability factors are density, Poisson's ratio, and seismic wave speed. The material parameters were assigned to 500 zones and then varied by 500 variability factors composing a Gaussian or exponential distribution.

Chapter 3

RESULTS AND ANALYSIS

3.1 Random Calculations

The random calculations were generated with the modified AFTON 1-D finite difference code. In the first phase of the analysis, the statistical properties of the variability factors were varied to examine the effects on the computed output, velocity and displacement time histories. Correlation distances of 30 and 50 cm were compared, and the standard deviation in the variability factors varied from 0 to 20 percent.

3.1.1 Correlation Distance Comparisons

The variability factors used in the random calculations to compare the difference in correlation distance were generated with an arbitrary standard deviation of 10 percent, and initial seed of 100. The correlation distances of 30 and 50 cm are compared in Figures 14 through 17. The waveforms in Figures 14 through 17 correspond to ranges of 200, 500, 900, and 2000 cm from the center of the cavity, respectively.

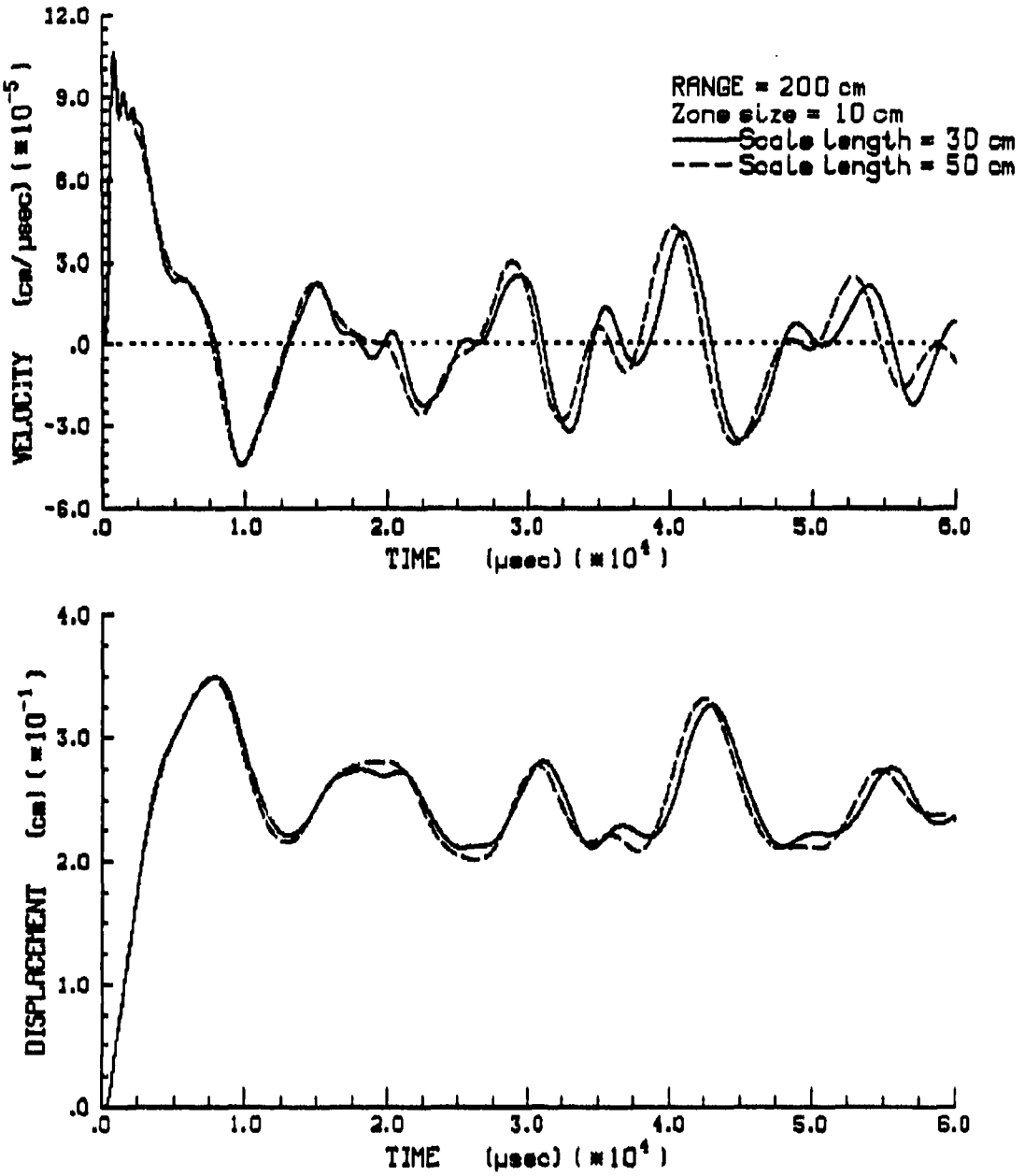

Figure 14. Correlation distance comparisons for 30 and 50 cm at a range of 200 cm.

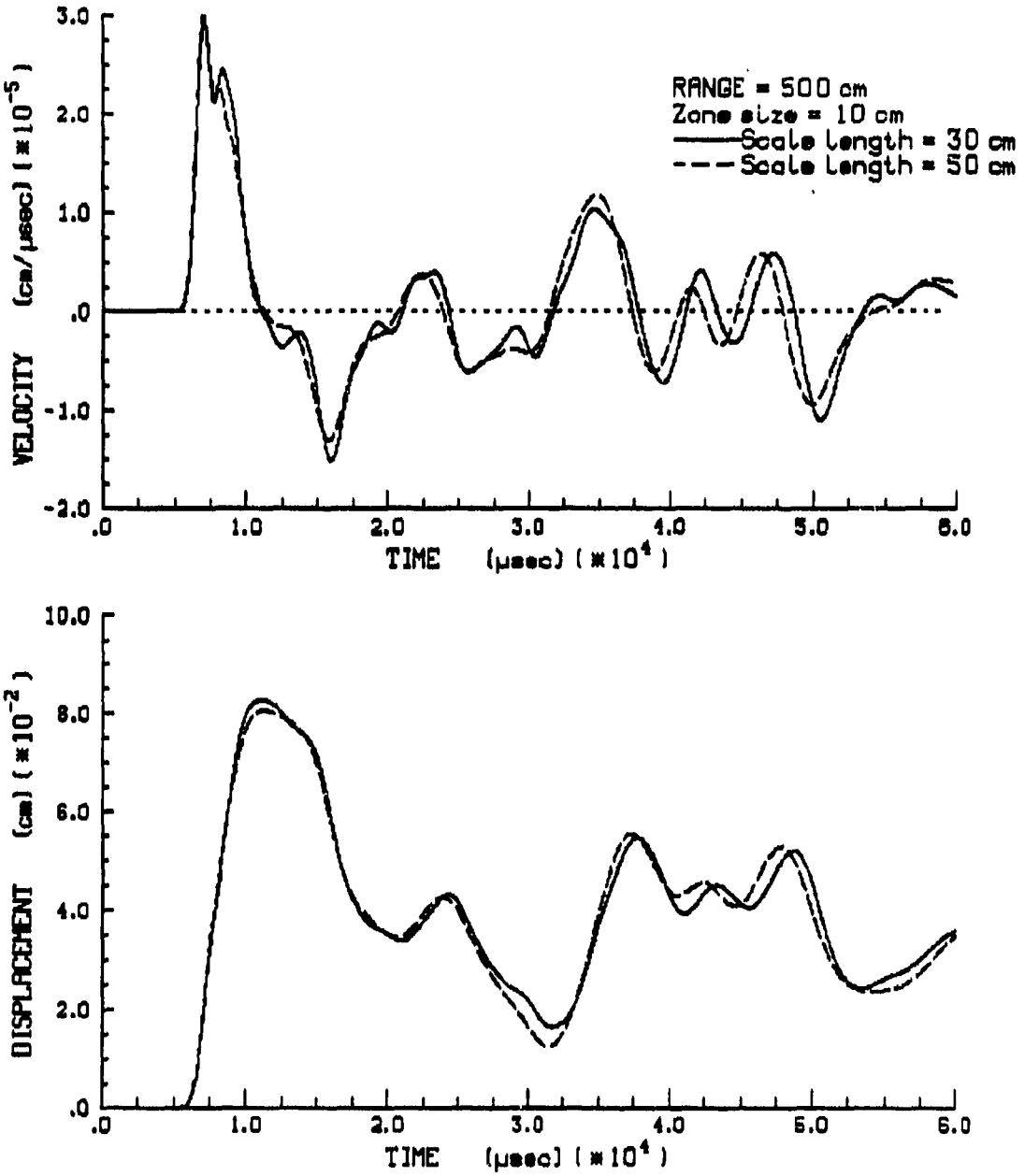

Figure 15. Correlation distance comparisons for 30 and 50 cm at a range of 500 cm.

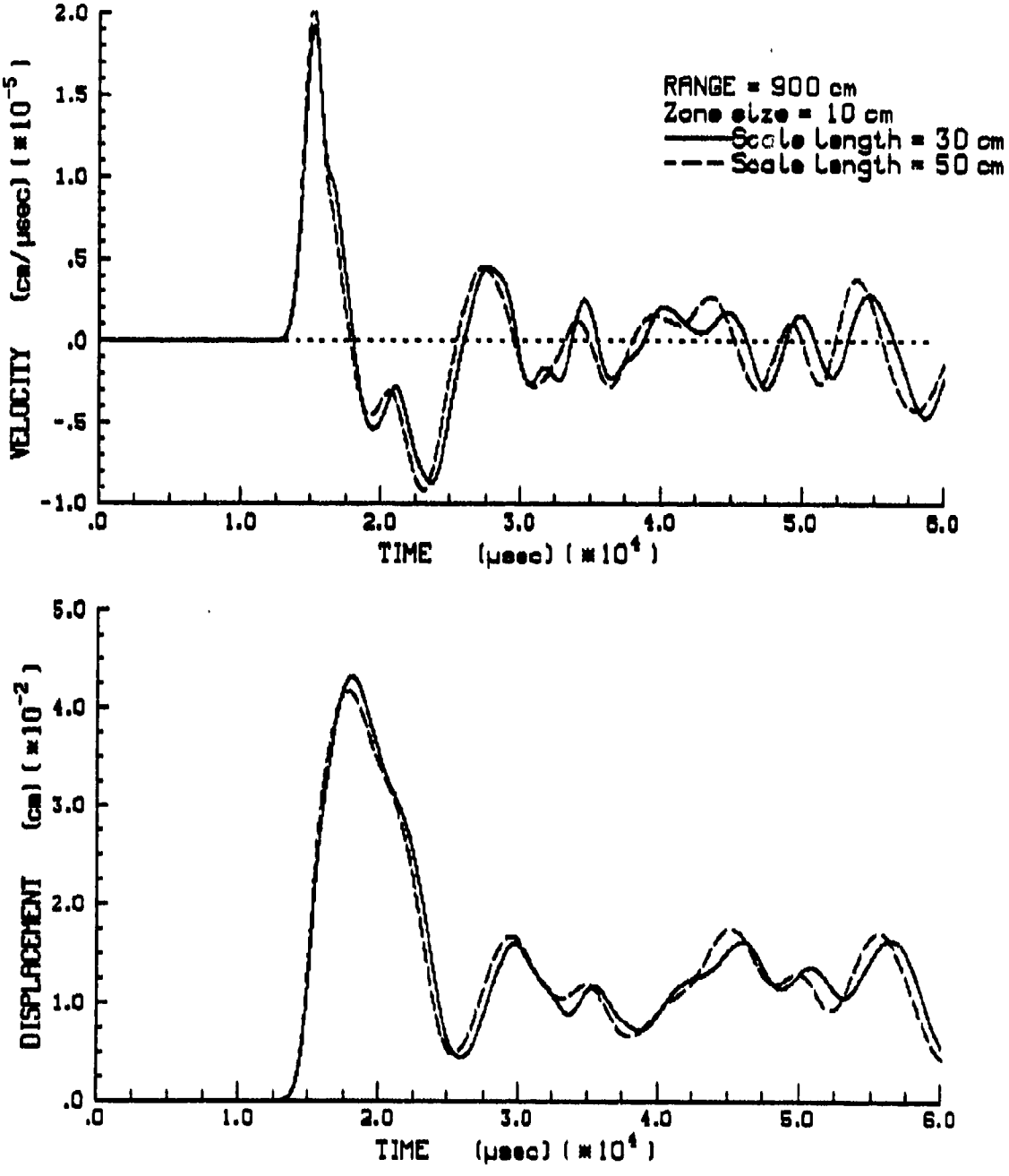

Figure 16. Correlation distance comparisons for 30 and 50 cm at a range of 900 cm.

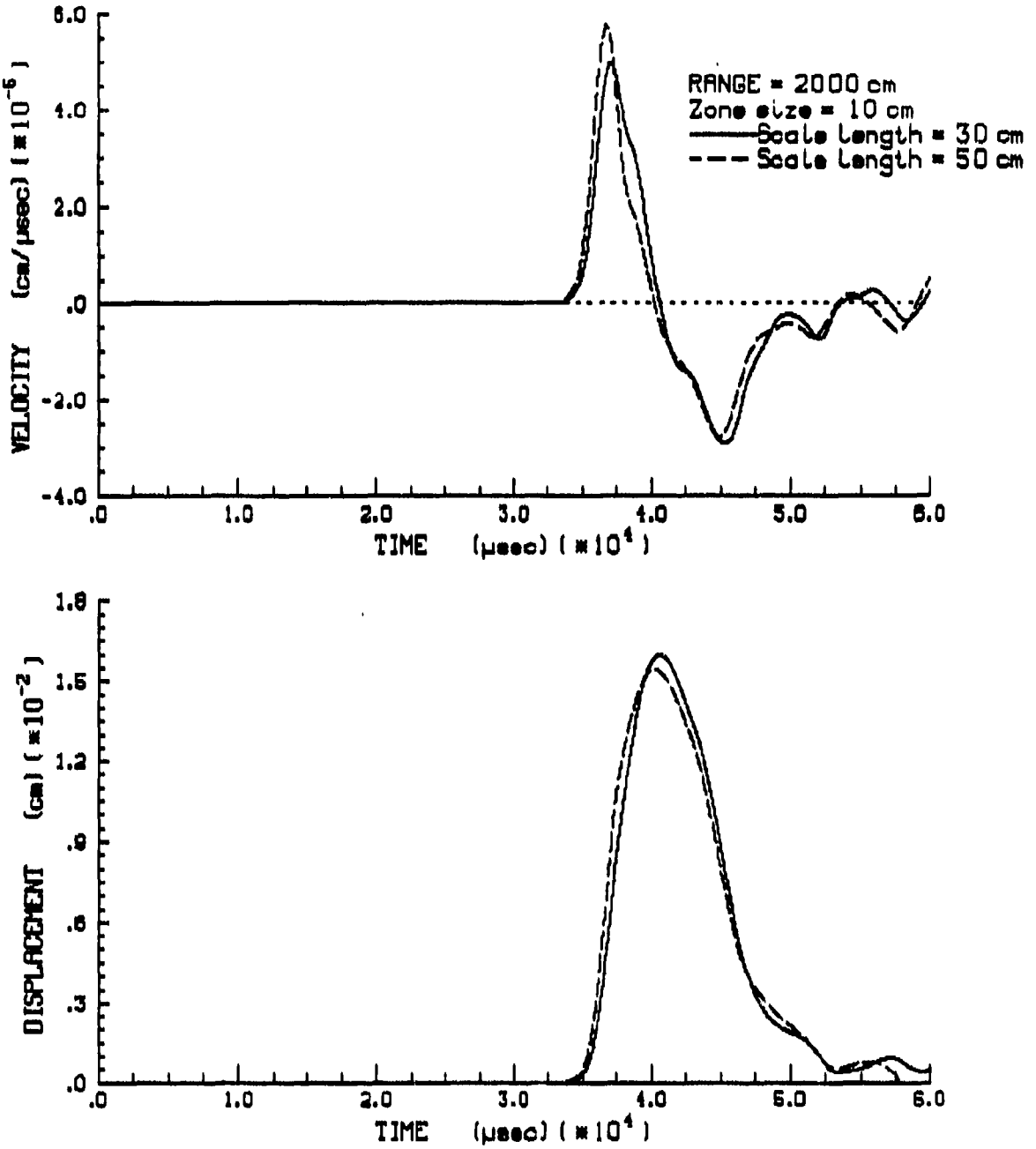

Figure 17. Correlation distance comparisons for 30 and 50 cm at a range of 2000 cm.

The waveforms generated with the two correlation distances vary slightly, but there are no significant differences. The time of arrivals are the same for both cases at the different ranges.

3.1.2 Standard Deviation and Initial Seed Comparisons

The differences in standard deviation and initial seed in the random calculations are shown in Figures 18 through 21. The three waveforms in each plot represent the soil properties modeled as a homogeneous half space (sd=0), and as random geologic material property profiles generated with a 50 cm correlation distance, different random seeds (s=100, s=456), and standard deviations (sd=5%, sd=10%, sd=15%, and sd=20%). These waveforms were generated at a range of 500 cm from the center of the cavity. Figures 18 through 21 represent 5, 10, 15, and 20 percent standard deviations, respectively.

The velocity time history waveforms generated from the homogeneous calculations (sd=0) show the initial peak and then decay to zero. For the time histories generated with the random variability profile calculations, the waveforms do not decay as rapidly with time, but rather show the late

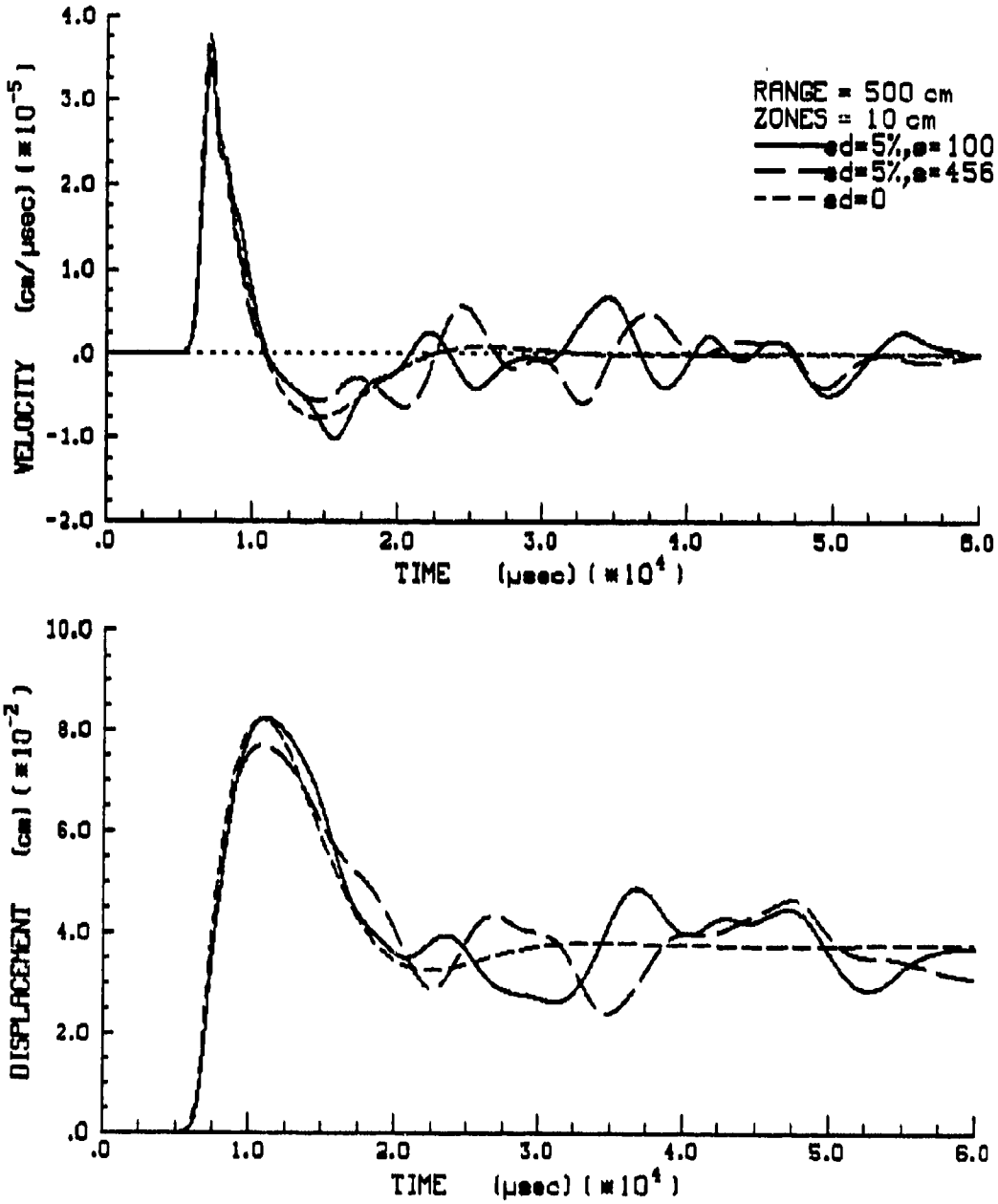

Figure 18. Random calculations generated with 5 percent standard deviation in variability factors.

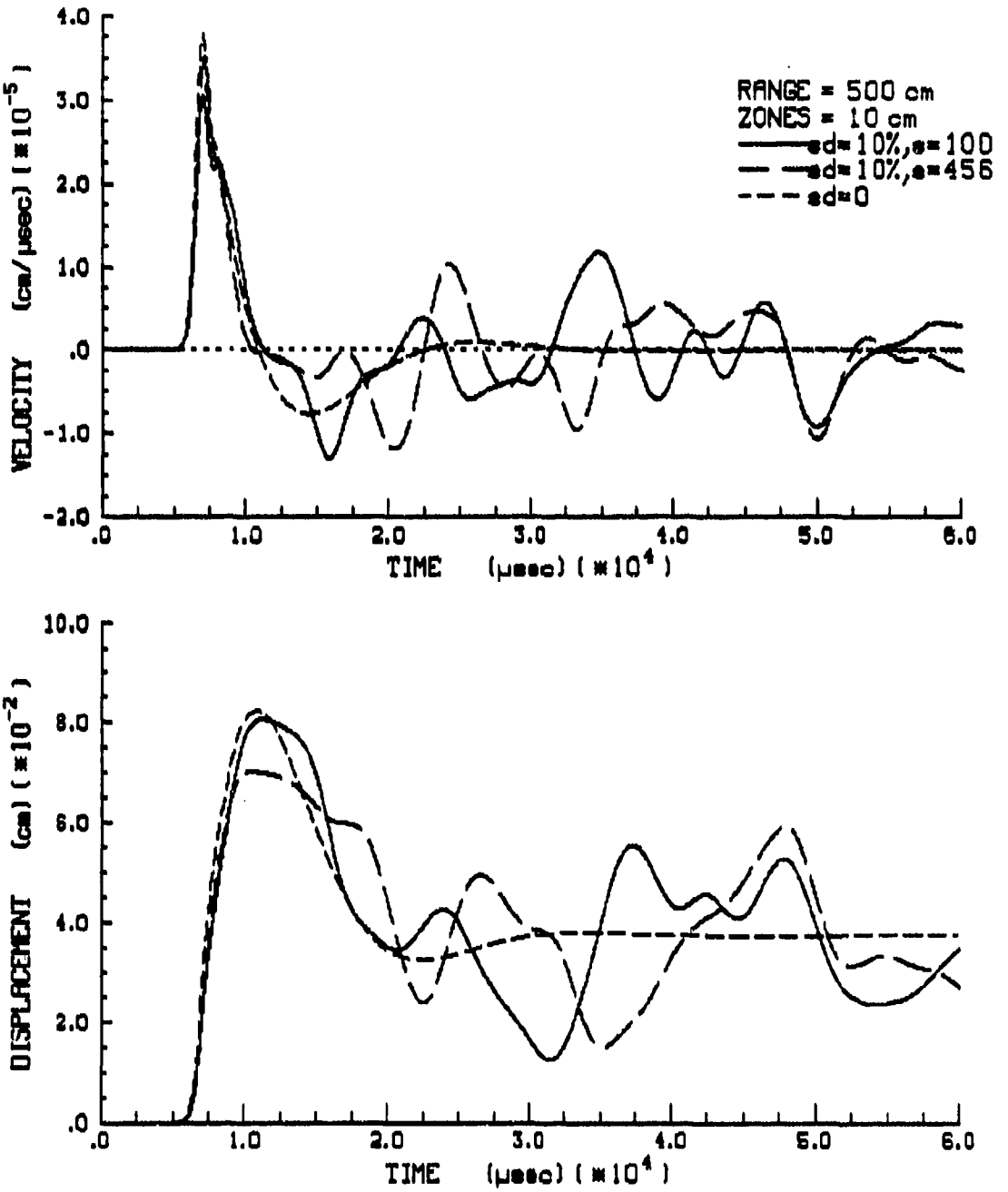

Figure 19. Random calculations generated with 10 percent standard deviation in variability factors.

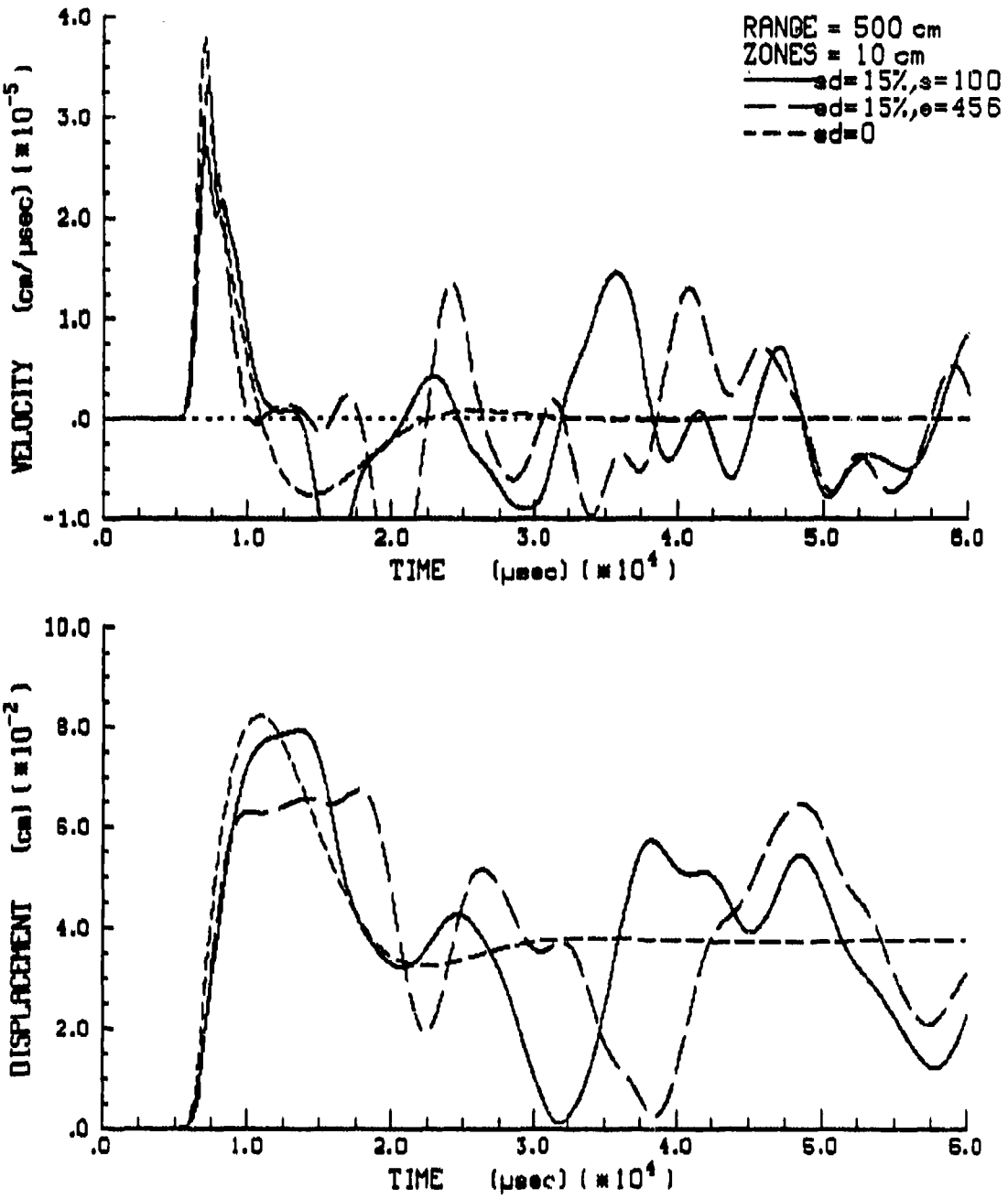

Figure 20. Random calculations generated with 15 percent standard deviation in variability factors.

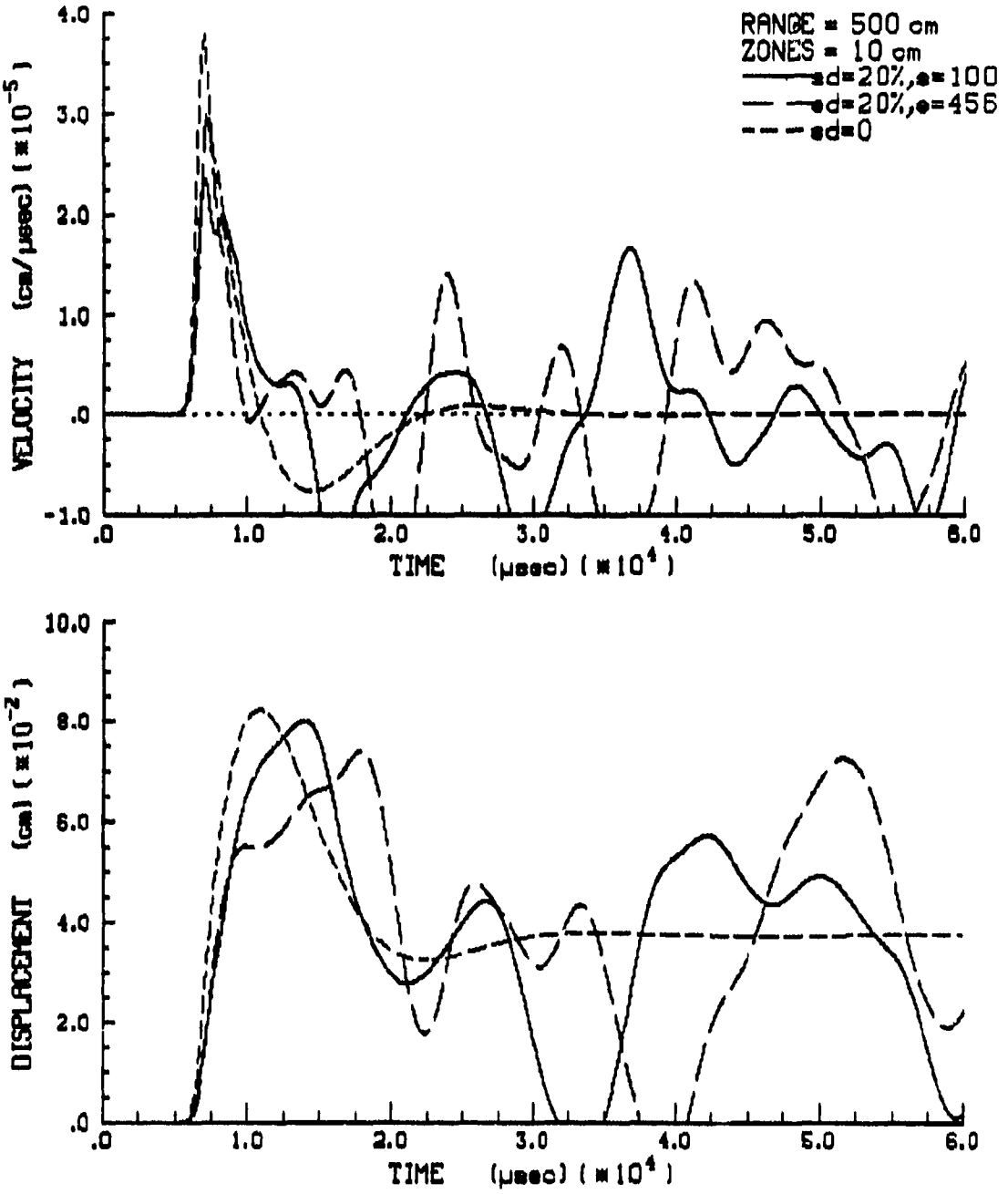

Figure 21. Random calculations generated with 20 percent standard deviation in variability factors.

time noise that is often present in measured field measurements. The other significant difference between the homogeneous and random calculations in Figures 18 through 21 is the reduction in the peak velocity value. As the level of variability in the soil properties increases (from 0 to 20 percent standard deviation), the attenuation of the ground shock motion increases.

Also illustrated in Figures 18 through 21 are the differences in the random calculations due to the initial seeds used in the random number generator. The random variability factors generated by the two initial seeds produced significant differences in the velocity and displacement waveforms. Even though the two sets of random variability factors are statistically the same, the initial seed used in the random number generator influences the computed velocity and displacement waveforms. In order to account for the differences produced by the initial seeds, representative random waveforms (mean and mean ± 1 standard deviation) were generated based on work performed by Vanmarcke (1979).

Vanmarcke developed a methodology to probabilistically characterize the variability of geotechnical parameters and design sampling and testing programs to maximize the

probabilistic information. Based on Vanmarcke's findings and experience, he suggests that a minimum of 6-8 data points are needed to estimate means and variances or coefficient of variation with a reasonable degree of reliability. Therefore, representative random waveforms were generated using 10 different seeds.

3.2 Representative Random Waveforms

In order to compare the results produced by the introduction of spatial subsurface variability to homogeneous ground shock calculations and experimental data, representative random waveforms (mean and mean ± 1 standard deviation) were generated. The representative random waveforms were generated with a 50 cm correlation distance, a Gaussian distribution, soil properties with a 10 percent standard deviation, and by using 3 sets of 10 different seeds (Set-1, Set-2, and Set-3). The seeds used in the 3 sets are shown in Table 2.

Representative velocity waveforms were generated at varying ranges from the pressure cavity center (200, 500, 900, and

Table 2. Three sets of random number generator seeds.

Set 1	Set 2	Set 3
234	1000	572
345	2000	802
456	3000	33
567	4000	534
678	5000	499
789	6000	955
890	7000	748
980	8000	554
1234	9000	624
2345	10000	89

2000 cm) for the 3 sets of independent seeds. The waveforms are presented in Figures 22 through 27.

The soil properties in these random calculations were varied by 10 percent based on down hole seismic cone investigations conducted at the McCormick Ranch test site by The Earth Technology Corporation (Final Report to Air Force Weapons Laboratory, Contract No. F8PR0171120007, 1987).

3.2.1 Analysis of Representative Random Waveforms

The representative random velocity waveforms presented in Figures 22 through 27 are shown in Figures 28 and 29 as

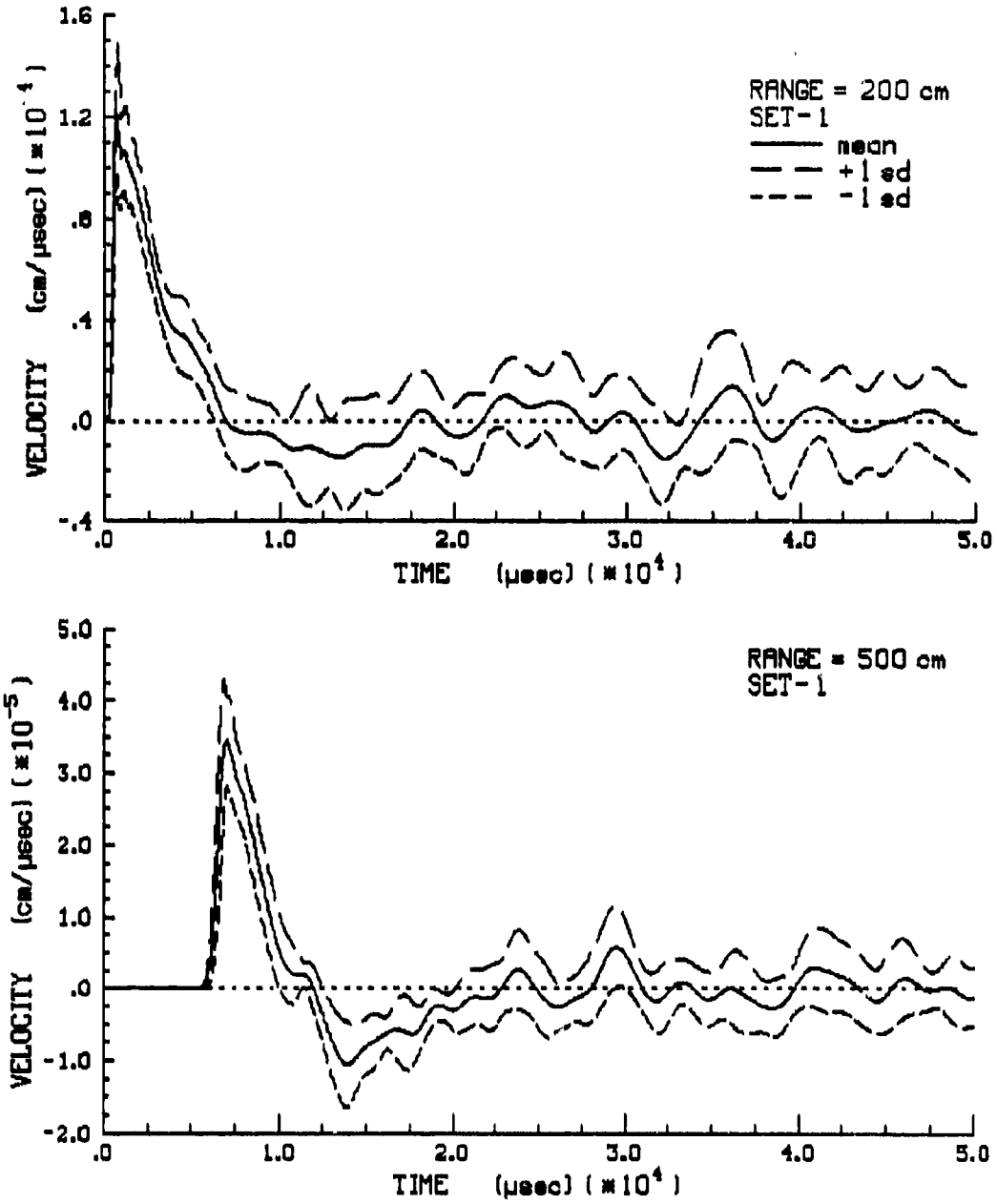

Figure 22. Representative velocity waveforms from Set-1 at 200 and 500 cm from the cavity center.

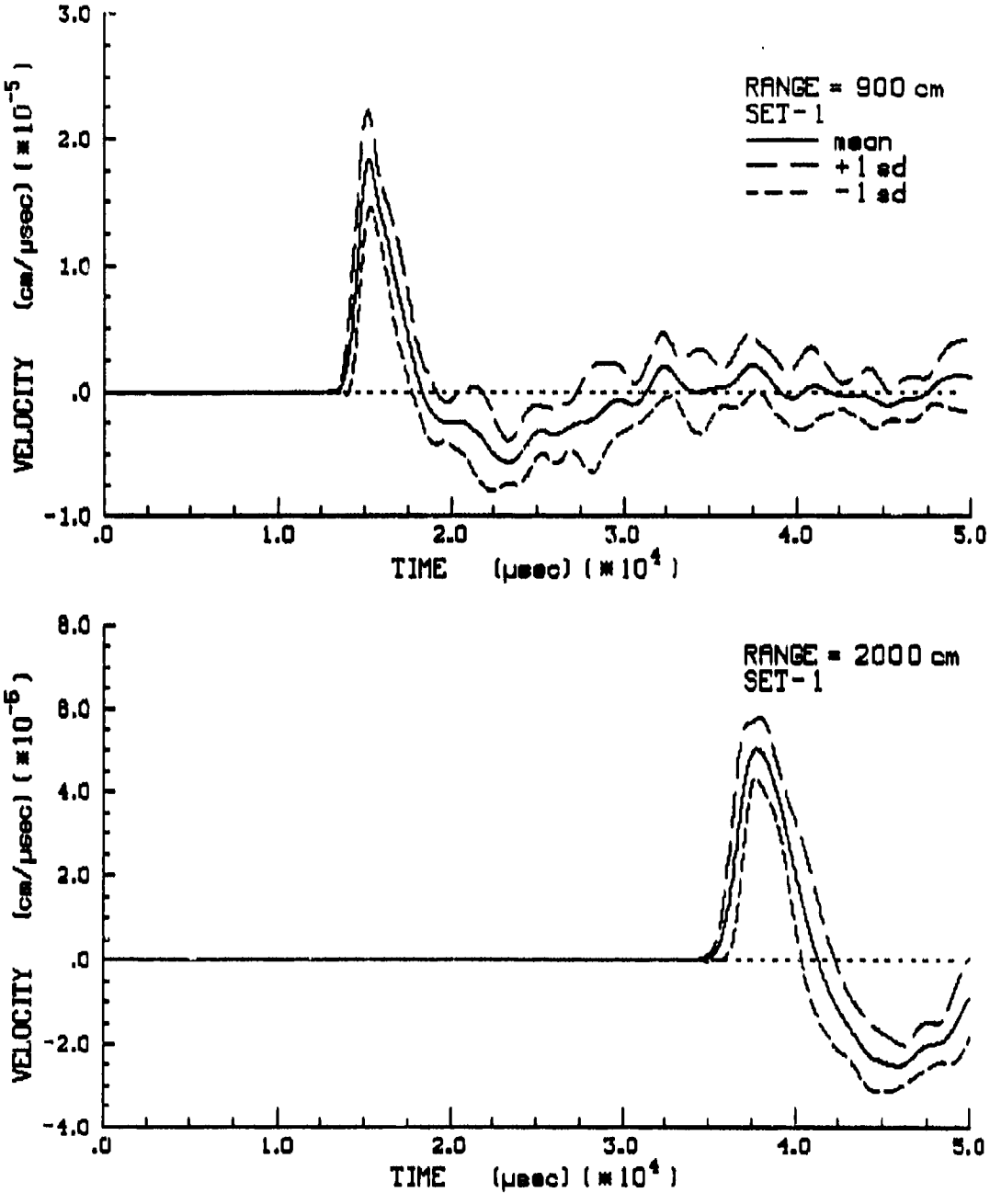

Figure 23. Representative velocity waveforms from Set-1 at 900 and 2000 cm from the cavity center.

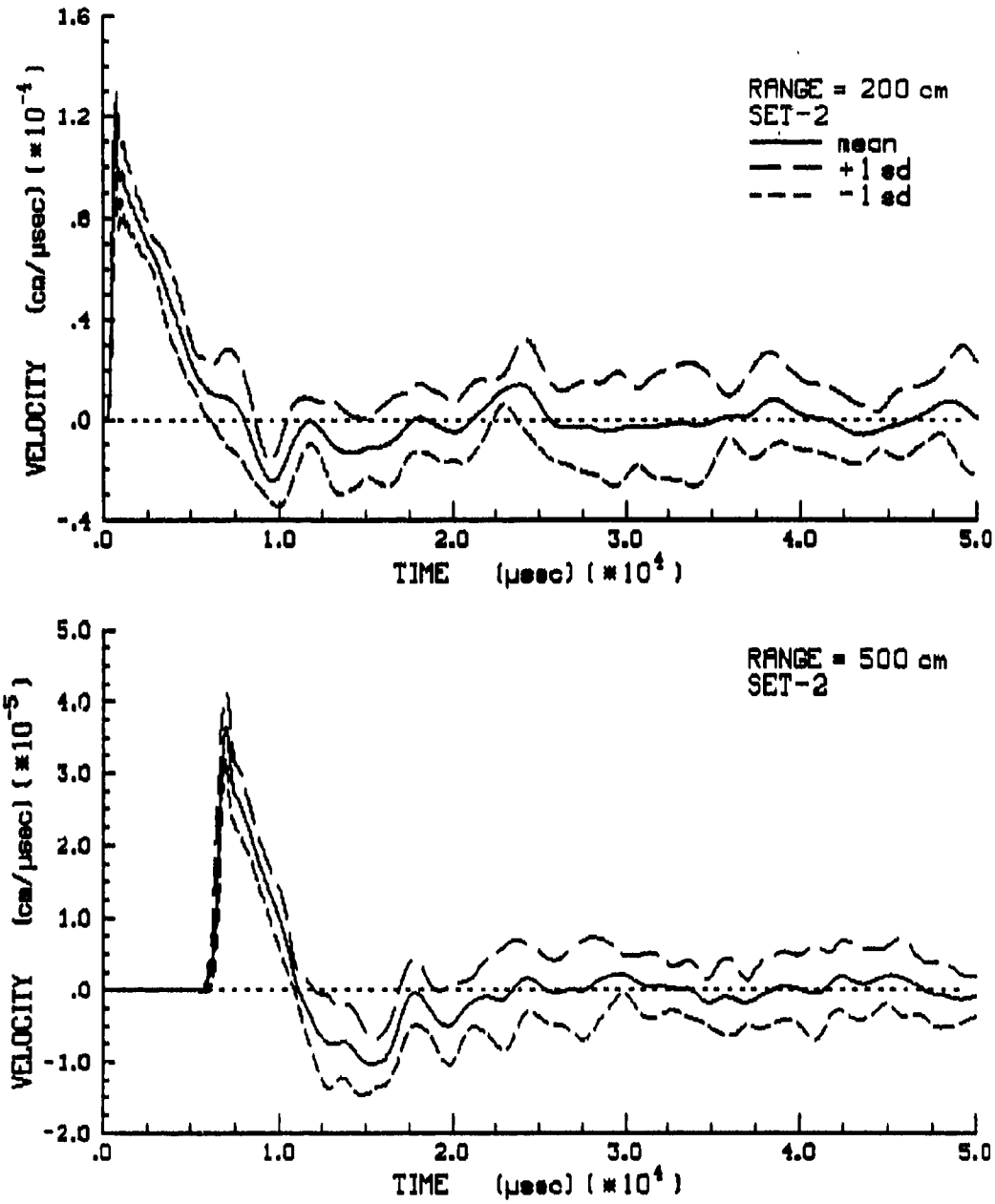

Figure 24. Representative velocity waveforms from Set-2 at 200 and 500 cm from the cavity center.

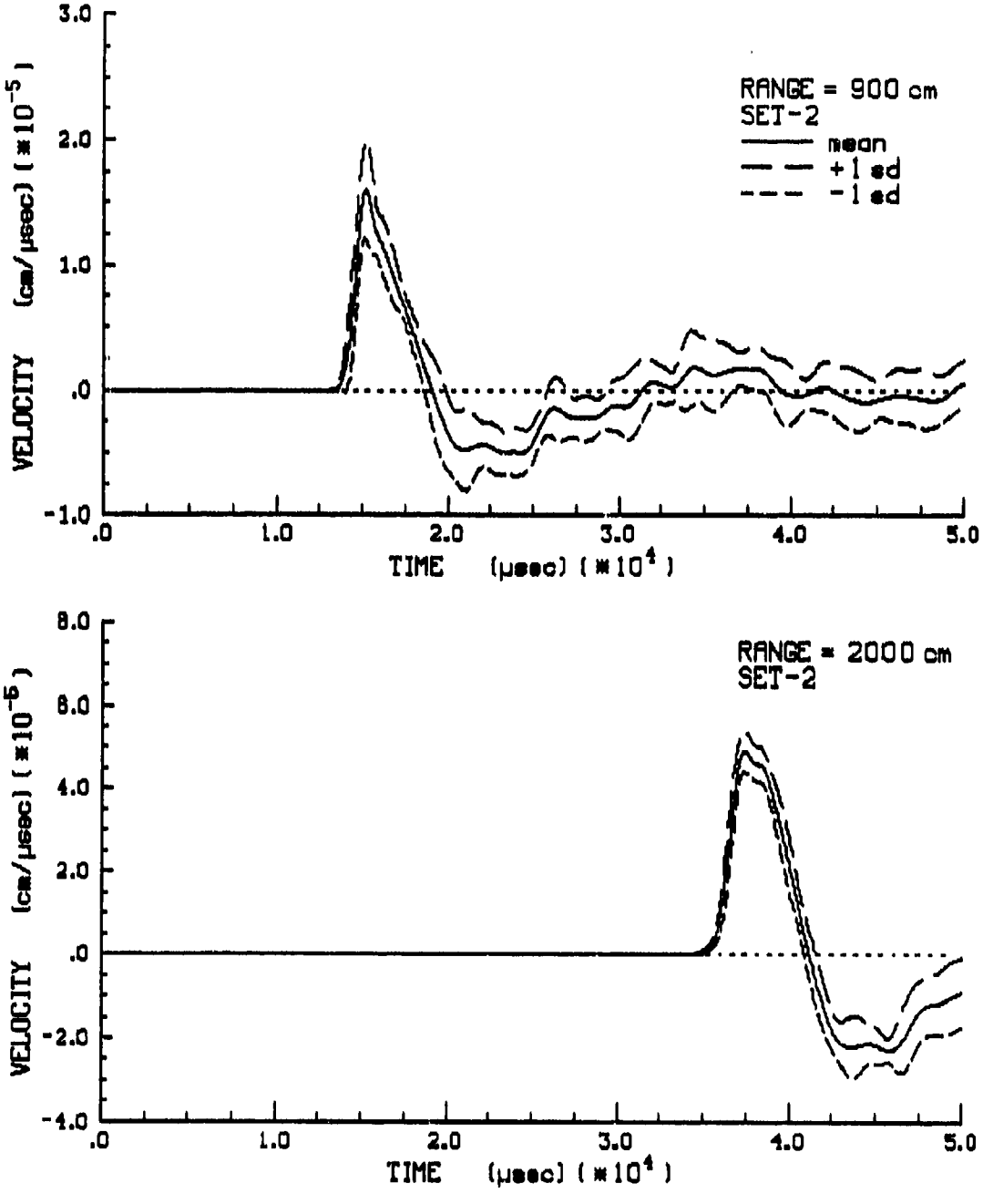

Figure 25. Representative velocity waveforms from Set-2 at 900 and 2000 cm from the cavity center.

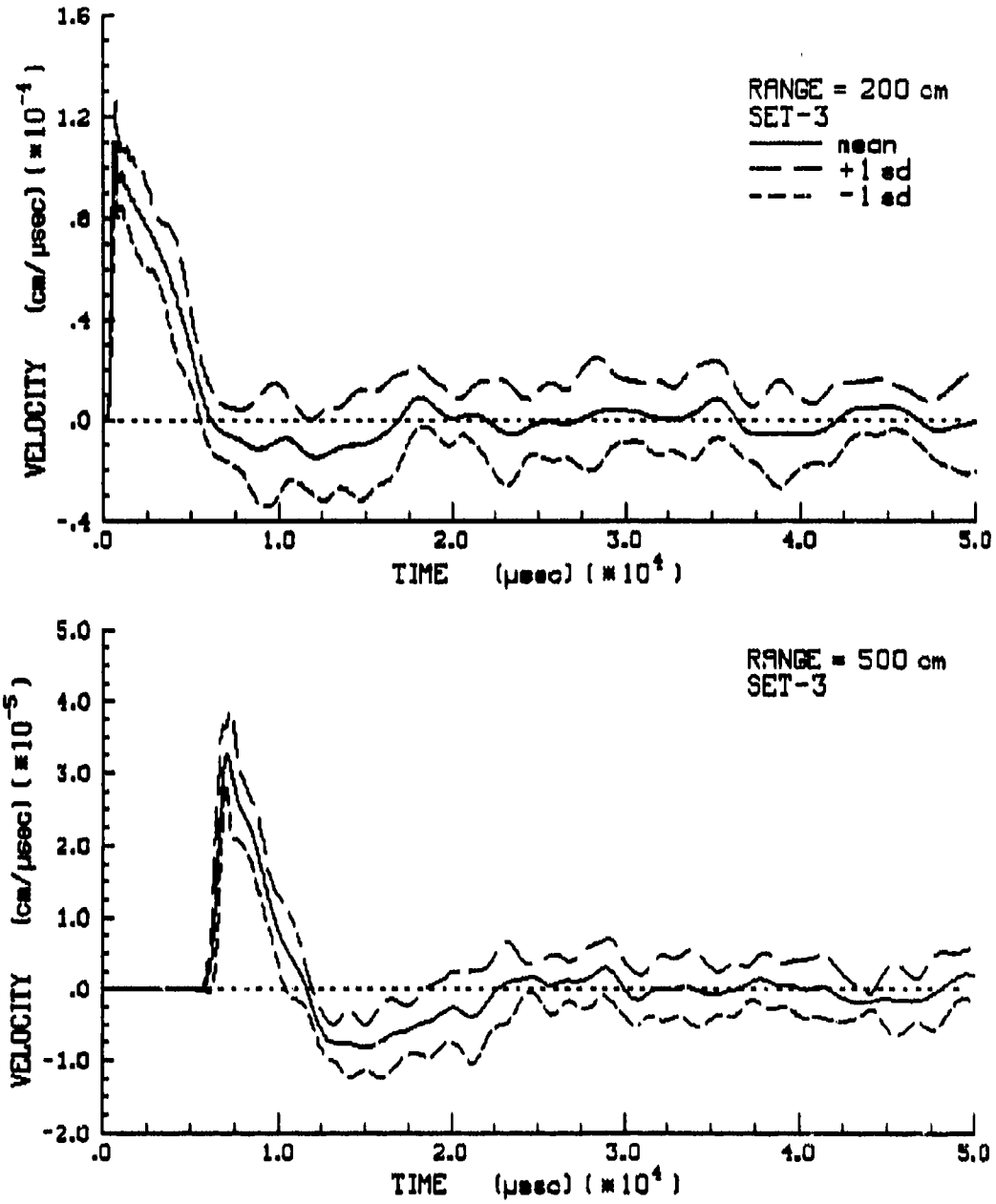

Figure 26. Representative velocity waveforms from Set-3 at 200 and 500 cm from the cavity center.

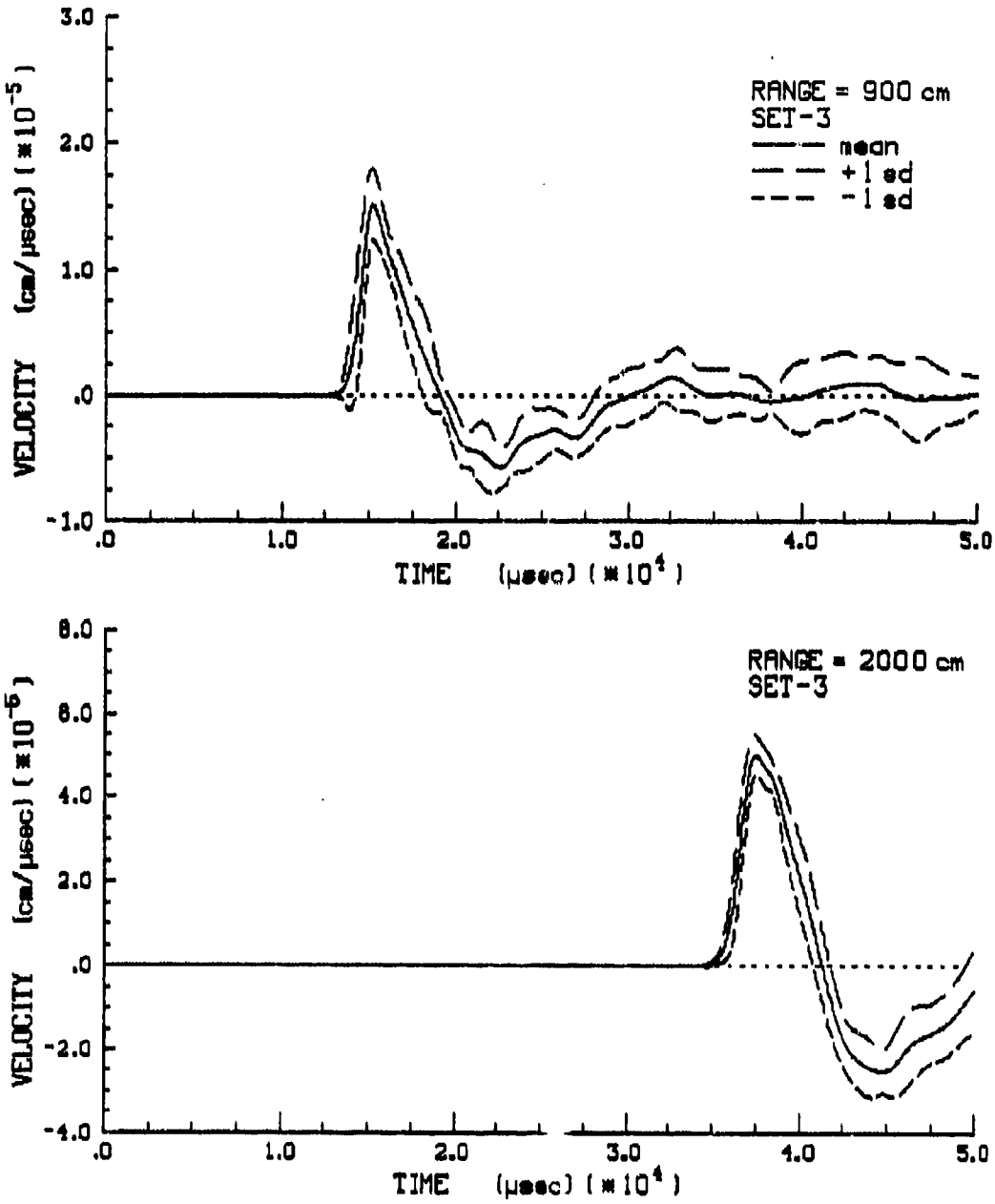

Figure 27. Representative velocity waveforms form Set-3 at 900 and 2000 cm from the cavity center.

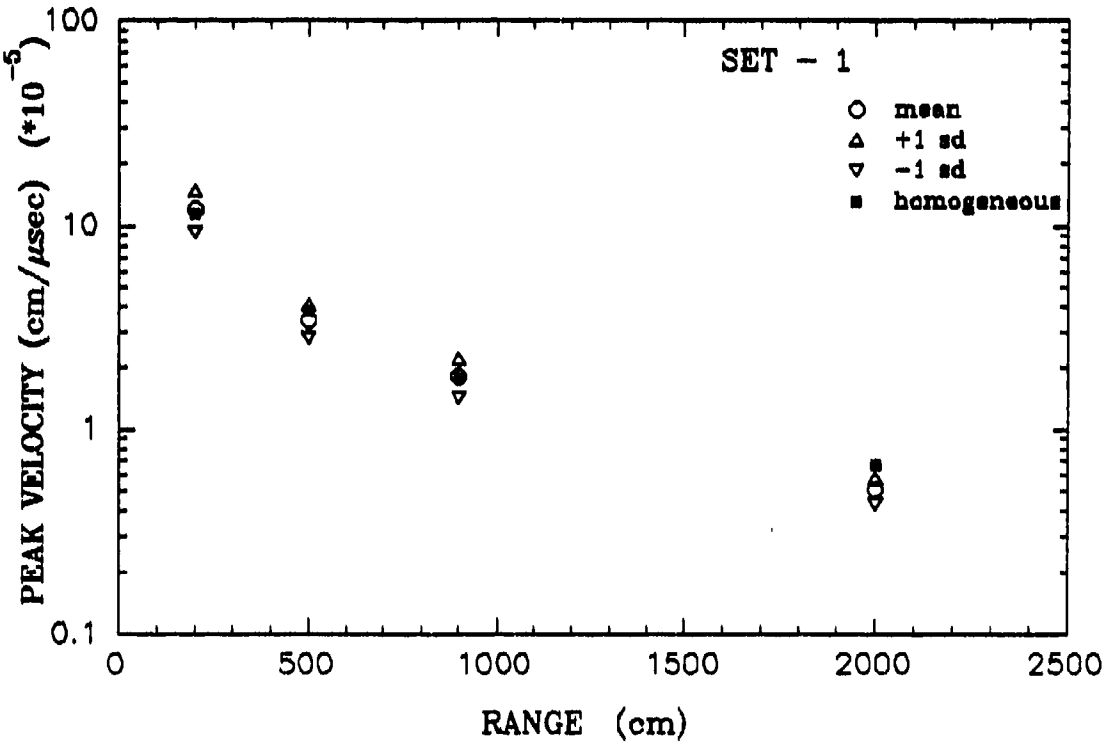

Figure 28. Random and homogeneous peak velocity amplitudes versus range for Set-1.

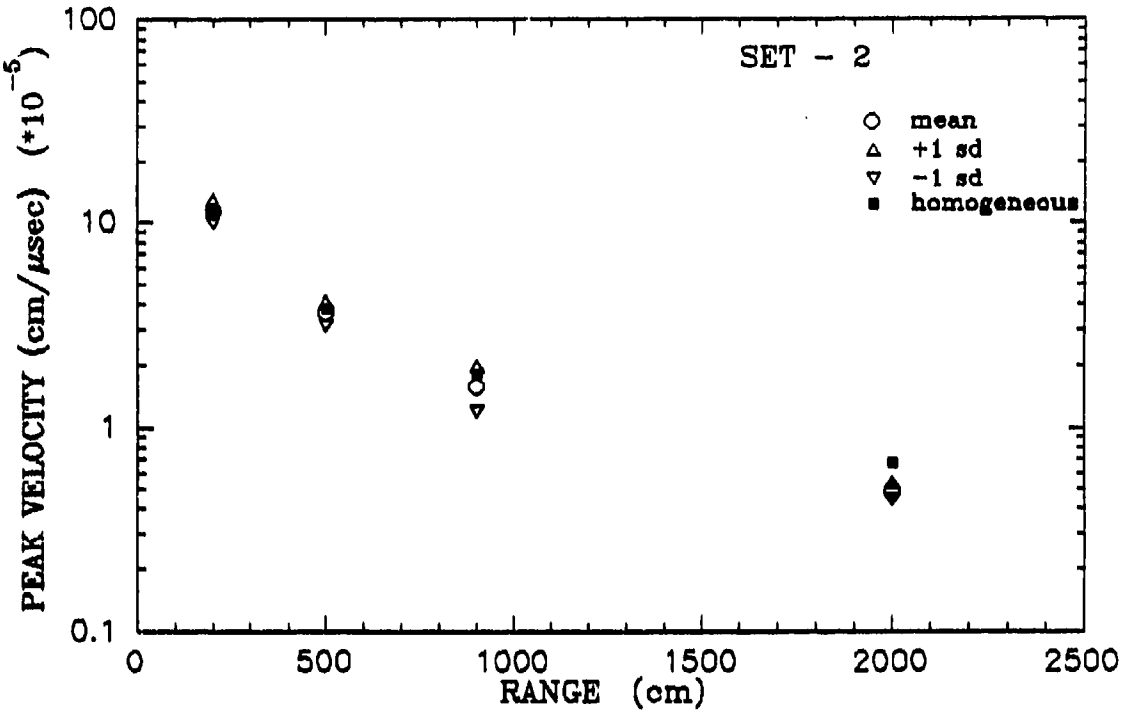

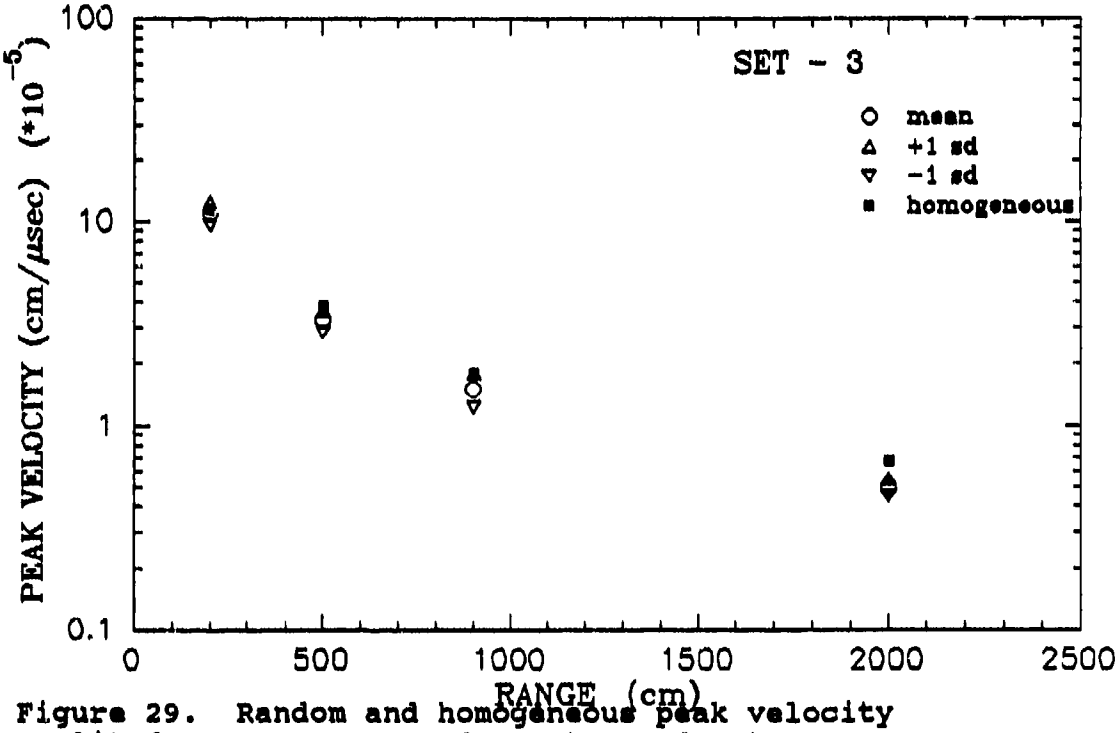

Figure 29. Random and homogeneous peak velocity amplitudes versus range for Set-2 and Set-3, respectively.

peak velocity amplitudes versus range for Set-1, Set-2, and Set-3, respectively. This type of data presentation is useful for analyzing the decay rate of the random and homogeneous calculations for the three cases. Figures 28 and 29 show the mean, mean +1 standard deviation, mean -1 standard deviation, and homogeneous peak velocity amplitudes.

In general, the peak velocity amplitudes from the homogeneous calculation are larger than the mean amplitudes and in some cases are not within the ±1 standard deviation bounds. These plots indicate that the ground shock attenuation rate is larger for the random calculations relative to the homogeneous calculations.

3.2.2 Coefficients of Variation

The peak velocities obtained from the random and homogeneous calculations were normalized to the mean amplitudes for the three random cases to eliminate a biased comparison between the sets of independent seeds. The ratio is known as the coefficient of variation (Bendat and Piersol, 1971).

The coefficients of variation for the peak velocity amplitudes are shown in Figure 30 as a function of range. The mean +1 standard deviation, mean -1 standard deviation, and homogeneous peak velocity amplitudes were normalized to the mean amplitude at the different ranges for each set. The mean ±1 standard deviation for the three sets are represented by the open triangle, diamond, and circle symbols. The homogeneous velocity amplitudes normalized to the mean of each set are represented by the closed triangle, diamond, and circle symbols for Set-1, Set-2, and Set-3, respectively.

The widths of the ±1 standard deviation bounds or error bounds are consistent for the three sets of seeds, except for Set-1 at the 200 cm range. The error bound for Set-1 is approximately 23 percent from the mean, where Set-2 and and Set-3 are only 13 percent from the mean. However, the widths of the error bounds at the different ranges do vary. The widths of the largest error bounds at the different ranges are 23, 18, 25, and 14 percent for the 200, 500, 900, and 2000 cm ranges, respectively. The average error bound is 20 percent for all ranges.

Figure 30 also shows the homogeneous peak velocity amplitudes with respect to the mean amplitude and bounds.

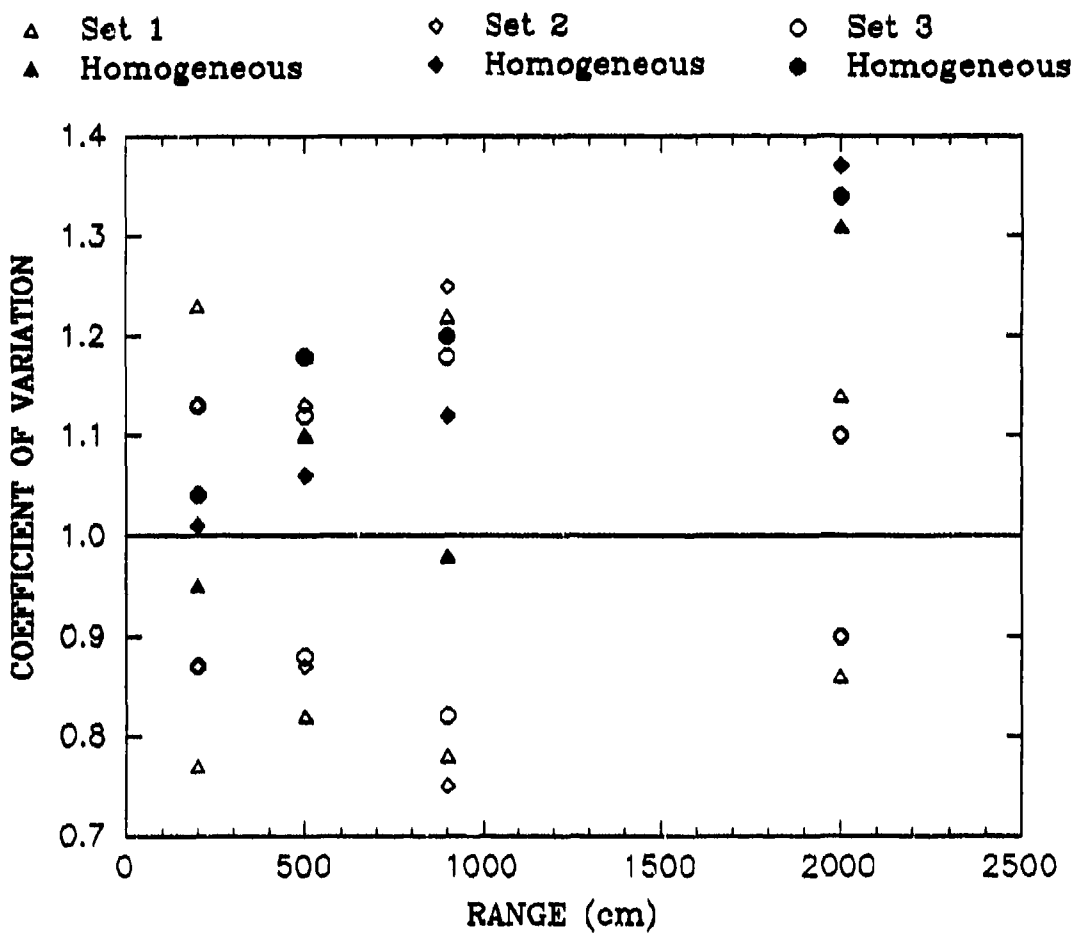

Figure 30. Coefficients of variations with respect to range for Set-1, Set-2, and Set-3. The open symbols represent the bounds for the 3 sets of random calculations, and the closed symbols represent the homogeneous calculations normalized to the mean of each set.

The homogenenous amplitudes for the three cases are closest to the mean and within the bounds at the 200 cm range. At the 500 and 900 cm ranges, the homogeneous amplitudes normalized to the Set-3 means are outside the bounds. At the 2000 cm range, the homogeneous amplitudes for the three cases are outside the bounds. The average homogeneous amplitude is 30 percent from the mean, where the largest error bound is 14 percent at 2000 cm.

Figure 30 shows that the ground shock decay rate with range for the homogeneous calculations is smaller than the random calculations.

3.2.3 Other Random Waveform Effects

In the previous sections, only the peak amplitudes from the homogeneous calculations were compared to those of the representative random calculations. In this section, the complete homogeneous velocity waveforms will be compared to the mean random velocity waveforms.

Four homogeneous velocity waveforms are shown in Figure 31 as a function of range. The mean random waveforms for Set-1, Set-2, and Set-3 are shown in Figures 32 through 34,

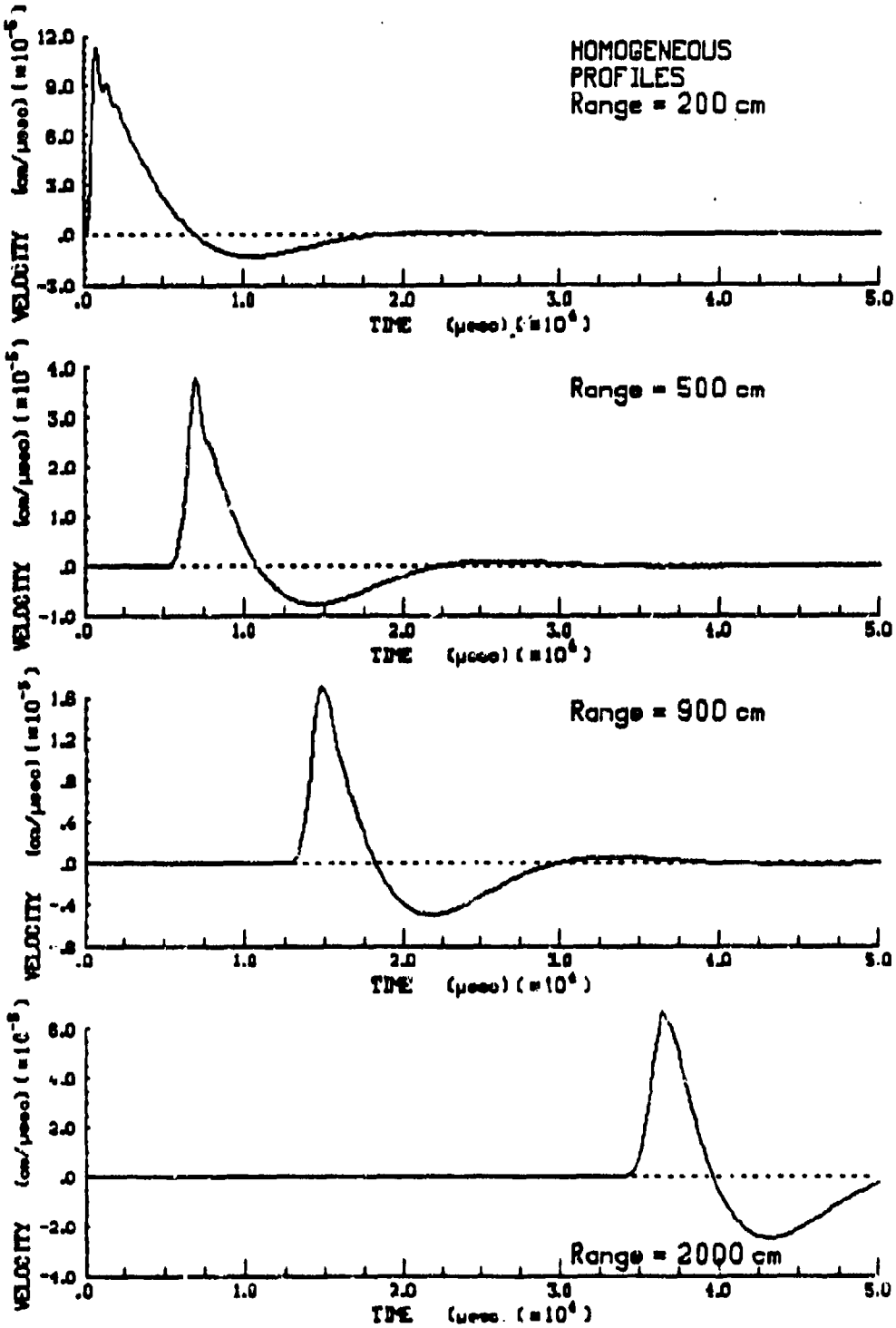

Figure 31. Homogeneous velocity waveforms as a function of range.

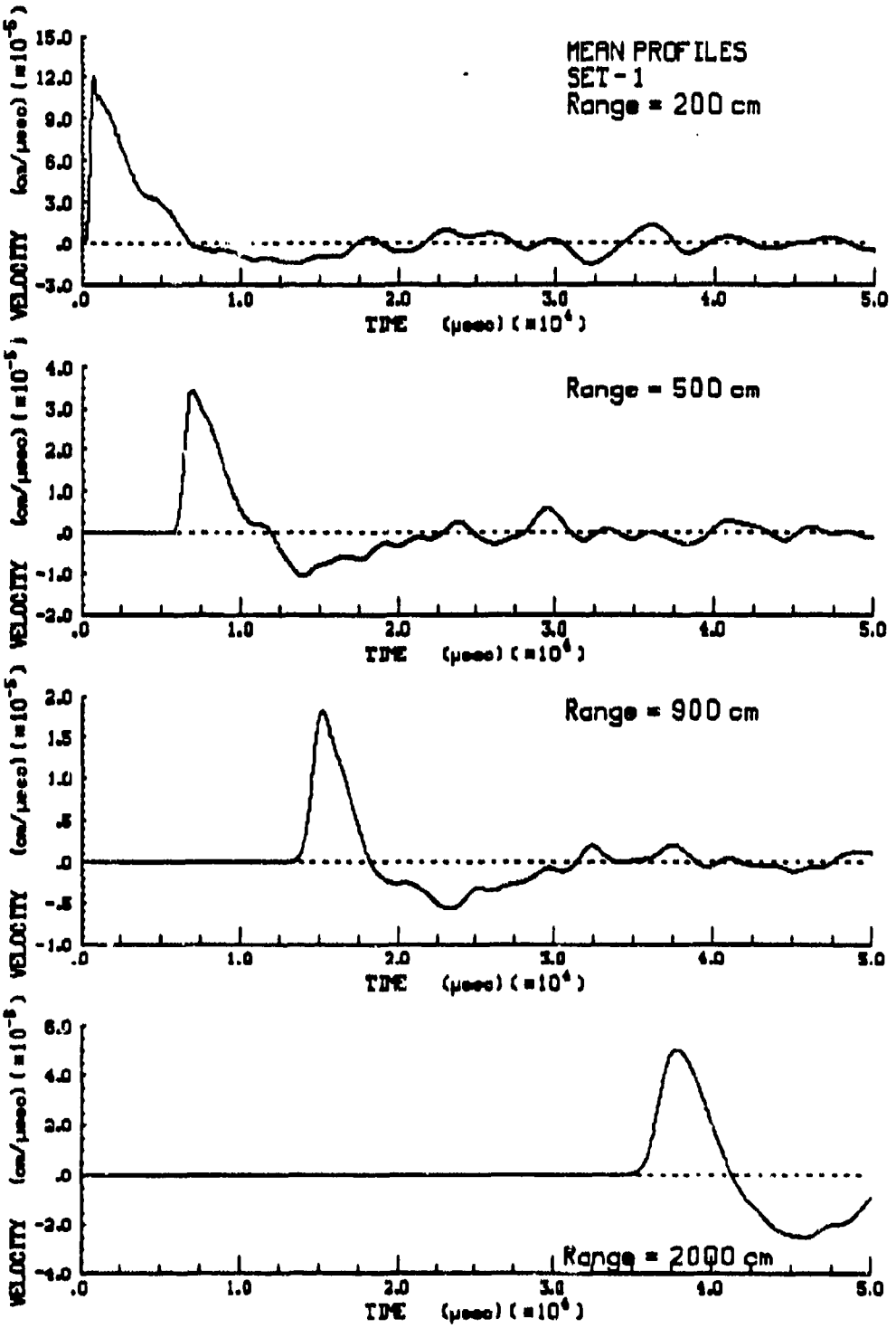

Figure 32. Representative mean velocity waveforms as a function of range for Set-1.

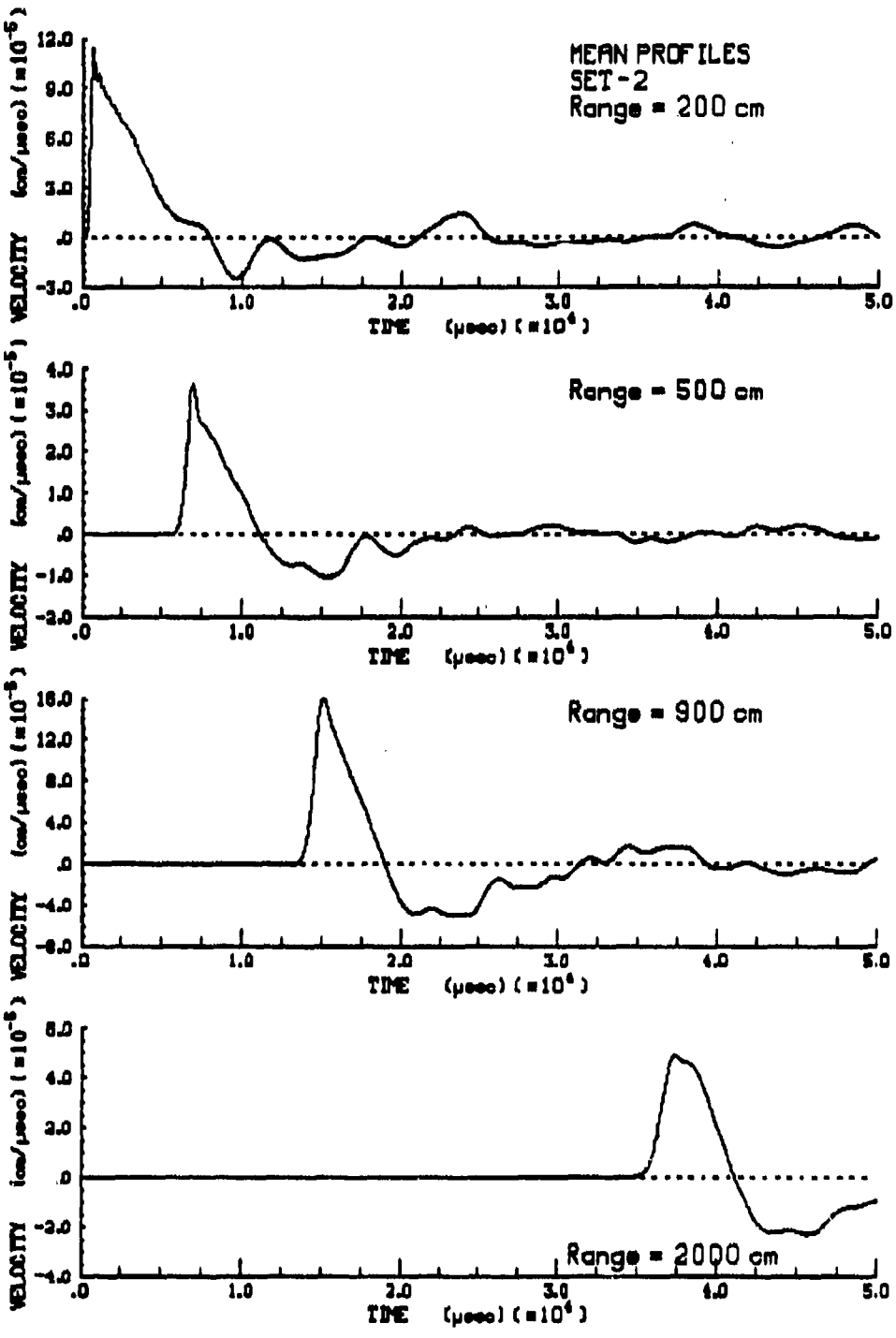

Figure 33. Representative mean velocity waveforms as a function of range for Set-2.

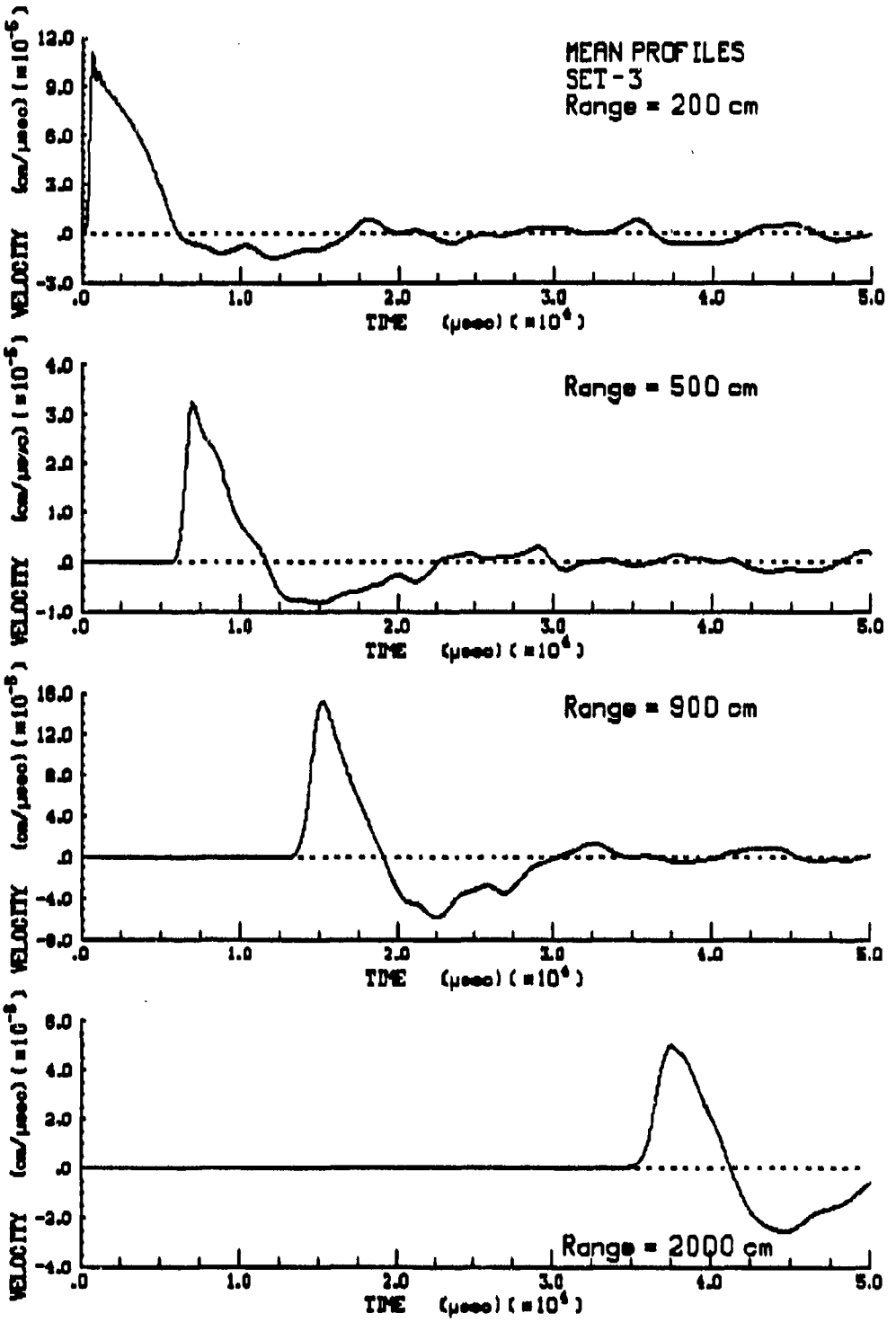

Figure 34. Representative mean velocity waveforms as a function of range for Set-3.

respectively. The mean random waveforms which take into account the spatial subsurface variability show a reduction in the peak amplitudes as well as a shift to a lower frequency. The energy is spread out with time in the initial positive cycle for the mean random waveforms. The mean random waveforms also show the late time ringing or noise often seen in experimental data.

3.3 Experimental Data Comparison

In the final phase of the analysis, the random calculations were compared to experimental data. The analysis was more qualitative than quantitative for the following reasons:

1. The random calculations performed in this study were purely linear elastic calculations. All near source explosion data involve non-linearity.
2. The calculations were 1-dimensional, where the actual conditions are 3-dimensional.

When an explosive test is buried sufficiently deep (no surface effects), the experiment can be assumed to be 1-dimensional. Therefore, the random calculations were compared in a qualitative way to three approximately 1-

dimensional explosive tests. These three tests are MERLIN, MP-2, and CHEAT.

3.3.1 MERLIN Test

MERLIN was a contained underground nuclear experiment conducted in desert alluvium in Yucca Flats, Nevada Test Site (Perret and Bass, 1975). MERLIN was a 10 kiloton test at a depth of 296 m (971 ft) with numerous gages placed at shot depth approximating a one-dimensional configuration.

The instrumentation layout for the MERLIN test is shown in Figure 35. The ranges at stations U3, U4, U5, and U7 are 350, 700, 1100, and 2503 ft, respectively, from the charge. The velocity waveforms are shown in Figure 36. The velocity waveform at U7 was obtained from an accelerometer measurement and not a velocity measurement, therefore, the symbol $\int$ was placed in the plot. As seen in Figure 36, the late time ringing or noise introduced into the random calculation by the subsurface variability (see Figures 32-34) is also seen in the MERLIN results for the various ranges. In previous analyses of data of this type, the late time ringing has been attributed to reflections from various interfaces, or from surface spall impact (Murphy,

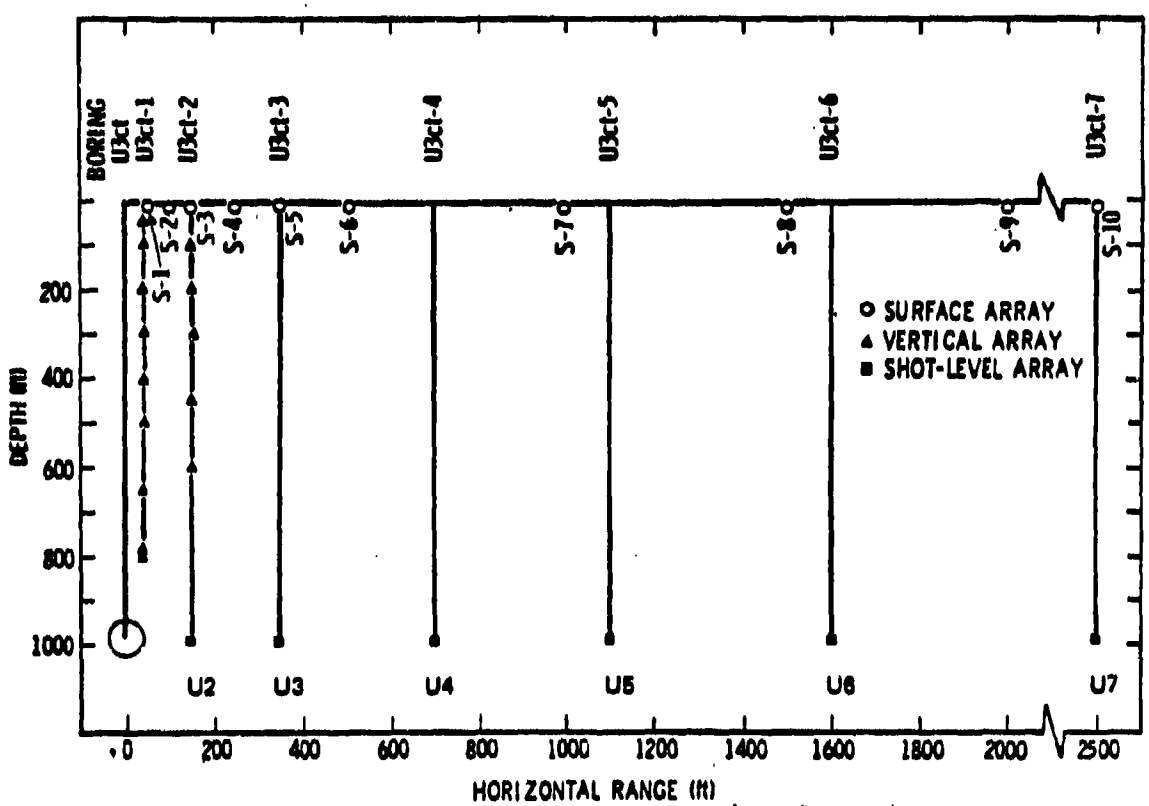

Figure 35. MERLIN test instrumentation layout. (From Perret and Bass, 1975)

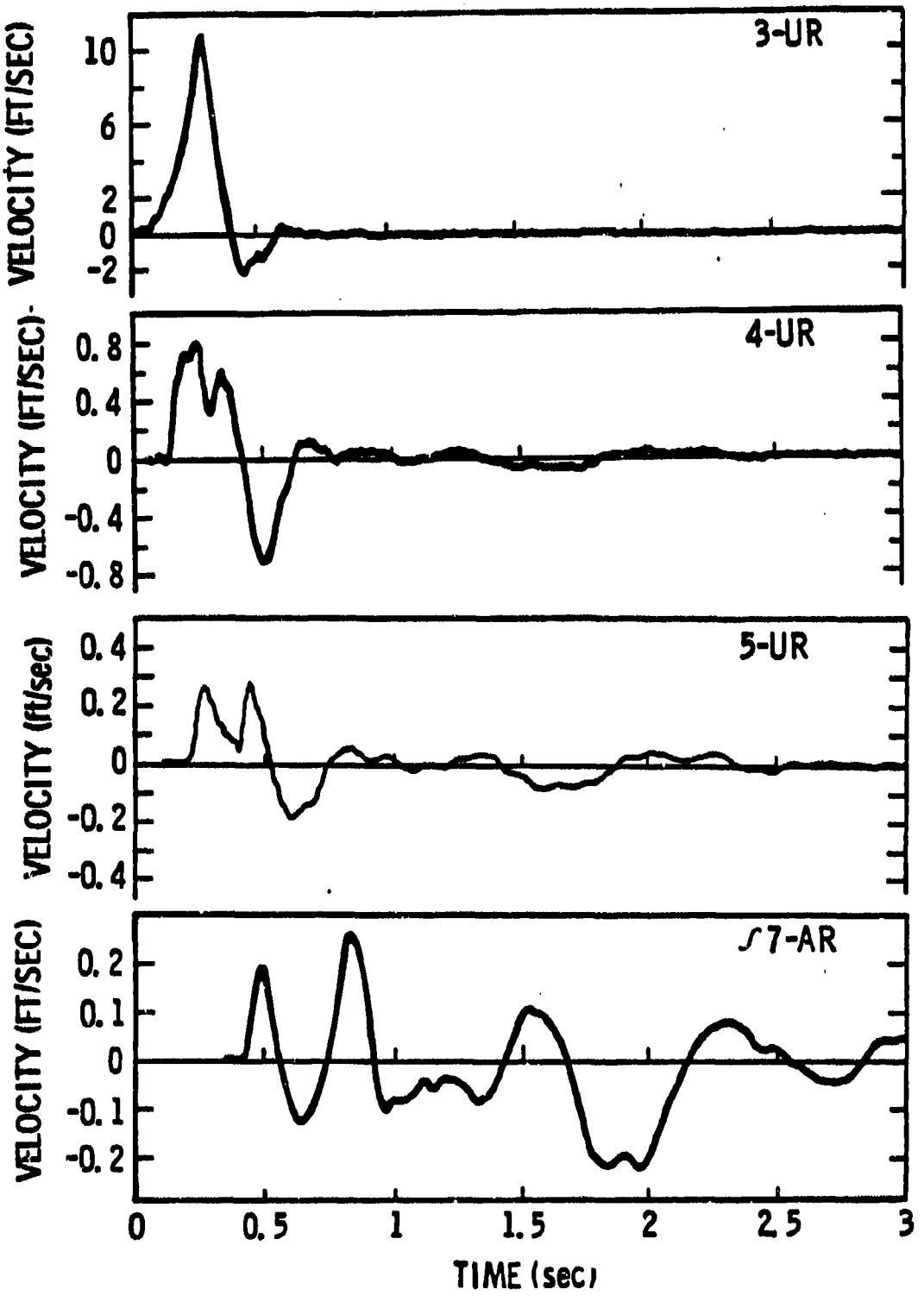

Figure 36. MERLIN results at ranges 350, 700, 1100, 2503 ft from the charge (top to bottom).
(From Perret and Bass, 1975)

1991). The random calculations, however, demonstrate that a relatively small amount of spatial variability in the material properties can produce similar effects.

3.3.2 Material Properties Test 2 (MP-2)

The MP-2 test consisted of a 20 ton nitromethane charge buried 20 m below the surface in dry alluvium at the Yuma Test Site, Yuma, Arizona (Rinehart and Veyera, 1986). A total of 178 gages were placed in this test on 5 different azimuths. The results from this test were used to study the variation in peak particle velocities at approximately the same ranges for 5 azimuths.

Figure 37 shows two velocity plots with 5 waveforms for approximate ranges of 9.5 m (top plot) and 12.6 m (bottom plot). These plots show the variability in recorded measurements at the same distance, but different azimuths. The peak particle velocities at the 9.5 m range vary from 20.5 to 27.5 m/sec, with an average velocity of 23.4 m/sec and a coefficient of variation of 11 percent. The peak particle velocities at the 12.6 m range vary from 4 to 18 m/sec, with an average velocity of 11.6 m/sec, and a coefficient of variation of 14 percent. These ±1 standard

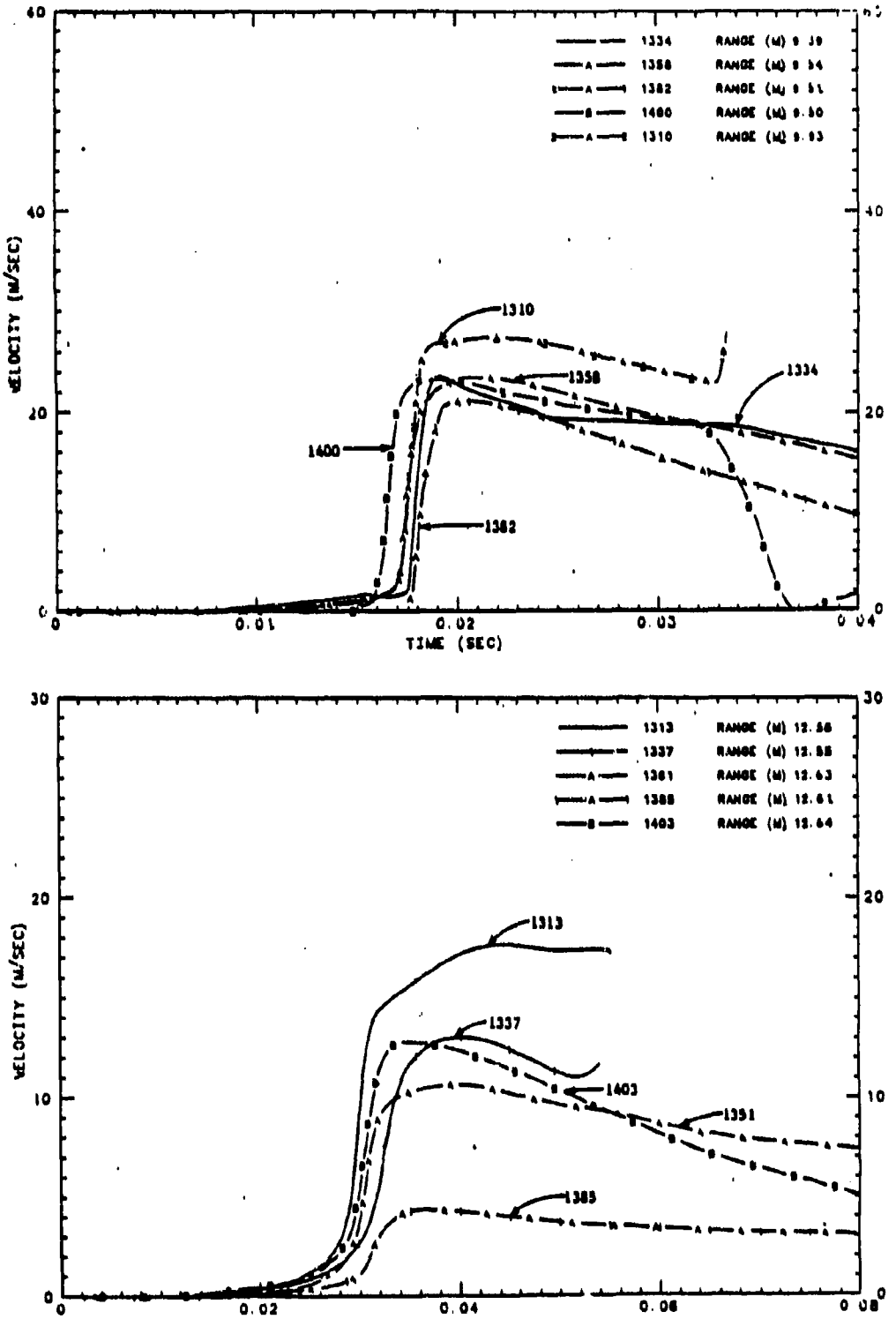

Figure 37. Velocity time histories from MP-2 at approximately 9.5 m (top) and 12.6 m (bottom) ranges. (From Rinehart and Veyera, 1986)

deviation bounds are similar to the uncertainty bounds for the random calculations shown in Figure 30.

3.3.3 Contained High Explosive Alluvium Test (CHEAT)

The CHEAT experiment consisted of a 253 lb TNT charge detonated at a depth of 11.5 m in dry alluvium at McCormick Ranch (Stump and Reinke, 1987) at a site near where the cone penetrometer study was conducted. The instrumentation layout is shown in Figure 38 (top plot) for the CHEAT experiment.

The only measurement of interest for this study is located at a depth of 7.5 m from the surface, since all the other measurements are close to the free surface. The acceleration, velocity, and displacement time histories are shown in Figure 38 (bottom plots). The velocity time history for this test again shows the late time noise or ringing seen in the random velocity waveforms. Stump and Reinke attributed some late time features of the waveforms to free surface effects, but again the random calculations show that a small amount of spatial variability can introduce similar late time features into the waveforms.

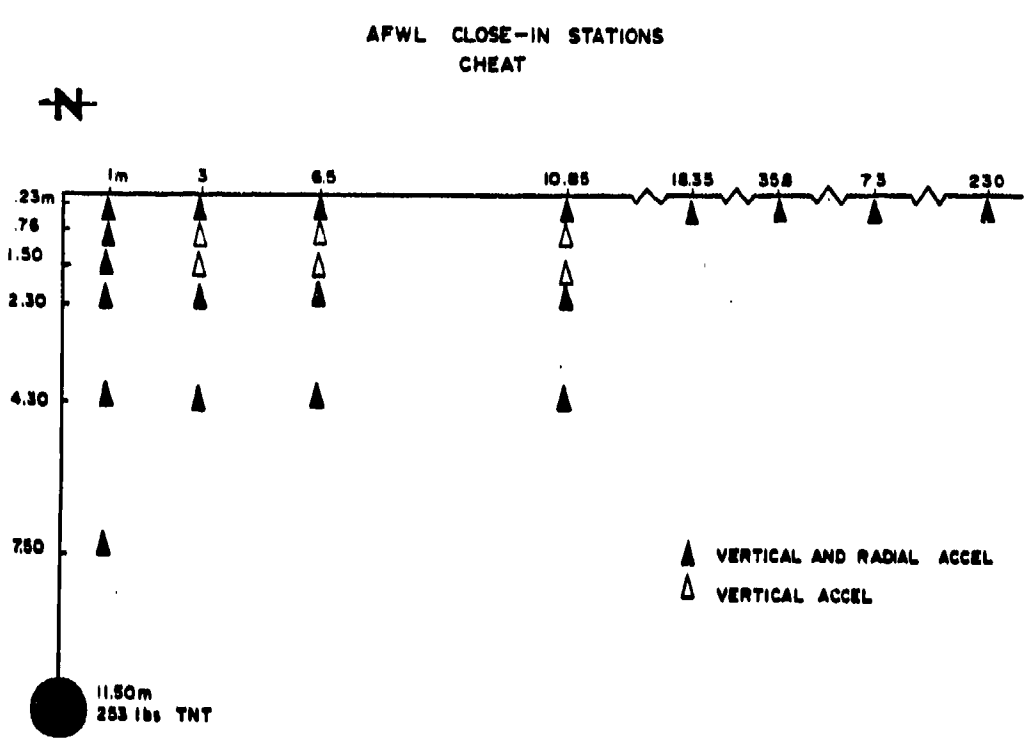

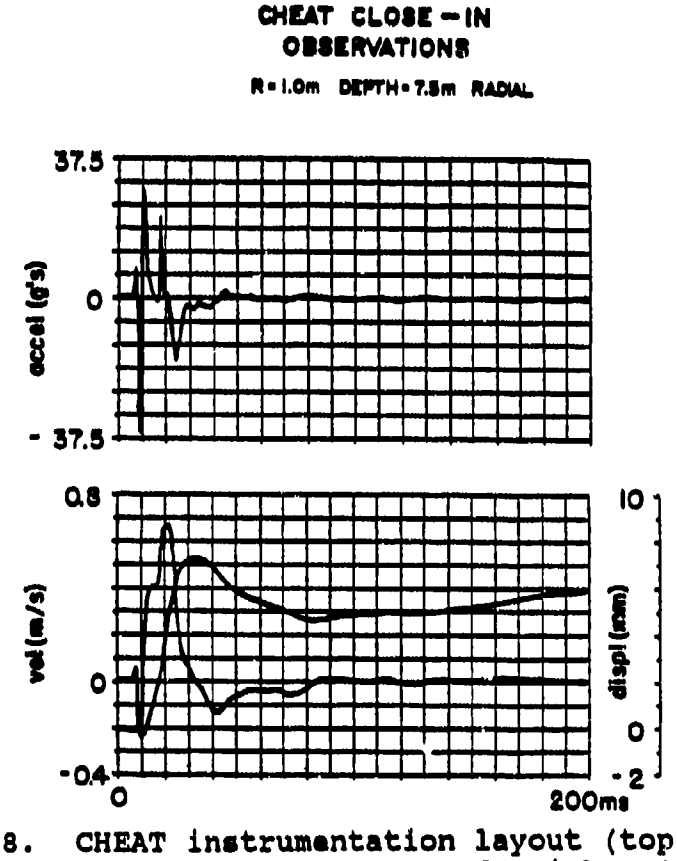

Figure 38. CHEAT instrumentation layout (top) and time histories (bottom). (From Stump and Reinke, 1987)

Chapter 4

CONCLUSIONS

4.1 Techniques

One-dimensional techniques for modeling ground shock propagation through spatially random geologic media were developed in this study. The subsurface spatial variability was defined by a statistical distribution which defines the subsurface heterogeneity, the correlation distance of the variability, and the mean and standard deviation of the material property being considered. These parameters were chosen based on the results of a field investigation effort conducted in dry alluvium.

A technique was developed to construct spatially random geologic variability factors which were incorporated into the AFTON 1-D finite difference code to simulate the subsurface inhomogeneities. This technique was named the Random Geology Generator in this study.

4.2 Implications

The results of the calculations which incorporated the

spatial subsurface variability into the geologic material model have several important implications for the explosive effects community. The implications are as follows:

1. The calculations have shown that relatively small percentages of variability (5 percent standard deviation) result in changes in the ground motion waveforms relative to the homogeneous calculations. Understanding the effects that spatial subsurface variability has on ground motion will reduce the uncertainty involved when performing ground shock calculations/predictions.

2. The introduction of spatial random variability into the elastic material caused broadening of peaks, and the attenuation rate to increase relative to the homogeneous calculations. Dynamic material model parameters are often obtained by adjusting finite difference code input parameters until the calculated waveforms match experimental waveforms in terms of attenuation rate, and pulse width. By adjusting certain parameters, the increased attenuation rate and pulse broadening might be in correctly modeled as non-linear material effects, when they can be caused by spatial variability in a linear-elastic material.

3. The presence of spatial variability means a single gage record at a given range for an experiment does not provide a definitive view of the ground motion field. Multiple gage records at the same range on different azimuths are required to adequately define the ground motion uncertainty and variability.

4. Incorporation of spatial variability into calculational predictions of explosive effects on structures would better define the uncertainty in the predictions. For structures of large areal extent, spatial variability in the ground motion field means that different portions of the structure are subjected to different loadings.

5. Random spatial variability may have a significant influence on the determination of explosive yields under nuclear testing treaties using near-source ground motion data. The calculations performed in this study have shown an increase in the attenuation rate relative to the homogeneous cases. In addition, there is a significant uncertainty band (maximum band was ± 25 percent) for the velocity amplitudes. Again a single gage at a given range may not adequately define this uncertainty. Near-source heterogeneity may also have

strong influences on the distant seismic signals recorded from underground nuclear tests (Gupta, Lynnes, and Wagner, 1991).

4.3 Recommendations

Since a site characterization effort cannot be done in such detail to determine each and every heterogeneity in the subsurface material for a test site, a new site must be characterized statistically. Therefore, a methodology for statistical in situ characterization must be developed to account for the spatial subsurface variability.

Since the geologic material behavior in explosions is in general non-linear, the 1-dimensional modeling techniques developed in this study should be applied to an elastic-plastic material model. Therefore, a methodology for estimating the variability in the material parameters used in an elastic-plastic model must be developed.

Following this step, the modeling techniques should be extended to a two-dimensional environment. A two-dimensional random geology generator should be developed and incorporated into a two-dimensional ground shock code.

REFERENCES

Bendat, Julius S. and Allan G. Piersol, 1971, **Random Data: Analysis and Measurement Procedures**, John Wiley & Son, Inc.

Chernov, Lev A., 1960, **Wave Propagation in a Random Media**, McGraw-Hill Book Company, Inc.

Fisk, M.D., G.D. McCartor, and W.R. Wortman, 1991, "Phase Screen Simulations of Seismic Wave Scattering Related to Monitoring Underground Nuclear Explosions", Phillips Laboratory, Technical Report PL-TR-91-2084.

Frankel, A. and R.W. Clayton, 1986, "Finite Difference Simulations of Seismic Scattering: Implications for the Propagation of Short-Period Seismic Waves in the Crust and Models of Crustal Heterogeneity', **Journal of Geophysical Research**, 91, No B6.

Gupta, I. N., C. S. Lynnes, and R. A. Wagner, 1991, "Studies of Near-Source and Near-Receiver Scattering and Low-Frequency Lg from East Kazakh and NTS Explosions", Phillips Laboratory, Technical Report PL-TR-91-2287.

Grant, L.T., 1988, "Experimental Determination of Seismic Source Characteristics for Small Explosions", MS Thesis, Dep. of Geology, Southern Methodist Univ., Dallas, TX.

Jewell, A., 1988, "Stochastic Site Characterization and Modelling", Final Report, 1988 USAF-UES Summer Graduate Student Research Program.

Law, Averill M. and W. David Kelton, 1982, **Simulation Modeling and Analysis**, McGraw-Hill BooK Company, Inc.

Lehmer D.H., 1951, "Mathematical Method in Large-Scale Computing Units", **Annuals Computation Lab. Harvard University**, 26, pp 141-146.

Lewis, P.A., A.S. Goodman, and J.M. Miller, 1969, "A Pseudo-Random Number Generator for the System/360", **IBM Syst.**, J. 8, 2, p6p 136-146.

Murphy, J. R., 1991, "Free-Field Seismic Observations for Underground Nuclear Explosions", in Explosion Source Phenomenology, American Geophysical Union.

PC-MATLAB for MD-DOS Personal Computers, by The MathWorks, Inc., South Natick, MA, 1989.

Perret, William R. and Robert C. Bass, 1975, "Free-Field Ground Motion Induced by Underground Explosions", Sandia National Laboratory Report, SAND74-0252.

Reinke, R.E. and B.W. Stump, 1988, "Stochastic Geologic Influences on Near-Field Ground Motions in Alluvium", **Bulletin of the Seismological Society of America**, Vol. 78, pp 1037-1058.

Reinke, R.E. and B.W. Stump, 1991, "Small-Scale Experimental Studies of Stochastic Geologic Influences on Near-Field Ground Motions", accepted for publication in an American Geophysical Union Monograph entitled "Explosion Source Phenomenology".

Rinehart, E. J. and G. E. Veyera, 1986, "Material Properties Test 2 (MP-2) Review and Final Data Analysis", Air Force Weapons Laboratory, Technical Report AFWL-TR-86-66.

Rohani, Behzad, 1982, "Probabilistic Solution for One-Dimensional Plane Wave Propagation in Homogeneous Bilinear Hysteretic Materials", U.S. Army Engineer Waterways Experiment Station, Misc Paper SL-82-7.

Schuster, Sheldon et al., 1984, "Crale Users Manual (Revision 1)", Air Force Weapons Laboratory, Technical Report AFWL-TR-83-48.

Sharpe, Joseph A., 1942, "The Production of Elastic Waves by Explosion Pressures. I. Theory and Empirical Field Observations", **Geophysics**, Vol. VII, pp 144-154.

Smith, S.W., J.E. Ehrenberg, and E.N. Hernandes, 1982, "Analysis of the El Centro Differential Array for the 1979 Imperial Valley Earthquake", **Bulletin of the Seismological Society of America**, Vol. 72, No. 1, pp 237-258.

Stump, Brian W. and Robert E. Reinke, 1987, "Experimental Seismology: In Situ Source Experiments", Bulletin of the Seismological Society of America, Vol. 77, No. 4, pp 1295-1311.

Sudicky, E.A., 1986, "A Natural Gradient Experiment on Solute Transport in a Sand Aquifer: Spatial Variability of Hydraulic Conductivity and Its Role in the Dispersion Process", **Water Resources Research**, Vol. 22, No. 13, pp 2069-2082.

Trulio, John G., 1966, "Theory and Structure of the AFTON Codes", Air Force Weapons Laboratory, Technical Report AFWL-TR-66-19.

Vanmarcke, Erik H., 1979, "Probabilistic Soil Sampling Program for MX-Related Site Characterization", U.S. Army Engineer Waterways Experiment Station, Misc Paper SL-79-26.

Vanmarcke, Eric, 1983, **Random Fields: Analysis and Synthesis**, The MIT press, Cambridge, Ma., 372 p.

Vernon, F.L., J. Fletcher, L. Carroll, A. Chave, and E. Sembera, 1991, "Coherence of Seismic Body Waves from Local Events as Measured by a Small-Aperture Array", **Journal of Geophysical Research**, Vol. 96, No. B7, pp 11981-11996.

Geologic Site Characterization Cone Penetrometer and Seismic Techniques, 1987, McCormick Ranch Site, Kirtland AFB, New Mexico, Letter Report by The Earth Technology Corporation, Long Beach, CA.

APPENDIX A

RANDOM GEOLOGY GENERATOR PROGRAM

This is the listing for the random geology generator program.
This program was written for use in the PC-MATLAB software. It requires
no formal coding language.

```
function x = randvar(dist,N,Mn,Sd,A,dg,s)
%
%   The Gaussian and Exponential correlation functions are defined in
%   the frequency domain.  The random variables are generated through
%   the random number generator (RAND) and then fourier transformed
%   (FFT).
%
%
%   INPUT PARAMETES:
%
%      dist = Gaussian (1), and Exponential (2)
%      N  =  number of random variables to be generated
%      Mn =  the mean
%      Sd =  standard deviation
%      A  =  number of sample intervals
%      dg =  spatial sample interval
%      (NOTE: a = A * dg = correlation distance)
%      s  =  seed
%
%*************************************************************************
%
%     Correlation Functions
%
for h=0:N/2;
  Tpi=2.*pi.*h;
     if (dist == 1)
        f(h+1)=A.*dg.*sqrt(pi).*exp(-(A^2.*Tpi^2./(N^2.))./4);
     elseif (dist == 2)
        f(h+1)=(2.*A*dg)/(1+(Tpi/N)^2.*A^2.);
     end
end
%
v=1
for h=N/2+1:N-1;
   f(h+1)=f(N/2+1-v);
   v=v+1;
end
%
disp('hit any key to plot Theoretical Transform of Autocorrelation')
```

```
pause
   plot(f)
%
%    Writing output to file called auto.out
%
for i = 1:N/2;
    fprintf('auto.out','%e     %e\n',i,f(i))
end
pause
%
%     Random Number Generator
%
   rand('normal');
   rand('seed',s)
   x=rand(1,N);
%
%     FFT on random numbers
%
   x=fft(x);
   y=x.*conj(x);
%
disp('hit any key to display Power Spectrum of Random Numbers')
pause
   plot(y)
pause
%
%     Realizations constructed by taking the square root of the
%     power spectrum and multiplying it to the phase term exp(i*phi)
%
   phi=atan2(imag(x),real(x));
   x=sqrt(f).*exp(sqrt(-1).*(phi));
   y=x.*conj(x);
%
disp('hit any key to display Filtered Power Spectrum of Random
Numbers')
pause
   plot(y)
pause
%
%     IFFT required to transform random numbers to the space domain
%
   x=ifft(x);
   x=real(x);
%
%     Data Standardization:  Transforming to match the original
%                            standard deviation
%
   x=(x-mean(x)).*Sd./std(x(1:N))+Mn;
%
disp('hit any key to plot Filtered Random Numbers')
```

```
pause
   plot(x)
pause
%
% Writing random number output to file called gaus.out for Gaussian
% Correlation and exp.out for Exponential Correlation
%
for i=1:N;
    if (dist == 1)
      fprintf('gaus.out','%e    %e\n',i,x(i))
      fprintf('gausb.out','%e\n',x(i))
    elseif (dist == 2)
      fprintf('exp.out','%e    %e\n',i,x(i))
      fprintf('expb.out','%e\n',x(i))
    end
end
pause
%
%   Construct autocorrelation by FFT of padded sequence
%
   xm=mean(x);
   x=(x-xm);
   x=fft(x,N*2);
   x=x.*conj(x);
   x=ifft(x);
   x=real(x);
   x=x./x(1);
%
for h=0:N*2-1
   r(h+1)=h.*dg;
end
%
for ec=0:N*2-1
   r1(ec+1)=ec.*dg;
     if (dist == 1)
        ex(ec+1)=exp(-(ec^2.*dg^2.)./((A*dg)^2.));
     elseif (dist == 2)
        ex(ec+1)=exp(-(ec*dg)/(A*dg));
     end
end
%
disp('hit any key to display Final Autocorrelation')
pause
plot(r1,ex,r,x)
pause
%  Writing theoretical and computed autocorrelation to file final.out
%
for i=1:N;
    fprintf('final.out','%e    %e   %e\n',r(i),ex(i),x(i))
end
```

APPENDIX B

CHI-SQUARE TEST

B.1 Chi-Square Test Deviations

The most direct way to test a random number generator is to use it to generate the desired random numbers, U_i's, and examine the U_i's statistically to determine how closely they appear to be uniformly distributed between 0 and 1. The chi-square test, serial test, and runs (or runs-up) test are a few empirical tests (Law and Kelton, 1982). A computer program of the chi-square test of uniformity was written to test the function,

$$Z_i = (7^5 Z_{i-1}) \pmod{2^{31} - 1} \qquad \text{(B.1)}$$

The following steps are required to apply the chi-square test:

1. The interval (0, 1) is divided into k subintervals of equal length, and $U_1, U_2, \ldots, U_n$ are generated. (As a rule, k should be at least 100, and n/k should be at least 5.)

2. For $j = 1, 2, \ldots, k$, let f_j be the number of the U_i's that are in the jth subinterval, and let

$$\chi^2 = \frac{k}{n} \sum_{j=1}^{k} \left(f_j - \frac{n}{k} \right)^2 \qquad \text{(B.2)}$$

3. For large n, χ^2 will approximately have a chi-square distribution with (k - 1) df (degrees of freedom) under the null hypothesis that the U_i's are IID U(0,1) random variables. The null hypothesis is rejected at level α if $\chi^2 > \chi^2_{k-1,1-\alpha}$, where $\chi^2_{k-1,1-\alpha}$ is the upper $1-\alpha$ critical point of the chi-square distribution with k-1 df.

4. For large values of k, the approximation

$$\chi^2_{k-1,1-\alpha} \approx (k - 1) \left(1 - \frac{2}{9(k-1)} + z_{1-\alpha} \left(\frac{2}{9(k-1)} \right)^{1/2} \right)^3 \qquad \text{(B.3)}$$

can be used, where $z_{1-\alpha}$ is the upper $1 - \alpha$ critical point of the N(0,1) distribution.

The input parameters used in the chi-square test are:

1. The initial seed: $Z_0 = 12,345,678$
2. $k = 2^{12} = 4096$
3. $n = 2^{16} = 65,536$

The approximation for the critical point at α=0.10 is:

$$\chi^2_{k-1,1-\alpha} \approx (k-1)\left(1 - \frac{2}{9(k-1)} + z_{1-\alpha}\left(\frac{2}{9(k-1)}\right)^{1/2}\right)^3$$

$$\chi^2_{4095,0.9} \approx (4095)\left(1 - \frac{2}{9(4095)} + 1.282\left(\frac{2}{9(4095)}\right)^{1/2}\right)^3$$

$$\chi^2_{k-1,1-\alpha} = 4211.11$$

$$\chi^2 = 4000.8$$

Therefore,

$$\chi^2 < \chi^2_{k-1,1-\alpha}$$

so we fail to reject the NULL hypothesis at the 0.10 level. The random numbers generated do not behave significantly different from truly IID U(0,1) random variables, based on the chi-squared test.

The program written to test the random number generator with the chi-squared test is included in the following section.

B.2 Chi-Square Empirical Test Program

CHI-SQUARE TEST

This listing is for the chi-square test program. The coding language is Fortran.

```
      PROGRAM RANDOM NUMBER GENERATOR TEST
c     The chi-square test is designed to check whether the random
c     numbers (U's) appear to be uniformly distributed between 0 and
c     1.  [0, 1] is divided into subintervals (s) of equal length
c     and U1, U2, U3,....Un are generated.
c
c
c     List of symbols:
c
c      bm = subinterval matrix
c      RNUM = generated random numbers (MATLAB)
c      s = number of subintervals
c      ds = size of subinterval
c      n = number of random numbers
c      f = summation of U's
c      chi2 = equation to calculate chi-squared
c
c
          double precision bm(4096,2),RNUM(66000),f(0:4096),ds,chi2,n,s
c
          open(unit=10,file='rout',status='old')
          open (unit=1,file='output')
c
          ds = 1.0/4096.0
          n = 65536.0
          s = 4096.0
c
c     This loop will generate the values for matrix b - subintervals
c
          do 100 i=1,4096
            bm(i,1) = ds * i
            bm(i,2) = 0.0
100       continue
c
c     These loops will count the number of U's in each subinterval
c
          do 10 i = 1,65536
             read (10,*) RNUM(i)
c
```

```
            if(RNUM(i) .lt. 0.25) then
               do 20 k=1,1024
                  if(RNUM(i) .lt. bm(k,1)) then
                    bm(k,2) = bm(k,2) + 1.0
                    go to 10
                  endif
20             continue
              else
                 if(RNUM(i) .lt. 0.50) then
                   do 30 k=1025,2048
                      if(RNUM(i) .lt. bm(k,1)) then
                        bm(k,2) = bm(k,2) + 1.0
                        go to 10
                      endif
30                 continue
                  else
                    if(RNUM(i) .lt. 0.75) then
                      do 40 k=2049,3072
                         if(RNUM(i) .lt. bm(k,1)) then
                           bm(k,2)= bm(k,2) + 1.0
                           go to 10
                         endif
40                    continue
                      else
                        do 50 k=3073,4096
                           if (RNUM(i) .lt. bm(k,1)) then
                             bm(k,2) = bm(k,2) + 1.0
                             go to 10
                           endif
50                       continue
                      endif
                    endif
                endif
10       continue
c
         f(0) = 0.d0
c
c  Generation of chi-squared value
c
         do 90 j=1,4096
            f(j) = (bm(j,2) - n/s)**2.d0
            f(j) = f(j-1) + f(j)
90       continue
c
         chi2 = s/n * f(4096)
c
c  Write format statements to generate output
c
         write (1,60)
60       format (1x,'CHI-SQUARE TEST RESULTS:',/)
```

```
      write (1,65) chi2
65    format (1x,'chi2 = ',e17.10,//)
      write (1,66)
66    format (5x,'SUBINTERVAL',6x,'NUMBER OF Us')
      write (1,70) ((bm(i,j),j=1,2),i=1,4096)
70    format (2(1x,e17.10))
      stop
      end
```

APPENDIX C

SHARPE'S CLOSED FORM SOLUTION

C.1 Equation Deviations

The displacement in the medium corresponding to the application of unit function pressure to the interior surface of the cavity is as follows (Sharpe, 1942):

$$u = \frac{ap_0}{4G}\left[\left(\frac{a}{r}\right)^2 - \sqrt{\frac{3}{2}}\left(\frac{a}{r}\right)^2 e^{-\omega\tau/\sqrt{2}}\sin(\omega\tau + \tan^{-1}\sqrt{2})\right. \qquad \text{C.1}$$

$$\left. + \sqrt{2}\left(\frac{a}{r}\right) e^{-\omega\tau/\sqrt{2}}\sin\omega\tau\right]$$

where, u = displacement

For displacements at distances more than a few times the radius, Equation C.1 is simplified to the following expression

$$u = \frac{a^2 p_0}{2\sqrt{2}Gr} e^{-\omega\tau/\sqrt{2}} \sin\omega\tau \qquad \text{C.2}$$

where,

- a = cavity radius
- p_0 = applied pressure
- G = shear modulus
- r = range of interest
- $\omega = 2\sqrt{2}C_p/3a$
- C_p = P-wave velocity

τ = t-((r-a)/C_p)

t = time required to reach specified range

The velocity equation was obtained by taking the derivative of the displacement equation C.2 (du/dτ)

$$v = \frac{du}{d\tau} = \frac{a^2 p_0}{2\sqrt{2}Gr}\left[e^{-\omega\tau/\sqrt{2}}\,\omega\cos\omega\tau + (-\omega/\sqrt{2})\; e^{-\omega\tau/\sqrt{2}}\sin\omega\tau\right] \quad \text{C.3}$$

where, v = velocity

The shear modulus is obtained from the following equations:

$$G = \frac{M\,(1 - 2\nu)}{2\,(1 - \nu)} \quad \text{C.4}$$

$$C_p = \left(\frac{M}{\rho}\right)^{1/2} \quad \text{C.5}$$

where,

M = constaint modulus

ν = poisson's ratio

ρ = soil density.

If Equation C.5 is written as M = $C_p^2\rho$ and substituted into Equation C.4, the following expression is obtained

$$G = \frac{C_p^2 \rho (1 - 2\nu)}{2(1 - \nu)} \qquad \text{C.6}$$

Equation C.6 was simplified by letting the poisson's ratio, ν, equal 0.25:

$$G = 0.33\ \rho C_p^2 \qquad \text{C.7}$$

A MATLAB program was written with Equations C.2, C.3, and C.7 to generate the velocity and displacement waveforms using Sharpe's closed form solution.

The velocity and displacement waveforms were generated with the following input parameters:

Cavity radius (a) = 175 cm

Applied pressure (p_0) = 10e+10^6 dyne/cm^2 (10 Bars)

Density (ρ) = 1.643 g/cm^3

P-wave velocity (C_p) = 50800 cm/sec

Number of timesteps = 300

Timesteps = 0.0001 sec

Range of interest (r) = 200, 500, 900, and 2000 cm

C.2 Closed Form Solution Program

Sharpe's Closed Form Solution Program

This program was written for use in the PC-MATHLAB software. It require
no formal coding language.

```
function x = sharpe2a(crad,po,rho,r,tinc,T,c)
%
%  Sharpes solution for step function pressure applied to the wall
%  of a spherical cavity.
%
%  Symbols:
%        crad  =  cavity radius
%        po    =  applied pressure
%        rho   =  density
%        r     =  range
%        tinc  =  time step (make tinc small enough to catch
%                 waveform)
%        T     =  # of time steps to be evaluated
%        c     =  P wave velocity
%        G     =  shear modulus (rigidity) obtained from following
%                 equation (G = rho*c*c*(1-2v)/(2(1-v)), where v is
%                 the poisson's ratio of 0.25)
%        u     =  displacement output
%        udot  =  velocity output
%
%  NOTE: any units can be used as long as all are consistent
%
%*************************************************************************
***
%
% Time, td, required for wave to reach specified range r is computed
%
    td=(r-crad)./c
    Td1=td/tinc
    Td1=round(Td1)
    om=2*sqrt(2)*c./(3.*crad);
%
% Shear Modulus Computation
%
    G = 0.33*rho*c^2.
%
% Delay or travel time is tacked onto front of sharpes waveform
%
for i=1:(Td1-1);
```

```
    ti(i)=(i-1).*tinc;
    u(i)=0.0;
    udot(i)=0.0;
end;
%
h=0;
for i=Tdl:(T+Tdl);
    h=h+1;
    tau=(h-1)*tinc;
%
% Evaluation of equation 13 and its derivative from Sharpes part 1
% follows:
%

u(i)=(crad.^2.*po./(2*sqrt(2).*G.*r)).*exp((-tau.*om)/sqrt(2)).*sin(t
au*om);
  ud=(crad.^2.*po./(2*sqrt(2).*G.*r));
  deriv=exp((-tau*om)./sqrt(2)).*om.*cos(tau*om);
  deriv=deriv+((-om./sqrt(2)).*exp(-tau*om/sqrt(2)).*sin(tau*om));
  udot(i)=ud.*deriv;
end
%
for h= Tdl:(Tdl+T)
   ti(h)=(h-1)*tinc;
end
%
disp('hit any key to plot displacement')
pause
plot(ti,u)
pause
disp('hit any key to plot velocity')
pause
plot(ti,udot)
pause
%
% Convert units to time = usec; velocity = cm/usec; displacement = cm;
%
for i = 1:(T+Tdl);
   ti(i) = ti(i)./1.0e-6;
   udot(i) = udot(i).*1.0e-6;
end;
%
disp('displacement plot - cm vs sec')
pause
plot(ti,u)
pause
disp('velocity plot - cm/usec vs usec')
pause
plot(ti,udot)
pause
```

```
%
% writing output to file called sharp.out, col 1 is time, 2 is
% velocity,
% 3 is displacement
%
for i = 1:(T+Td1)
   fprintf('sharp.out','%e  %e  %e\n',ti(i),udot(i),u(i))
end
```

DISTRIBUTION LIST

DNA-TR-92-130

DEPARTMENT OF DEFENSE

ASSISTANT TO THE SECRETARY OF DEFENSE
ATTN: EXECUTIVE ASSISTANT

DEFENSE ADVANCED RSCH PROJ AGENCY
ATTN: DIR AEROSPACE & STRATEGIC TECH

DEFENSE INTELLIGENCE AGENCY
ATTN: DB-TPO
ATTN: DIW-4

DEFENSE NUCLEAR AGENCY
ATTN: DFTD D LINGER
ATTN: OPNS
2 CYS ATTN: OSIA
ATTN: PRPD
ATTN: SPSD
ATTN: SPSD P SENSENY
ATTN: SPSP MAJ K BRADLEY
ATTN: SPSP T FREDERICKSON
2 CYS ATTN: SPWE E TREMBA
2 CYS ATTN: TDTV F RENSVOLD
2 CYS ATTN: TITL

DEFENSE TECHNICAL INFORMATION CENTER
2 CYS ATTN: DTIC/FDAB

FIELD COMMAND DEFENSE NUCLEAR AGENCY
ATTN: FCNV M OBRIEN
ATTN: NVCG
ATTN: NVTV G S LU

FIELD COMMAND DEFENSE NUCLEAR AGENCY
2 CYS ATTN: A MARTINEZ
ATTN: FCNM
ATTN: FCTP J RENICK
ATTN: FCTP E RINEHART
ATTN: FCTP R REINKE
ATTN: FCTT
ATTN: NMHE

STRATEGIC AND THEATER NUCLEAR FORCES
ATTN: DR E SEVIN

DEPARTMENT OF THE ARMY

HARRY DIAMOND LABORATORIES
ATTN: SLCIS-IM-TL

U S ARMY BALLISTIC RESEARCH LAB
ATTN: SLCBR-SS-T
ATTN: SLCBR-TB-B R RALEY

U S ARMY CORPS OF ENGINEERS
ATTN: CERD-L

U S ARMY ENGINEER DIV HUNTSVILLE
ATTN: HNDED-SY

U S ARMY ENGINEER DIV OHIO RIVER
ATTN: ORDAS-L

U S ARMY ENGR WATERWAYS EXPER STATION
ATTN: CEWES J K INGRAM
2 CYS ATTN: CEWES-SD DR J G JACKSON JR
ATTN: D RICKMAN CEWES-SE-R
ATTN: E JACKSON CEWES-SD-R
ATTN: J ZELASKO CEWES-SD-R
ATTN: RESEARCH LIBRARY

U S ARMY MATERIAL TECHNOLOGY LABORATORY
ATTN: TECHNICAL LIBRARY

U S ARMY NUCLEAR & CHEMICAL AGENCY
ATTN: MONA-NU DR D BASH
ATTN: MONA-NU MR LONG

U S ARMY SPACE & STRATEGIC DEFENSE CMD
ATTN: CSSD-SA-EV
ATTN: CSSD-SL

USA SURVIVABILITY MANAGMENT OFFICE
ATTN: SLCSM-SE J BRAND

DEPARTMENT OF THE NAVY

NAVAL CIVIL ENGINEERING LABORATORY
ATTN: CODE L64 LORY

NAVAL POSTGRADUATE SCHOOL
ATTN: CODE 1424

NAVAL RESEARCH LABORATORY
ATTN: CODE 2627

NAVAL SURFACE WARFARE CENTER
ATTN: CODE K42 R ROBINSON
ATTN: CODE K42 S HUGHES

NAVAL WEAPONS EVALUATION FACILITY
ATTN: CLASSIFIED LIBRARY

NEW LONDON LABORATORY
ATTN: TECH LIBRARY

OFFICE OF CHIEF OF NAVAL OPERATIONS
ATTN: OP 03EG

OFFICE OF NAVAL RESEARCH
ATTN: CODE 1132SM

DEPARTMENT OF THE AIR FORCE

AFIS/INT
ATTN: INT

AIR FORCE TECHNICAL APPLICATIONS CTR
ATTN: R HANSEN

AIR UNIVERSITY LIBRARY
ATTN: AUL-LSE

PHILLIPS LABORATORY
ATTN: NTES LTCOL T BRETZ

UNITED STATES STRATEGIC COMMAND
ATTN: J 533
ATTN: JIC/ODM

DEPARTMENT OF ENERGY

DEPARTMENT OF ENERGY
NEVADA OPERATIONS OFFICE
ATTN: OTIS D H MARTIN

LAWRENCE LIVERMORE NATIONAL LAB
ATTN: L-140 R DONG
ATTN: L-200 D GLENN
ATTN: L-203 R SCHOCK
ATTN: L-84 G POMYKAL
ATTN: W CROWLEY

LOS ALAMOS NATIONAL LABORATORY
ATTN: BOB DEUPREE
ATTN: FRED APP
ATTN: R P WEAVER
ATTN: D STROTTMAN
ATTN: REPORT LIBRARY
ATTN: S TAYLOR
ATTN: R KIRBY

MARTIN MARIETTA ENERGY SYSTEMS INC
ATTN: DR C V CHESTER

SANDIA NATIONAL LABORATORIES
ATTN: A CHABAI DIV 9311
ATTN: DIV 5214 J S PHILLIPS
ATTN: DIV 9311 L R HILL
ATTN: DR CARL W SMITH DIV 9311
ATTN: MIKE FURNISH
ATTN: P YARRINGTON
ATTN: TECH LIB 3141
ATTN: 9311 C W SMITH
ATTN: 9311 D GARBIN

OTHER GOVERNMENT

CENTER FOR SEISMIC STUDIES
ATTN: L GRANT

CENTRAL INTELLIGENCE AGENCY
ATTN: OSWR/NED

DEPARTMENT OF THE INTERIOR
ATTN: D RODDY

FEDERAL AVIATION ADMINISTRATION
ATTN: L MOLINAR

DEPARTMENT OF DEFENSE CONTRACTORS

AEROSPACE CORP
ATTN: LIBRARY ACQUISITION

APPLIED RESEARCH ASSOCIATES, INC
ATTN: C J HIGGINS

APPLIED RESEARCH ASSOCIATES, INC
ATTN: S BLOUIN

APPLIED RESEARCH ASSOCIATES, INC
ATTN: R FRANK

APPLIED RESEARCH ASSOCIATES, INC
ATTN: J L DRAKE

APPLIED THEORY, INC
ATTN: J TRULIO

BDM FEDERAL INC
ATTN: E DORCHAK
ATTN: J STOCKTON

BOEING TECHNICAL & MANAGEMENT SVCS, INC
ATTN: ROBERT M SCHMIDT

CALIFORNIA INSTITUTE OF TECHNOLOGY
ATTN: T AHRENS

CALIFORNIA RESEARCH & TECHNOLOGY, INC
ATTN: J THOMSEN
ATTN: K KREYENHAGEN

CARPENTER RESEARCH CORP
ATTN: H J CARPENTER

HORIZONS TECHNOLOGY, INC
ATTN: B LEE

IIT RESEARCH INSTITUTE
ATTN: A BUTI
ATTN: DOCUMENTS LIBRARY
ATTN: M JOHNSON

INSTITUTE FOR DEFENSE ANALYSES
ATTN: CLASSIFIED LIBRARY

KAMAN SCIENCES CORP
ATTN: L MENTE
ATTN: LIBRARY

KAMAN SCIENCES CORP
ATTN: DASIAC

KAMAN SCIENCES CORPORATION
ATTN: DASIAC

KTECH CORP
ATTN: E GAFFNEY

LACHEL AND ASSOCIATES, INC
ATTN: J BECK

LOCKHEED MISSILES & SPACE CO, INC
ATTN: PHILIP UNDERWOOD

LOCKHEED MISSILES & SPACE CO, INC
ATTN: TECH INFO CTR

LOGICON R & D ASSOCIATES
ATTN: C K B LEE
ATTN. D SIMONS
ATTN: LIBRARY

LOGICON R & D ASSOCIATES
ATTN: B KILLIAN
ATTN: J WALTON
ATTN: L GERMAIN

MAXWELL LABORATORIES, INC
ATTN: J MURPHY

MCDONNELL DOUGLAS CORPORATION
ATTN: R HALPRIN

MISSION RESEARCH CORP
ATTN: TECH LIBRARY

NEW MEXICO STATE UNIVERSITY
2 CYS ATTN: A A MARTINEZ
ATTN: A K AYER
ATTN: T WARD
ATTN: W MCCARTHY

PACIFIC-SIERRA RESEARCH CORP
ATTN: H BRODE
ATTN: L JOHNSON

S-CUBED
ATTN: DR J L STEVENS
ATTN: DR K L MCLAUGHLIN
ATTN: K D PYATT JR
ATTN: R LAFRENZ
ATTN: S PEYTON

S-CUBED
ATTN: L KENNEDY

SCIENCE APPLICATIONS INTL CORP
ATTN: DR M MCKAY
ATTN: H PRATT
ATTN: H WILSON
ATTN: S MELZER
ATTN: TECHNICAL REPORT SYSTEM

SCIENCE APPLICATIONS INTL CORP
ATTN: W LAYSON

SCIENCE APPLICATIONS INTL CORP
ATTN: TECH LIBRARY

SOUTHERN METHODIST UNIV
ATTN: DR BRIAN STUMP

SRI INTERNATIONAL
ATTN: A FLORENCE
ATTN: D KEOUGH
ATTN: DR B S HOLMES

TECH REPS, INC
ATTN: F MCMULLAN

TERRA TEK, INC
ATTN: C FELICE

TITAN CORPORATION
ATTN: LIBRARY
ATTN: S SCHUSTER

TRW SPACE & DEFENSE SECTOR
ATTN: W WAMPLER

WEIDLINGER ASSOC, INC
ATTN: H LEVINE

WEIDLINGER ASSOCIATES, INC
ATTN: T DEEVY

WEIDLINGER ASSOCIATES, INC
ATTN: J WRIGHT
ATTN: M BARON

FOREIGN

BUNDESAN STALT FUR GEOWISSEN SCHAFFEN
ATTN: S REAMER